NON-LINEAR ANALYSIS OF SEEPAGE INTO DRAINS

BY

NURUDDEEN ABDULRAHMAN RAFIN**DADI**

B.Eng.(Civil)

A Thesis Submitted in Partial Fulfillment of the Requirements for the Degree of M.Sc. (Water Resources Engineering) to the Postgraduate School, Ahmadu Bello University, Zaria.

August, 1986

CERTIFICATION

This project thesis entitled "Non-Linear Analysis of Seepage Into Drains" by Nuruddeen Abdulrahman Rafindadi, meets the regulations governing the award of the degree of M.Sc. (Water Res.) of Ahmadu Bello University and is approved for its contribution to knowledge and literary presentation.

Dr. S. Mustafa,
Chairman, Supervisory Committee Date 22/12/86

Dr. L. I. Ogigie
Member, Supervisory Committee Date 22/12/86

Professor J. A. Ogunronbi
Head of Department Date 22/12/86

Professor G. E. Osuide
Dean, Postgraduate School Date ----------

DEDICATION

I dedicate this piece of work to

My Dear Father

ALHAJI ABDULRAHMAN N. RAFINDADI

DECLARATION

I hereby declare that this thesis has been written by myself and that it is a record of my own research work at Ahmadu Bello University. It has not been accepted in any previous application for a higher degree.

All sources of information have been specifically acknowledged in the reference section.

18/12/96

N. A. RAFINDADI.

ACKNOWLEDGEMENTS

I wish to express my profound gratitude and appreciation to Dr. S. Mustafa of the Department of Water Resources and Environmental Engineering, for affording me the opportunity to carry out this project, from conception to completion, under his supervision, and for his continuous show of brotherly concern in the process. His guidance during the execution of the project was indispensable.

I also wish to express sincere appreciation to other individuals who through their comments and criticisms have contributed to the completion of the project. Special thanks are due to Dr. L. I. Odigie also of the Department of Water Resources and Environmental Engineering for reading, discussing and constructively criticizing the draft thesis report. Professor Rashid of the Mathematics Department kindly reviewed some of the mathematical formulations. Preparation for and execution of the model experiments were done with the help of the technical staff of the hydraulics and soil mechanics laboratories, and of the Civil Engineering Departmental workshop. Their kind assistance is gratefully acknowledged.

My post-graduate course at the department was sponsored by the Kaduna-Karaduwa River Basin & Rural Development Authority, Dutsinma. I wish to express gratitude to the Board and Management of the Authority for for their kind consideration.

My special thanks are finally due to my family and in particular my wife, Saratu, for putting up with the inconveniences that were unavoidable during the period of the course.

ABSTRACT

The sustenance of viable agriculture depends strategically upon the provision of adequate subsurface drainage.

The goals of providing adequate aeration and salinity control in irrigated lands have been translated into a number of criteria upon which drainage systems are designed. A brief review of these shows that most criteria for design can be reduced to that of an equivalent steady state condition.

Many theories have been developed for the design of subsurface drainage systems. Some of these theories derive exact mathematical solutions while others use simplifying assumptions to derive approximate results that can be applied to field conditions.

Most commonly used drainage theories are based on the extensive use of the experimental law of Darcy which postulates a linear relation between macroscopic velocity and hydraulic gradient despite the acknowledged fact that the law fails in flow situations of high Reynold's number.

In this study, approximate analytical solutions are proposed for the water table profile between parallel drains, along with drain spacing formulae which generalize those conventionally used and based on the Darcy's linear law. The validity of these proposed equations is investi-gated experimentally using a sand tank seepage flow m under high velocity flow regimes. They are found to close agreements with experimental results as well as with similar studies reported in the literature, and provide for greater economy in drainage systems design.

TABLE OF CONTENTS

		Page
Title Page		
CERTIFICATION		ii
DEDICATION		iii
DECLARATION		iv
ACKNOWLEDGEMENTS		v
ABSTRACT		vi
LIST OF TABLES		ix
LIST OF FIGURES		x
LIST OF PLATES		xii
LIST OF SYMBOLS		xiv
CHAPTER 1: INTRODUCTION		1
1.1.	Objective of study	1
1.2.	Background of study	2
CHAPTER 2: LITERATURE REVIEW		8
2.1.	Drainage - general	8
2.2.	The need for drainage	11
2.3.	Evaluating drainage requirements ..	20
2.4.	Porous media flow theory	28
2.5.	Solutions for linear seepage flow ..	40
2.6.	Solutions for nonlinear flows ..	56
2.7.	Seepage flow models and analogues ..	62
2.8.	Summary	65
CHAPTER 3: ANALYSIS OF STEADY NONLINEAR SEEPAGE INTO DRAINS		67
3.1.	Introduction and assumptions ..	67

Page

3.2. Continuity of flow 68

3.3. Purely linear flow 70

3.4. Transitional non-Darcy flow 73

3.5. Tully turbulent flow 79

3.6. Evaporation 81

3.7. Summary 83

CHAPTER 4: EXPERIMENTAL SET-UP AND PROCEDURE .. 84

4.1. Introduction 84

4.2. The rainfall simulator 84

4.3. The sand tank 85

4.4. Water supply to the model 87

4.5. Model experiment procedure 90

4.6. The permeameter experiment 91

CHAPTER 5: EXPERIMENTAL RESULTS AND ANALYSES .. 94

5.1. The porous medium 94

5.2. Permeameter test 94

5.3. Analysis of permeameter data .. 97

5.4. Calculation of precipitation rates .. 107

5.5. Determination of theoretical water table profiles 109

5.6. Flow regimes .. ..

5.7. Discussion of results 121

CHAPTER 6: CONCLUSIONS AND RECOMMENDATIONS .. 125

6.1. Conclusions 125

6.2. Recommendations 127

REFERENCES 130

LIST OF TABLES

		Page
Table 5.1:	Particle size distribution of sample porous medium	96
Table 5.2:	Permeameter data for determination of flow coefficients	98
Table 5.3:	Calculation of the mean square error MSE of experimental data unto I = av	100
Table 5.4:	Summation for least squares regression of experimental data to fit into $I = av + bv^2$ ..	102
Table 5.5:	Calculation of the mean square error MSE for regression of experimental data unto $I = av + bv^2$ ..	103
Table 5.6:	Summations for least squares regression of experimental data to fit into log I = A+B logV ..	105
Table 5.7:	Calculation of the mean square error MSE for regression of experimental data unto log I = A+B logV ..	106
Table 5.8:	Water table profiles: $R = 1.8063 \times 10^{-4}$ m/sec ..	113
Table 5.9:	Water table profiles: $R = 2.1725 \times 10^{-4}$ m/sec ..	114
Table 5.10:	Water table profiles: $R = 2.2026 \times 10^{-4}$ m/sec ..	114
Table 5.11:	Water table profiles: $R = 2.4645 \times 10^{-4}$ m/sec ..	115

LIST OF FIGURES

Fig. 2.1: Schematic Representation of Darcy's experiment. 31

Fig. 2.2: Analysis of flow to drains using potential theory (Kirkham, 1958). 42

Fig. 2.3: Seepage flow towards drains from D-F theory. 47

Fig. 2.4: Seepage of steady rainfall into parallel ditch drains. 50

Fig. 2.5: Combining radial and horizontal (D-F) flow assumptions (Hooghoudt, 1940). 53

Fig. 2.6: One dimensional vertical infiltration (non-Darcy flow; Gill, 1976). 57

Fig. 2.7: Steady non-Darcian seepage through embankment (Basak, 1976). 67

Fig. 3.1: Typical water table profiles for various values of dimensionless parameters P and Q; S/h = 16. 82

Fig. 3.2: Typical water table profiles under evaporation; S/h = 16. 91

Fig. 4.1: Rainfall simulator - Plan and Views. 101

Fig. 4.2: Sand tank model; experimental set-up. 103

Fig. 4.3: Schematic diagram of the constant head permeameter experiment. 111

Fig. 5.1: Particle size distribution of sample of porous matrix. 124

Fig. 5.2: Regression of experimental plots along linear flow relation. 134

Fig. 5.3: Regression of experimental plots along non-linear flow relation. 137

Fig. 5.4: Regression of experimental plots along non-linear flow relation. 105A

Fig. 5.5: Theoretical and experimental water table profiles; R = 1.8063×10^{-4} m/s. 112A

Fig. 5.6: Theoretical and experimental water table profiles; R = 2.1725×10^{-4} m/s. 112B

Fig. 5.7: Theoretical and experimental water table profiles; R = 2.2026×10^{-4} m/s. 112C

Fig. 5.8: Theoretical and experimental water table profiles; R = 2.4645×10^{-4} m/s. 112D

Fig. 5.9. Variation of dimensionless spacing (S/H) with the ratio (h/H) for three assumed flow conditions; R = 2.4645×10^{-4} m/s. 123

LIST OF PLATES

Plate I:	Front view of sand tank model	90A
Plate II:	Discharge pipe P_1 with measuring container	90B
Plate III:	Manometric glass tubes, and precipitation from rainfall simulator.	90C
Plate IV:	Porous matrix bed after application of precipitation	90D
Plate V:	Porous matrix bed bounded by perforated metal sheet as vertical ditch surface	90E
Plate VI:	Ditch water level and overflow from ditch, to be discharged out through pipe P_1	90F

LIST OF SYMBOLS

The following notations are used in this thesis. All quantities are defined where they first appear.

a : Coefficient of linear resistivity.

A : Dimensionless constant in the logrithmic flow equation.

b : Coefficient of quadratic resistivity.

B : Dimensionless constant in log flow equation.

c : Dimensionless nonlinear flow parameter.

C_d : Coefficient of discharge.

d : Effective depth of impervious layer below drain level.

Δ_1, Δ_2: Manometric water level differences in constant head permeameter.

E : Evaporation rate.

g : Acceleration due to gravity (= 9.81 m/s^2).

h : Depth of impervious layer below drain level.

H : Depth of impervious layer below the maximum groun**d** water level between drains.

I : Hydraulic gradient.

K : Hydraulic conductivity.

M : Material flow constant.

m : H**e**ight of maximum water table level above drain axis.

MSE : Mean square error.

n : non-Darcy exponent; dimensionless.

μ	:	Viscosity of water.
P	:	Dimensionless coefficient of quadratic resistivity = bR^2 or bE^2.
ϕ	:	Hydraulic head potential.
Q	:	Dimensionless coefficient of linear resistivity = aR.
Q_E	:	= aE.
Q_d	:	Quantity of discharge (m^3/sec).
R	:	Rainfall rate.
r	:	Distances from drain axis.
ρ	:	Density of water.
S	:	Spacing distance between drains.
t	:	Time period
u,v,w;		Orthogonal velocity components.
V	:	Macroscopic velocity.
x	:	Horizontal coordinate; and distance measure.
X	:	Distance measure = (S/2 - x).
y	:	Vertical coordinate, and vertical distance measure.

CHAPTER ONE

INTRODUCTION

1.1. OBJECTIVE OF THE STUDY

In this thesis, a study is presented into the shape of the static water table profile established by the seepage of steady rainfall or equivalent irrigation recharge through soil into parallel drains.

The use of non-linear constitutive laws describing the variation of the flow velocity with the hydraulic gradient, in preference to the linear law which is most commonly used (the Darcy's law) is introduced. Consequently, approximate analytical solutions are proposed for the water table profile between the drains along with drain spacing formulae. These proposed equations and formulae are found to be generalizations of those conventionally used and based on the Darcy's linear law.

To investigate the validity of the proposed equations it is intended to carry out a series of experiments on a sand tank seepage flow model to obtain actual water table profiles, using sieved sand (effective size D_{10} = 2.86 mm). A rainfall simulator is used in the model, constructed from galvanized iron sheets and perforated with 2 mm diameter drills at 5 cm cross spacings. A steady uniform recharge will be maintained using the rainfall simulator upon the porous matrix bed. The static water table will be measured by the use of a series of manometric glass tubes fixed to the sides of the sand tank model.

Comparison can then be made between the experimental water table profiles, those from the proposed equations and those presented by other research works.

1.2. BACKGROUND TO THE STUDY

1.2.1. Drainage Problems:

The ever rising demand for increased food production to cater for soaring populations has inspired tremendous efforts aimed at increasing the food production per hectare of agricultural lands particularly through the development and judicious management of the Limited water resources available. In the last one and a half decades, the Federal Government has invested thousands of millions of Naira in the development of water resources for agriculture in the various river basins of the country. Indeed, improved water management along with other agronomic, engineering and economic technologies is a necessary input for increased efficient food production through water resources development.

The term 'Water Management' implies partial or total control of the water on the land and in the soil so as to enhance high levels of production and reduce damages to a minimum. In this country, emphasis has tended to concentrate on the provisions for irrigation of agricultural lands, but a no less important phase of water management involves the drainage of agricultural lands, which is the orderly removal of water that is excess to economic crop production from the plants' soil environment or, in the case of irrigated lands in arid and semi-arid climates, the establishment and maintenance

of proper salt balance in the soil. Without adequate provision for drainage, excessive soil moisture accumulates in the plants' soil environment, creating toxicity conditions that seriously hamper the growth of plants and cause deteriorative changes in the soil's physical structure.

A review of available literature shows that millions of hectares of agricultural lands around the world have been put out of production through the establishment of extensive irrigation projects without commensurate provisions for adequate drainage of the land. Indeed, the downfall of some early civilizations, such as that of Mesopotamia, which thrived in the fertile valleys of Tigris and Euphrates in the Middle East, has been attributed to the damaging consequences of the problems of water-logging salinity and alkalinity associated with poor drainage of irrigated lands. Conversely, millions of hectares of damaged agricultural lands have been reclaimed by the installation of adequate drainage facilities in the land along with other chemical treatments (Russel, 1973).

Reports of water-logging problems in Nigerian irrigated lands have also recently begun to emerge. For instance, the Kano river project was established in 1970 with the plan of putting about 62,000 hectares of land under irrigation during the first two phases, but with evidently no provisions for effective sub-surface drainage. According to Nwa (1982), a ground-water survey in the area before the project construction

showed that there was no water table existing within 1.5 m of the ground surface even during the rainy season. However, a study initiated in 1977 revealed that high groundwater table has become a problem in the Kadawa sector of the project within seven years of continuous irrigation, with widespread reported crop failure as a result.

1.2.2. Flows In Porous Media:

The mechanism whereby excess subsurface water is removed from the plant's soil environment involves the physics of flow of fluids through porous media and consequently depends heavily on the properties of the soil. In fluid mechanics, we learn that in order to describe the motion of a fluid, we require the kinematic, dynamic, and thermodynamic relationships of flow. The first of these leads to a statement of conservation of mass, the second may be derived from a momentum balance, the third takes the form of equations of state relating the fluid's pressure, temperature and density.

The classical dynamical relation for Newtonian (viscous) fluids derived in texts of hydrodynamics are the Navier-Stokes equations, and these are the equations applicable to groundwater flow. The Navier-Stokes equations, however, do not lend themselves to solution in very many situations of practical interest. For this reason, simple empirical constitutive equations have been developed as equivalent dynamic relations derived mostly from experimental observations of macroscopic velocity responses to applied hydraulic gradients.

By far, the most widely used of these relations in the derivations of groundwater flow equations is the experimental law based on the work of Henry Darcy in 1856 which postulates a linear relationship between the macroscopic velocity of flow and the applied hydraulic gradient.

However, while Darcy's law holds good for most flow conditions in fine grained soils, researches over the years have indicated the existence of upper limits of its validity in which viscous forces no longer predominate and inertial forces become significant. Flows of this nature are encountered in rock aquifers, coarse-grained soils and rock-fill banks, unconsolidated aquifers, especially in areas adjacent to open water bodies such as streams or wells; and in flow in filters.

1.2.3. Steady State Drainage Flow:

In the evaluation of the drainage requirement of a given land, a number of criteria have been evloved upon which to base the design of drainage systems. In the analyses of seepage flow towards drains, the steady state condition provides the simplest approach in obtaining solutions to drainage flow problems. The steady state is said to be attained when subsoil water is drained at a steady rate equal to that of a steady rainfall or irrigation recharge, and the resulting water table profile between drains becomes static with time. Solutions and requirements based on the steady state conditions, such as the fluctuating or falling watwr table conditions.

To analyse the drainage of steady precipitation into drains, various theoretical approaches have been developed for the determination of the position of the water table in equilibrium with rainfall and the derivation of the drain spacing formula. Some of these solutions are exact in the sense that an exact mathematical solution is found to the differential equations and boundary conditions that are assumed applicable (e.g. Kirkham, 1958; Engelund, 1957). Other solutions are approximate in nature because they use simplifying assumptions to derive simple results that can be applied approximately to field conditions (Van Schilfgaarde, 1957; Dagan, 1964).

One of the most widely used of these simplifying assumptions is the "Dupuit-approximation "(also known as the Dupuit-Forchheimer theory) used in the analyses of problems of unconfined flow systems that are shallow relative to their aereal extents and exhibit relatively small curvature of the free surface.

Most available solutions to drainage flow problems, however, have been based on the assumption of applicability of Darcy's linear flow law. Although the inadequacy of Darcy's law at high Reynold's numbers has been widely acknowledged, the treatments of practical situations of seepage through soils into drains involving Non-Darcy flow have been few.

The two most widely used forms of nonlinear velocity-hydraulic gradient relationships are:

(i) that of Izbash as reported by Basak (1976)

which is of the form

$$v = MI^n \qquad (1.1)$$

in which v = macroscopic velocity of flow

I = applied hydraulic gradient

M = a material constant

and n, is a non-Darcy exponent which lies between $\frac{1}{2}$ and 1;

(ii) that developed originally by Forchheimer in 1901; which is of the form:

$$I = av + bv^m \qquad (1.2)$$

where $1.6 \leq m \leq 2$

a and b above are resistivity coefficients.

While Izbash's equation is purely empirical, Forchheimer's equation, though initially based on experimental results alone, has been found to have theoretical basis (Irmay, 1958; Ahmad & Sunada, 1969)

Basak (1977) presented one of the few available solutions of drainage flow based on a nonlinear flow law. Using the Izbash flow equation (1.1)above, he derived an equation for the steady state water table profile between two parallel drains and a drain spacing formula. In this study the proposed analytical solution shall be based on the Forchheimer equation (1.2) above. utilizing the same flow system as that analyzed by Basak (1977).

CHAPTER TWO

LITERATURE REVIEW

2.1. DRAINAGE - GENERAL

The significance of effective drainage for agricultural lands has been recognized for over 2,000 years. It has been known that the presence of excessive soil moisture in a plant environment creates conditions that seriously hamper the growth of plants.

Recorded examples in the practice of the art of drainage, particularly in irrigated lands date back to the times of the early Egyptian civilization in the Nile valley, and the Roman Empire. Examples of the devastating effects of poor drainage of irrigated lands have also been known for centuries. Thus for instance, although varied causes have been cited for the downfall of the civilization in Mesopotamia which thrived in the valleys of the Tigris and Euphrates rivers in the Middle East, most authorities are said to agree that the finality was determined by problems of water-logging and salinity associated with poor drainage of irrigated lands.

In the past century, huge irrigation projects have been established around the world, in many cases without adequate natural drainage, and have invariably resulted in the wastage of millions of hectares of agricultural land, on account of high groundwater tables and salinization. One typical case of such projects is the Punjab Irrigation Project of the Indus valley in Pakistan, started in the 1920s. According to Mehta (1957),

development of damages to land by water-logging and salinity in the Punjab project had, by 1945 exceeded 20,000 hectares and was on the increase. Subsequent studies (e.g. Framji, 1974) reported that water-logging continued significantly in the Punjab, reaching the largest damage extent, with over 1.6 million hectares affected, by 1963.

In another case study, an estimate of the extent of water-logging and salinization of various lands in parts of India where canal irrigation had been introduced in the absence of any in-built drainage measures, gave a total of over 3.1 million hectares in 1974 (Framji, 1974).

Reports on studies of drainage problems in irrigated lands in Nigeria have also been available recently. A typical review of the history of irrigated agriculture and the status of salinity and water-logging problems in the irrigated lands of Northern Nigeria was presented by Maurya and Singh(1979). Early studies carried out by, among others, Allison, L.E. of the U.S. Salinity Laboratory in 1962, on the salinity status of Irrigation Schemes of Northern Nigeria, found that in general, harmful amounts of salinity and exchangeable sodium were not detected from most irrigation sites. But a similar report, on a feasibility study on South Chad Irrigation projects by McDonald and Partners (1973) found that although levels of salinity existing at the area were predominantly low, about 20 - 40% of the older flood plains in the Hadejia River Basin contained soils with

alkaline sub-surface horizons and low salinity, resulting in the formation of alkali soils at the basement complex plains in the lowland areas.

At the Institute of Agricultural Research of the Ahmadu Bello University in 1978, a salinity survey of major irrigation projects was initiated, with monitoring at six-month intervals. As at 1979, results of samples collected from Tungan Tudu, Hadejia, Tallum, and Thomas irrigation projects in Kano State showed that except for a few locations, improved drainage was required in most areas to forestall the possible future development of salinity and alkalinity (Maurya, 1979). In particular, at Tungan Tudu, the report indicated the existence of a hard pan subsoil layer at 60 cm depth, and water table fluctuations between 50 - 60 cm during the rainy season.

In another study, Nwa (1982) reported on the problems of water-logging in some parts of the Kano river project, one of the projects identified in a Federal Government commissioned reconnaissance study of the Chad Basin within Nigeria in 1968, lying within the Hadejia-Jama'are River Basin and covering a projected total of 93,000 hectares to be executed in phases. By 1980, 6,000 hectares consisting mainly of wheat, maize and vegetables were under irrigation. The study reported that in 1966 - 67, prior to the commencement of construction works, a study of about 500 holes augered to an average depth of 1.5 m showed only one hole containing groundwater table to within 1.5 m of the surface. In another study, initiated in 1977, in the Kadawa section of the project, it was determined that at most locations, groundwater level lay

between zero to 60 cm at peak of rains and between zero to 40 cm at peak of irrigations, below the ground level. Widespread total crop failure was reported particularly in the lowlands of the project during the rainy season, and surface crust formation was observed at various sites. Thus high groundwater table or water-logging had become a problem in the Kadawa sector of the Kano River project within seven years of continuous irrigation principally because effective provision of drainage was not incorporated in the project design and construction initially. While improved irrigation efficiencies and manipulation of the cropping patterns can minimize the problems, the study concluded that the ultimate solution lies in the establishment of an effective drainage system for the area.

Centuries of experience of drainage problem of irrigated lands have pointed to the same important lesson, that establishment of effective drainage system at fairly early stages of projects is as important as the irrigation facilities themselves.

2.2. THE NEED FOR DRAINAGE

According to Luthin (1957), among various sources of drainage water which create poor drainage conditions in irrigated lands, two factors are most prominent.

(i) Low conveyance efficiencies resulting from high seepage losses in canals. As much as 30% of the total water delivered for irrigation projects has been reported lost through canal seepage, particularly unlined canals.

(ii) Low application efficiencies resulting from excessive application of irrigation water on the land. Thus, in most surface irrigation methods, some percolation of excess applied water below the plants root zone occurs. According to various studies, this percolation is, in fact, essential to maintain a favourable salt balance in the soil of irrigated lands.

In a soil environment which does not possess adequate natural (or artificial) capacity to drain off the excess water, these conditions result in a gradual accumulation of subsurface water and therefore a general rise in the level of the groundwater table. Water-logging conditions are generally said to exist when crop failure commences as a result of high groundwater table. It is very essential to avoid these conditions by ensuring adequate drainage of agricultural lands. The principal effects of poor drainage are enumerated below.

2.2.1. Wet Soil Conditions (Water-logging):

High groundwater creates soil environments with excessively high moisture levels; and crop productions are harmed just as much by excessive as by deficient soil moisture.

The adverse effect of excessive soil moisture on crop production centres around deficient aeration (Van't Woudt and Hagan, 1957). Aeration is the process by which roots absorb oxygen from the atmosphere through the soil air channels for respiration and other metabollic activities and exchange it, through diffusion, with carbon dioxide. In water-logged soils, these channels of gaseous

diffusion get blocked and become inefficient for exchange of gases, thus creating a deficiency in oxygen, or anaerobic conditions. This shortage of oxygen causes some species of bacteria to carry out a number of chemical reductions, producing reduced organic and inorganic compounds which are very toxic to root cells (Ponnamperuma, 1972). These reduced substances include nitrites, sulphites, ferrous (Iron II) and manganous (Manganese III) compounds; hydrogen sulphide, methane, and hydrogen gases. The presence of these substances in toxic concentrations weakens the plants' root system, often sufficiently to become susceptible to pests and diseases. Thus, Grable (1966) reports that several diseases have been identified which are prevalent in conditions of water-logging and nitrogen deficiency. Scalding, a damaging crop disease which results in the burning and scorching of plant tissues, has been reported (Van't Woudt and Hagan, 1957) to be generally ascribed to conditions of excessive soil moisture and high temperatures.

Anaerobic conditions also create a slowing down in the rate of decomposition of organic matter in the soil and thus a deficiency in the end products of nitrogen and phosphate, which are very important plant nutrients (Russel, 1973). Thus, in a study of the relationship between groundwater level and crop yield, Harris et al (1962) reported that a rise from 100 cm to 40 cm below the ground surface of the water table reduced the crop yield to 63% of the original yield. This deficiency was corrected by the application of a nitrogen fertilizer,

thus confirming that the reduction in yield was due to insufficient nitrogen in the plant environment. Similarly, Nicola and Amer (1969) reported increases in the yields of wheat, maize, and cotton, ranging between 21% and 47% without fertilizer application due to the installation of tile drainage in the farm land.

Anaerobic conditions are also harmful to the growth of scme important organisms in the plants' soil environment such as those bacteria responsible for nitrogen fixation (the reduction of nitrogen gas from the atmosphere to ammonia in soil solution) and nitrification (the production of nitrates for ready use by plants from ammonia) - processes which are essential for plant development (Van de Goor, 1972).

Numerous other problems associated with water-logged soils have been subjects of studies. Some of these include:

(i) Inhibited root formation and transpiration rate of some plants due to increased concentrations of carbondioxide in the plants' root system (Van't Woudt & Hagan, 1957).

(ii) Poor trafficability of the soil, making it difficult or impossible for machinery activities on the land for tillage and non-tillage operations (Reeve & Fausey, 1974).

(iii) High specific heat capacity of wet soils in comparison with drier soils, thus causing the soil of temperate lands unable to readily warm up in the spring, and resulting in germination delays.

(iv) Creation of health hazard situations due to mosquitoes and other harmful insects breeding in small ponds in the field (Luthin, 1972).

2.2.2. Salinity:

A saline soil as defined by the U.S. Salinity Laboratory is a non-alkali soil containing soluble salts in such quantities that they interfere with the growth of most crop plants (Hayward & Wadleigh, 1949).

Saline soils mostly occur in regions of arid or semi-arid climate and are frequently produced artificially by injudicious irrigation and poor drainage. They result from the accumulation of salts in the soil added through the application of irrigation waters which usually contain high salt concentrations in comparison with rain water (Allison, 1964). Salts also result from the geologic origin of the parent rocks of the soil. Gradually, evaporation and consumptive use of the water by plants raises the concentration of the salts in the residual soil water.

The salt content of irrigation waters is commonly specified in practice by its electrical conductivity in m.mhos/cm. (U.S. Salinity Laboratory, 1954). The term "salt tolerance" indicates the degree of salinity a plant can withstand without being appreciably affected in its growth and development, and is generally stated in terms of the electrical conductivity of the saturation extract of the soil in the root zone of the plants (see Maas & Hoffmann, 1977). Thus, if crop yields are not to suffer from salinity, the conductivity of the soil

solution must be kept below the value for the crop tolerance. But since the soil solution becomes more concentrated as the crop removes water from the soil, then the more saline the water, the less water can the crop be allowed to remove before irrigation is reapplied. The re-application must, more over, be in sufficient quantity in order to wash down, or "leach" the concentrated solution below the root zone of the crop.

The proportion of applied irrigation water that must be used for leaching out the residual salts from the soil profile is called leaching requirement. Naturally, leaching can only be done if the groundwater is sufficiently low and good drainage is maintained on the land. In poorly drained land, leaching would only give rise to water-logging and increased undesirable salt movement into the upper root zone.

According to Russel (1973), salinity may have two types of effects on the growth of crops.

The more prominent effect is the increase in the osmotic pressure of the soil solution that occurs with increase in the total soluble salt content, and which inhibits the growth of plants. Plant growth is inhibited because the high osmotic pressure, like soil moisture tension, decreases the amount of water that is physiologically available to the plant, thereby inducing modifications in plant behaviour normally associated with water deficiency in the tissues. Thus crops in high salt content conditions would require relatively more irrigation water application in order to maintain an optimal growth

rate. Because salt accumulations are often greater at seed depths than at lower levels in the soil profile, this effect has been reported to cause widespread germination failures (Bernstein, 1974).

The second effect is the damage that occurs to crops due to toxic accumulation of specific salts or ions which are otherwise harmless in lower concentrations. Thus, for instance, excessive sodium concentration (sodium toxicity) in soil solution results in high pH, which creates nutritional imbalance by impeding plants' absorption of many important nutrients such as phosphates, iron, zinc and manganese. Chloride ion accumulation causes damage usually in the form of leaf burn or defoliation (Fireman, 1957). Boron, though essential for plant growth in allowable quantities is exceedingly toxic to most plants at concentrations greater than 0.3 parts per million. Presence of the bicarbonate ion in high concentrations inhibits the intake of calcium and magnesium and occasionally gives rise to ion chlorosis (Allison, 1964). Other specifically toxic ions identified include sulphate, calcium, magnesium and nitrates at varying concentrations (Hayward & Wadleigh, 1949).

Because high concentrations of salts are already present under saline conditions, the nutritional imbalances caused by specific ion effects cannot be corrected by adding the deficient element to the soil as such amount would be excessive, costly and would cause further undesirable increases in salinity (Bernstein, 1974).

2.2.3. Alkalinity:

An alkali soil is a soil which contains sufficient exchangeable sodium in its complex to interfere with the growth of most crop plants and does not contain appreciable quantities of soluble salts. The development of an alkali soil is caused by the same factors responsible for the salinization of soils.

As soluble salts from irrigation water become more concentrated in solution, the solubility limit of certain salts, notably the alkaline earth (calcium and magnesium) carbonates and sulphates are exceeded, causing them to precipitate out of solution, with a corresponding increase in the relative proportion of sodium in the soil solution. Ca^{++} and Mg^{++} ions are the dominant cations normallly found in soils of arid regions. However, due to the dynamic equilibrium between soluble and adsorbed ions, sodium replaces some of the calcium and magnesium originally present in the exchange complex of the soil. This "alkalization" process leads eventually to the formation of alkali or sodic soils (Allison, 1964).

one long term effect of alkalization resulting from the precipitation of alkaline earth carbonates and sulphates is the formation of layers of large accumulations of gypsum or carbonate minerals at shallow depths below the surface, forming a hard pan barrier that is essentially impermeable except for cracks and other discontinuities.

The characteristics of clay soils (shrinkage, swelling, structural stability, etc.), are influenced by the strength of attraction between the clay particles,

which is largely determined by the exchangeable cations composition. Thus, the bivalent cations of calcium and magnesium are more strongly attracted to clay particles than is the monovalent sodium ion, and allow these particles to flocculate into stable larger particles which can result in better structured agricultural soils. In sodic soils, however, as the soil solution becomes more dilute due to leaching, then following the Guoy-Chapmann diffuse double layer theory for exchangeable cations which describes the thickness of the mantle of bound water in which the exchangeable ions are distributed around the clay particles, there is an increase in the thickness of the diffuse double layer of exchangeable sodium on the clay particle surface. The clay mineral consequently undergoes swelling and inter-particle repulsive forces develop, eventually becoming sufficient to rupture the Van-der-waals forces of attraction between individual particles. The clay particles thus deflocculate and block the pores through which water percolates thus rendering the soil impermeable.

This loss of soil structure, known as "dispersion" is responsible for the tendency of soils high in adsorbed sodium to become plastic and sticky when wet, and impede water movement, as reported by Firemann (1957). Dispersed soils are not conducive to vigorous plant growth because of the following properties which they possess:

(i) The poor structural status of the soil lowers the nutrient and water availability to plants even in conditions of abundant water supply.

(ii) The soils' capacity for gaseous interchange is lowered leading to oxygen deficiency in the plant environment.

(iii) On drying. the soil forms large, dense. hard clods or "crusts" on the surface, separated by few deep cracks. These dense clods impede infiltration and can prevent seedling emergence.

(iv) In the absence of interparticle forces of attraction, individual particles become free units and may often get "translocated", or washed down to the sub-soil where they form an impervious layer, further impeding the downward movement of applied water.

2.3. EVALUATING DRAINAGE REQUIREMENTS FOR DIFFERENT CONDITIONS

In order to establish an effective artificial drainage system for an agricultural land a number of methods exist (see Reviews by Schwab et al, 1966; Donnan & Schwab, 1974). These include open ditch. surface field, subsurface or tile, and interceptor drains, as well as pumped tube wells. Generally, the usual practice for a given piece of land is to install the drains running parallel to each other at specified spacings apart. Under such arrangement, maximum water table heights would occur half way between the drains. In this section, a number of different conditions for evaluating the drainage requirement of a given field, are examined and a suitable one is proposed.

For any selected method of drainage, the drainage requirement of a given field is the desired capacity of

the field to drain a given precipitation such as to ensure adequate control of the groundwater level (Bourver, 1974). Where such requirement is not satisfied by the natural drainage intensity then there is a need for the design of a drainage system. Drainage requirements are evaluated for a number of conditions.

2.3.1. Steady State Condition:

The steady state is said to exist when a certain uniform and steady rate of precipitation establishes a water table profile, known as the 'equilibrium" or 'static' water table, that does not rise or fall with time. This implies that the subsoil water is drained at a rate equal to the steady rate of application.

The idea of steady state in drainage is to control the maximum height the water table would rise between the drains given the soil characteristics, depth of drain and the application rate. These parameters are connected together by the various drainage design equations developed by a number of authors, as discussed in Section 2.5.

Drainage provisions based on the steady state condition thus assume approximately uniform and steady precipitation patterns such as low intensity long duration rainfall events or continuous irrigation applications. Thus the design requirement can be described by a certain combination of application rate and the desired maximum water table level.

The desirable maximum water table level to be applied in design varies with the types of conditions. For instance, leguminous plants are said to perform well with

groundwater depths of about 50 cm below the surface. Plants such as grasses or clovers grown for their vegetative parts, and vegetables are said to produce favourably with water tables at 30 - 50 cm below the surface (Van't Doudt & Hagan, 1957). Harris et al (1962) in their experiments indicated a range of 60 - 100 cm depths for maize, sweet corn, and vegetables. Van De Gour (1972) reports that in Netherlands, the highest average yields of grassland are found when groundwater table depths are between 60 - 80 cm for fine-textured soils and 40 - 60 cm for sandy soils. Generally, for humid climates minimum permissible water table depths of 40 cm for grassland and 50 cm for arable land are assumed.

The value of application rate to be assumed is a mean value of variable rainfall rates taken as steady precipitation. Bouwer (1974) reports that an upper limit of 7 mm/day is commonly used in the Netherlands based on the observation that on well drained fields, the drainage rate seldom exceeded 7 mm/day, while water table seldom rose closer than 50 cm to the field surface. For typical Nigerian conditions, a higher value would be expected. Actual values should, however, be properly chosen keeping in view the nature of rainfall and soil conditions.

In irrigated agriculture, salinity control requirement is to prevent high groundwater levels during leaching exercises. The leaching requirement, i.e. the proportion of the applied irrigation water to be used

for leaching, is also the ratio of the salt concentration in the irrigation water to the crop salt tolerance. The required minimum groundwater depth is generally greater than for humid climates so as to avoid salt accumulation in the root zone through upward movement of salt ladden water by capillary action. A range of depths between 120 and 190 cm midway between drains has been indicated by various authors depending on the soil texture. The drainage coefficient range is 0.5 - 2.5 mm/day (Bouwer, 1974).

Trafficability control is also often used as a basis for drainage design on the steady state condition. Trafficability depends on the traction or shearing resistance of the topsoil, which in turn depends on the soil water content. The maximum value of the soil water content required to give a certain shearing resistance of the topsoil can be determined through the Coulomb equation (Terzaghi and Peck, 1967):

$$s = C + (P - U_w) \tan \phi$$

in which P = total pressure on the soil

s = shearing strength of soil

U_w = pore water pressure

ϕ = angle of shearing resistance, a property of the soil material; and

C = cohesion of soil material.

Thus, the moisture level that givss a required shearing resistance can be determined, from which the required water table depth can be selected to provide the right moisture content using established experimental relation-

ships between water table depths and moisture contents (Reeve and Fausey, 1974). The drain spacing is then computed such as to obtain the selected water table depth.

2.3.2. Falling Water Table Condition:

In climates with precipitation patterns of high intensity short duration events the water table would usually undergo a rapid rise, reaching the ground surface during torrential rainfall events. Thus the main idea of the falling water table in drainage of such lands is that the water table should drop from the field surface to a required safe depth within a given safe period of time. The design requirements in such cases can therefore be described by a certain combination of a minimum fallen depth and a safe time period.

The safe time period is determined from studies on tolerance of crops to temporary high water tables which varies with crop type, stage of growth, weather conditions and soil characteristics (e.g. capillary fringe, drainable porosity). Wesseling and Van Wijk (1957) indicated that in most cases, growth is not seriously affected if a 50 cm drop of the water table is achieved within 48 hours.

2.3.3. Fluctuating Water Table Condition:

Drainage design based on the fluctuating water table condition considers the overall fluctuation pattern of the groundwater table throughout a season. Drainage requirement is such as to prevent an undesireable pattern of water table fluctuation. For the drainage requirement to be evaluated, a rational assessment of two factors is required.

(i) A prediction of the pattern of water table fluctuation (water table hydrograph) for a given pattern of rainfall or irrigation recharge.

(ii) The effect of a given water table hydrograph on the crop yield.

Early solutions to the problem of unsteady (transient) flow to predict water table changes, were provided by Glover of the USBR (Van Schilfgaarde, 1957) who derived equations relating the spacing of tile drains to the rate of drop of the water table at given heights above the drain.

Maasland (1959) considered the problem of water table fluctuations in response to repeated recharges. He presented an analysis of the effect on water table of intermittent constant recharge (recharge applied intermittently at constant rate) and of intermittent instantaneous recharge (recharge applied instantaneously at regular intervals). Maasland (1964) also considered a similar problem involving repeated irrigation recharges.

Van Schilfgaarde (1965) presented a method which takes into account the probability distribution of precipitation events for a certain drainage system to determine the pattern of water table fluctuations (water table hydrograph). The results of his method are expressed in terms of water table frequency diagrams showing lengths of period per year or season that a certain water table position is exceeded in relation to the drain spacing. The approach was parallel to the use of recurrence intervals in hydrologic analyses.

To enable design of drainage systems based upon an anticipated long term sequence of recharge and drainage, especially for irrigated areas, where, with regular irrigation, recharge events are regarded as periodic in temporal distribution, the concept of dynamic equilibrium was evolved (McWhorter, 1977). In this concept, drain spacing is selected such that the depth of water table is the same at the end of an irrigation season as at the beginning, and the resulting dynamic equilibrium position is at a safe depth.

Glover (1978) in his work on transient groundwater hydraulics, has presented an extensive review of various methods of analyses of water table depths in the transient state.

The effect of a water table fluctuation pattern on crop yields has also been a subject of a number of studies. For instance, Sieben, as reported by Van de Gour (1972) found a relation between yield reduction of wheat and frequency of high groundwater surface in the North-East polder of the Netherlands. He introduced the SEW-value (sum of excess water tables levels above a specified depth) which is obtained by summing all daily values, in cm, by which the groundwater levels (midway between drains) exceed a reference level.

It was found that the SEW-value, as a parameter for groundwater regime in the upper layer of the soil showed, above a certain minimum, negative relations with crop yields. Thus, for instance, optimum crop yields were found to be obtained if the sum of excess water table levels

above 30 cm depth(SEW_{30})did not exceed 200 cm-days.

Some other studies have indicated that no effect is observed on yields even when the water table rose to 30 cm, provided it remained below 60 cm for 75% of the time (Wesseling & Van Wijk, 1957).

2.3.4. Conclusion:

It is seen that among the various conditions considered for the evaluation of drainage requirements, the steady state is the simplest to analyse and apply. Further, in all the conditions considered, the common end product is a calculated drainage spacing S between parallel drains. It is therefore possible to define, for any given condition of drainage, an equivalent steady state condition as being a certain combination of minimum required water table depth and drainage coefficient which would give the same required spacing for effective drainage as the given condition. The Drainage Coefficient in turn is the amount of water that must be removed in a 24 hour period, and therefore, for steady state is synonymous to the application rate.

Thus, the various objectives for a designed drainage system could be used in the evaluation of the drainage requirement but the drainage requirement itself could be expressed in terms of an equivalent steady state criterion. Thus, Bowser (1974) has reported on studies indicating that optimum drainage provisions based on the fluctuating water table conditions for which SEW_{30} values did not exceed 200 cm-days could be obtained if an equivalent steady state with drain [illegible] cm-day [illegible]

minimum groundwater depth = 30 cm were assumed. Adjustments could also be made to the steady state criterion to cater for changes in drainable porosity, which is the volume of water that can be drained from a unit volume of soil.

2.4. POROUS MEDIA FLOW THEORY

To enable the rational assessment of the drainage problem, theoretical approaches have been devised which employ mathematical treatments of the theory of fluid flow in porous media. These theoretical treatments are made possible by introducing simplifying assumptions, many of which are not strictly true for actual field conditions. In spite of these simplifications, however, drainage theories have been found useful in enhancing quantitative judgement through understanding of the principles, and give fairly accurate predictions of the water table conditions provided proper judgement is used in deciding whether the assumptions made in the theoretical derivations correspond to the actual situations encountered in the field.

2.4.1. Basic Equations:

The study of flow of fluids through porous media is a special subject in hydrodynamics. The theory of hydrodynamical analyses has evolved three important relations that are necessary in order to fully describe the motion of a fluid (Lamb, 1932). Firstly, we require a kinematic relation, relating the flow velocity components at various points in space with density. This relation is expressed through statements of mass conservation, and results in the continuity equations. Secondly, we require

a dynamic relation relating momentum with energy of fluid flow at various points of the flow domain. These are expressed through equations of momentum balance, employing Newton's second law of motion for continuous media. By combining the equations for momentum balance and a mass conservation equation, for a small space-element through which fluid moves, using spatial coordinates, the classical dynamic relation used for fluids subject to Newton's law of viscosity are obtained, known as the Navier-Stokes equations.

In vector notation, the Navier-Stokes equations for drainage flow under gravity can be written as

$$\frac{DV}{Dt} = g - \left(\frac{1}{\rho}\right)\nabla P + \frac{1}{3}\left(\frac{\mu}{\rho}\right)\nabla\nabla.V + \left(\frac{\mu}{\rho}\right)\nabla.\nabla V \quad . \quad . \quad . \quad (2.1)$$

where

$\frac{DV}{Dt}$ is the total time derivative of the flow velocity V, with 3 components u. v, w, in the x, y, z directions, respectively, and

$$= \frac{Du}{Dt} + \frac{Dv}{Dt} + \frac{Dw}{Dt}$$

The vector notations are expressed as

$$\nabla P = \partial p/\partial x + \partial p/\partial y + \partial p/\partial z$$

$$\nabla\nabla.V = \frac{\partial}{\partial x}\left(\frac{\partial u}{\partial x} + \frac{\partial v}{\partial y} + \frac{\partial w}{\partial z}\right) + \frac{\partial}{\partial y}\left(\frac{\partial u}{\partial x} + \frac{\partial v}{\partial y} + \frac{\partial w}{\partial z}\right)$$

$$+ \frac{\partial}{\partial z}\left(\frac{\partial u}{\partial x} + \frac{\partial v}{\partial y} + \frac{\partial w}{\partial z}\right)$$

$$\nabla.\nabla v = \left(\frac{\partial^2 u}{\partial x^2} + \frac{\partial^2 u}{\partial y^2} + \frac{\partial^2 u}{\partial z^2}\right) + \left(\frac{\partial^2 v}{\partial x^2} + \frac{\partial^2 v}{\partial y^2} + \frac{\partial^2 v}{\partial z^2}\right)$$

$$+ \left(\frac{\partial^2 w}{\partial x^2} + \frac{\partial^2 w}{\partial y^2} + \frac{\partial^2 w}{\partial z^2}\right)$$

and

ρ = fluid density

p = fluid pressure

t = time

μ = coefficient of viscosity.

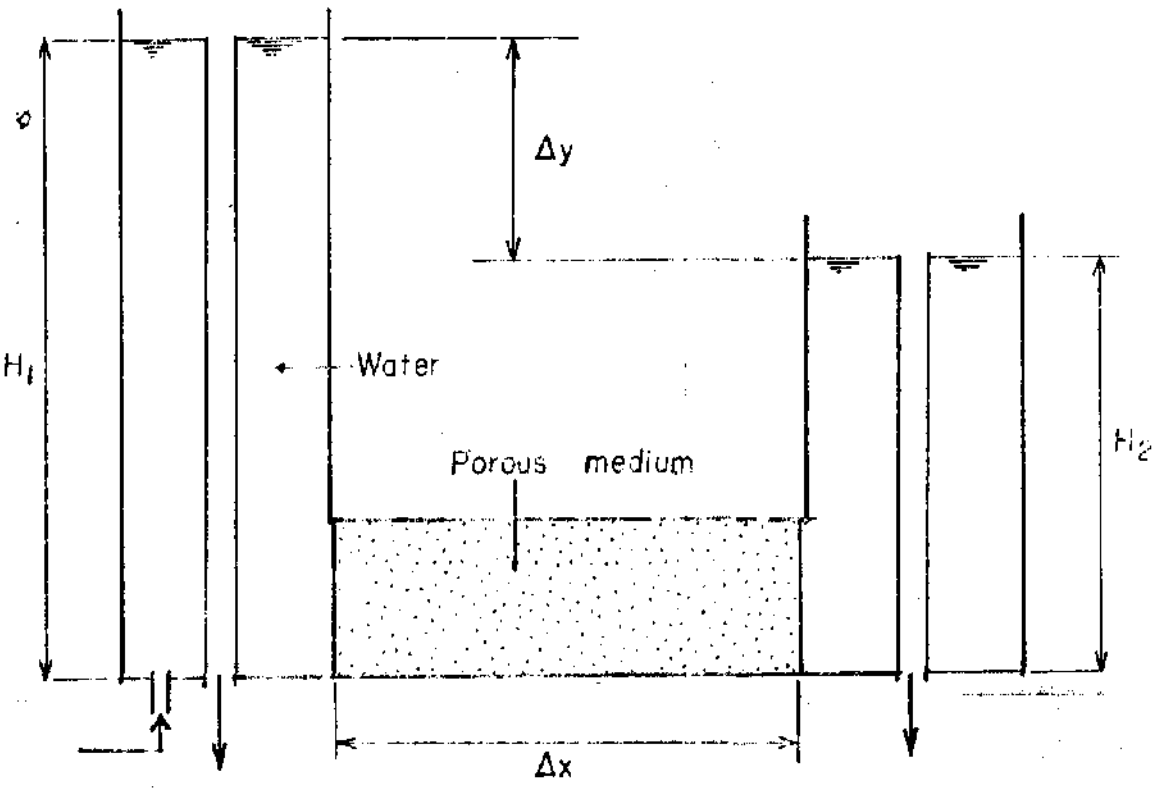
Thirdly, we require a thermodynamic relation which takes the form of equations of state, describing the variation of the fluid's physical properties such as pressure, temperature, and density. For incompressible flow which groundwater flow is normally assumed to be, this takes the form, ρ = constant. In order to solve the Navier-Stokes equations subject to the conditions of continuity and incompressibility, we require, in addition, to identify the external boundaries of the flow domain and the appropriate boundary conditions. At a fixed boundary for instance, the fluid's velocity component perpendicular to the surface must be zero. For flow through a porous medium, identification of the external boundaries of the flow domain would involve the specification of the exact geometry of each pore space. In a medium consisting of natural soil or rock, this is practically impossible except, perhaps, in a statistical sense.

To facilitate practical analyses of flow problems in porous media therefore, simpler equivalent "constitutive equations" are normally used. These are empirical dynamical relations, mostly derived from experimental observations of velocity responses to applied hydraulic gradients.

2.4.2. The Linear Flow Theory:

By far the most widely used of these dynamical relations in the derivation of groundwater flow equations is the experimental law based on the work of Hency Darcy, a French hydraulic Engineer, in 1856. This law was deduced from the results of a large number of experiments on the filtration of water using sand filters. Figure 2.1 shows a schematic diagram of Darcy's experiment.

Fig. 2.1: Schematic diagram of Darcy's Experiment.



In the experiment the water levels H_1 and H_2 at the inlet and outlet of the sand-filled tube of length Δx are kept constant. This experiment seeks to establish a correlation between the discharge of water passing through the porous medium, the difference in water levels $H_1 - H_2 = \Delta y$, and the dimensions of the filter.

Darcy's law postulates a linear relationship between the discharge across a unit area and the hydraulic gradient $\Delta y/\Delta x$; and can be expressed as:

$$V = - k \frac{\Delta y}{\Delta x} \qquad (2.2)$$

in which

V = macroscopic velocity

= discharge per unit cross sectional area

and $\frac{\Delta y}{\Delta x}$ = the hydraulic gradient I causing flow

and k is a material constant normally referred to as the hydraulic conductivity.

Attempts have been made by numerous authors to derive Darcy's law, or more generally the motion equations in porous media from the principles underlying the theory of hydrodynamics. Most of these involve conceptual model approaches to porous media and contain assumptions of negligible inertial forces in comparison with viscous forces in the flow system. Detailed reviews of these have been presented by Bear (1972), and Scheidegger (1960).

2.4.3. Nonlinear Flow Theories:

While Darcy's linear law holds good for most soil conditions containing low velocity flow regimes and in fine grained soils (Todd, 1959), researches over the years (e.g. Anandakrishnan and Varadarajulu, 1963; Arbh-abhirama and Dinoy, 1973;Volker, 1975) have indicated the existence of upper as well as lower limits of applicability of the linear law.

The Reynold's number Re, given by

$$Re = \frac{\rho VD}{\mu} \qquad (2.3)$$

has been used by numerous authors in defining the various flow regimes in porous media. In the equation (2.3),

ρ = density of the fluid

V = macroscopic velocity of flow; and

μ = viscosity of fluid.

D is some characteristic length dimension of the porous medium. Numerous authors (e.g. Muskat, 1937; Todd, 1959) have used the mean particle size as the applicable characteristic length. Others (e.g. Polubarinova - Kochina, 1962) have used the effective grains size D_{10}: i.e. the grain size that exceeds the diameter of 10% of the material by weight. Yet others (e.g. Arbhabhirama and Dinoy, 1973) have suggested the square root of permeability as the representative length dimension. According to Bear (1972), in practically all cases, Darcy's law remains valid as long as the Reynold's number, based on average grain diameter, does not exceed some value between 1 and 10.

Most early explanations as to why Darcy's law ceases to apply at higher flow regimes have employed the analogy with flow through straight or tortuous tubes. Thus, the failure of Darcy's linear law was seen as signifying the start of turbulence in flow through granular media in the same way that the failure of the Hagen-Poiseulle pipe-flow law signifies the onset of turbulence in pipes. However, in an experiment using 2.3 cm size gravel and a hot-wire anemometer arrangement for measurements of velocity and turbulence fluctuations, Wright (1968) found that although flow velocities began to deviate from Darcy's linear law

at Re = 2, the flow was substantially free from turbulence until Re exceeded a minimum of 90, reaching as high as 120. Schneebelli (1955) and others have also found the critical Re for onset of turbulence to be at least 60. In other words, non-Darcy laminar flow occurs in the Reynold's number range from a minimum of 1 - 10 to a maximum of 60 - 120.

Forchheimer, in 1901, in his original experimental study suggested that at high flow velocities, pressure is exercised by the seeping water upon the grains of the medium, making them more tightly pressed against each other, thus affecting the flow passages and the amount of flow through them (Leliavsky, 1965).

Various authors have identified a number of regimes of flow through porous media on the basis of the velocity gradient relationship in those zones. In a typical review, Basak (1977) noted five possible zones of flow regimes for any type of soil. These are:

(i) The no-flow zone:
which occurs only in media of high colloid content such as dense clays. Surface forces are strong enough to counteract the applied hydraulic gradient up to a value known as threshold or initial gradient. Irmay (in Bear et al, 1968) mentions that for clay soils the initial gradient may exceed 30. He attributes this phenomenon to the rheological non-Newtonian behaviour of water.

(ii) The non-Darcy prelinear zone:
in which interaction between strong negative charges on clay particles and the dipolar water molecules causes the velocity-gradient response to be non-linear.

(iii) The Darcian laminar regime:
The zone of linear seepage law; in which the effects of surfaces forces are not felt and the influence of inertial forces are negligibly small compared to viscous forces.

(iv) The non-Darcian post-linear-laminar zone:
Also known as the transition or steady inertial regime. Flow is still laminar but a gradual increase in inertial forces makes the flow deviate from Darcian linearity.

(v) Non-Darcy post linear turbulent zone:
where the applied hydraulic gradient is substantially dissipated in overcoming inertial forces and the rate of velocity gain hence becomes much less than the increase in hydraulic gradient.

Basak (1977) however notes that the existence and range of each of the above mentioned zones vary widely with soil types. The first two zones are almost exclusively found in clay soils.

The non-Darcy post linear laminar zone has been of particular interest to studies of non-Darcy flow regimes. Flows in this zone may be found in [illegible] aquifers, coarse grained soils, rock fill bunk, [illegible], unconsolidated aquifers under high [illegible] gradients [illegible] [illegible]

to open water bodies such as streams or wells, and in flow in filters.

Various flow equations have been proposed to describe the variation of flow velocities with applied hydraulic gradients in this region. Reviews of several of these equations are available in texts (e.g. Scheidegger, 1960; Bear, 1972). Most of these equations can be grouped under two broad forms, which are the most widely used non-Darcy flow equations:

1. The Izbash flow equation, which is of the form

$$V = MI^n \qquad (2.4)$$

in which

V = macroscopic velocity

I = hydraulic gradient

M = material constant with same dimension as hydraulic conductivity, and

n = a non-Darcy exponent varying between ½ and 1.

2. The Forchheimer equation, which reads

$$I = aV + bV^2 \qquad (2.5)$$

in which

I, V are as defined above and a, b are constants determined by the properties of the fluid and medium.

"a" is referred to as the coefficient of linear resistivity and has a dimension inverse to that of hydraulic conductivity and b is called the coefficient of quadratic resistivity. The coefficients a and b are theoretically dependent on the Reynold's number but may normally be assumed constant over a range of Reynold's numbers (Volker, 1975).

Typical values of a and b under different experimental conditions have been reported by numerous authors for different materials (Ahmed and Sunada, 1969; Arbhabhirama and Dinoy, 1973; Volker, 1975; Basak, 1976). A dimensionless nonlinear parameter defined as $C = b/a^2$ characterises the non-linearity in the flow relation. The higher the nonlinearity in the flow relation, the higher will be the parameter C. For sand, the value of C is reported to lie between 0.01 to 0.1. For more coarse media and higher flow regimes, C assumes greater values. For instance for gravel it has been reported to be nearly always more than 2.0 (Basak, 1976).

The Izbash equation, though purely empirical in origin, has been used by a number of authors because it can represent the three most common zones, i.e. the pre-linear laminar ($n > 1$, $I < 1$), the linear Darcian ($n = 1$) and the post linear laminar ($n < 1$, $I > 1$). The Forchheimer equation on the other hand was, like Darcy's law originally derived from experimental results of flow in high velocity regimes by Forchheimer in 1901.

Furthermore, the Forchheimer equation has been shown to have theoretical basis. Starting from the Navier-Stokes equations for incompressible fluids, Ahmed and Sunada (1969) employed a porous medium model of a homogeneous and isotropic nature composed of a spatial network of interconnected channels. They then averaged the Navier-Stokes equation over a representative control volume for a one-dimensional macroscopic flow without neglecting the inertial terms. Using the Gauss theorem they obtained an

equation similar to the Forchheimer equation. Irmay (1958) using a similar approach obtained a similar equation but with an additional time dependent term. Irmay's equation which was also the same as that proposed by Polubarinova - Kochina (1952) was of the form;

$$I = aV + bV^2 + C\frac{\partial V}{\partial t} \qquad (2.6)$$

where C is a constant term and the other terms as defined in equation (2.5). The latter author, however, showed that except for the very onset of motion (lasting a fraction of a second) this additional term tends very rapidly to zero.

Volker (1975) presented a numerical solution employing the finite difference method to problems involving unconfined nonlinear flow using the Forchheimer head loss equation and showed that solutions based on the Forchheimer relation agreed better with experimental data than solutions based on Darcy's law especially at large flow rates. Thus, for instance, in an experimental work using gravel (effective size 4.8 mm) in a tank with a central pumping well, a value of K (hydraulic conductivity) was determined for a flow with a discharge of 0.011 m^3/sec. When this value of K was used to predict discharge a discrepancy was obtained of over 50% between the measured and calculated values. The corresponding discrepancy was only 5% when the Forchheimer equation was employed in the calculation.

2.4.3. Experimental Determination of Flow Coefficients:

The principal type of apparatus for the

laboratory determination of flow coefficients of a soil sample is the permeameter. To perform a test with the permeameter a hydraulic gradient is established within the sample and water flows through the soil. For soils with high permeability such as coarse sand or gravel, the constant head permeameter is used (Terzaghi & Peck, 1967) in which the hydraulic head is kept constant and the discharge measured, from which the discharge (macroscopic) velocity is calculated. In contrast, the falling head permeameter used for soils of low permeabilities consists of a vertical column (glass tube) along which water level is allowed to fall, causing flow through the soil sample, and the rate of fall is measured.

The method of collecting data is the same for non-Darcian flow as for the Darcian flow. The hydraulic gradients and the corresponding seepage velocities are measured under different values of constant head. The hydraulic gradient is then plotted against seepage velocity, preferably on logrithmic scales. If the data plot on a straight line with an inclination of 45° the flow would be Darcian. If the angle is different from 45° the flow would be fully turbulent. ($a = 0$). If the data do not fall on one single straight line, the flow would be transitional ($a \neq 0$; $b \neq 0$). (Gill, 1977).

Gill (1977) used a least squares method of analysis of permeameter data to evaluate the coefficients a and b of equation (2.5) for a typical sample of porous medium in which non-Darcy flow takes place. In the method, values

of a and b are calculated such that the sum of the squares of actual deviations of the data points from the calculated curve is minimum. By this approach the expressions for a and b were given thus:

$$a = \frac{\sum_{n=1}^{N} Vn^4 \sum_{n=1}^{N} (Vn\ In) - \sum_{n=1}^{N} Vn^3 \sum_{n=1}^{N} (Vn^2\ In)}{\sum_{n=1}^{N} Vn^4 \sum_{n=1}^{N} Vn^2 - (\sum_{n=1}^{N} Vn^3)^2} \qquad (2.7)$$

$$b = \frac{\sum_{n=1}^{N} Vn^2 \sum_{n=1}^{N} (Vn^2)\ In) - \sum_{n=1}^{N} Vn^3 \sum_{n=1}^{N} (Vn\ In)}{\sum_{n=1}^{N} Vn^4 \sum_{n=1}^{N} Vn^2 - (\sum_{n=1}^{N} Vn^3)^2} \qquad (2.8)$$

in which Vn and In are the various experimental values (N in number) of velocities and hydraulic gradients obtained respectively. Using these expressions, and the permeameter data obtained by Anandakrishnan and Varadarajulu (1963) the values of a and b were evaluated for flow in a constant head permeameter through coarse sand (effective size 3.0 mm) which was identified to be in the transitional regime, as: a = 16.92 s/m and b = 21.54 $(s/cm)^2$.

2.5. SOLUTIONS FOR LINEAR SEEPAGE FLOW

In this section, some typical solutions of seepage flow through soils which are commonly encountered in literature are presented and discussed. These solutions result from the mathematical treatments of the theory of seepage flow through porous media, and, for the case of seepage through soil into drains, are developed for the purpose of determining the shape and position of

the static water table between drains and hence the required spacings between drains under given conditions. Many of these solutions are based on the assumptions of linear seepage law, the Darcy's law. Certain recent studies, however, have focussed on the implications of non-Darcian seepage (e.g. Gill, 1976; Basak, 1977) and will be treated in the next section.

The solutions for seepage flow can generally be classified into two broad groups, viz:

(i) Those that seek mathematically exact solutions to the differential equations and geometrical restraints that are assumed applicable;

(ii) those that use simplifying assumptions to derive results that apply approximately to field conditions.

Some typical instances of both classes of solutions and their theoretical bases are presented in the following sub-sections.

2.5.1. The Hodograph Solution:

The hodograph solutions result from a special application of the theory of comformal mapping which utilizes properties of analytic complex variables. The basic advantage of the hodograph method of solution arises in unconfined flow problems in which the saturated flow region is bounded along the upper side by the free surface, the shape and situation of which are not, as a rule, known before hand.

In the method, the free groundwater surface, referred to as the z-plane is mapped unto a hodograph plane, the w-plane, where w is a selected analytic function of z. The corresponding boundary condition on the w-plane (the hodograph plane) becomes simplified and well defined, reducing to a circle segment of known parameters in the case of steady precipitation. The procedure then determines the function relating the z-plane to the w-plane map. In this way, the floating (unknown) boundary conditions of the initial problem become fixed boundary conditions after a hodograph transformation is made.

Among the early uses of the hodograph theory was the work by Muskat (1937). Similarly, Polubarinova - Kochina (1962) used it extensively to analyse, among others, seepage from ditches, and confined flow under impervious dams. Engelund (1957) also used it for the analysis of drainage of homogeneous soils. The hodograph method provides exact mathematical solutions, but its use as applied to drainage flow problems leads to extremely complex analysis.

2.5.2. Infinite Series Solutions:

The infinite series solutions have been presented by numerous authors, prominent among whom was Kirkham (1958) who provided an exact mathematical solution for seepage of steady and uniform rainfall into a homogeneous soil drained by parallel tiles or ditches. In his analysis, Kirkham (1958) employed a rectangular model of flow (see Figure 2.2) bounded by ABCE as shown, and the

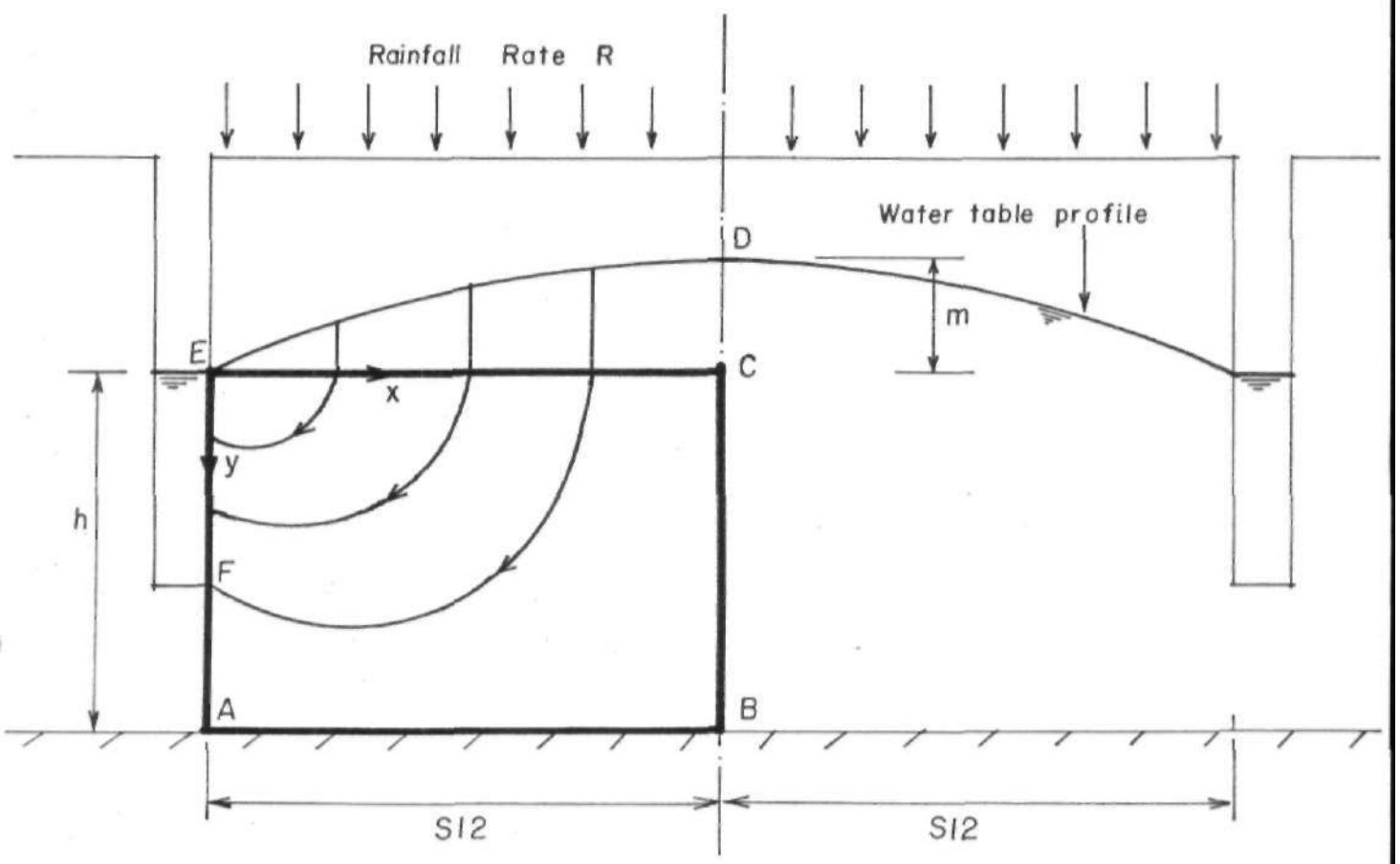


FIG. 2.2: Analysis of flow to drains using potential theory. (Kirkham, 1958)

centre line DB was effectively converted into an impervious vertical boundary.

Kirkham based his solutions on the physical assumption that the head loss along the arched region EDCE is negligible compared with that for the remainder of the flow region. This has the implication that the streamlines of flow can be assumed to be equally spaced along EC and also to be strictly vertical above the line EC. He then sought to find expressions for the stream function Ψ and potential function ϕ for the water seeping into drains, which satisfy the laplace equations of flow, viz:

$$\frac{\partial^2 \Psi}{\partial x^2} + \frac{\partial^2 \Psi}{\partial y^2} = 0 \qquad (2.9)$$

$$\frac{\partial^2 \phi}{\partial x^2} + \frac{\partial^2 \phi}{\partial y^2} = 0 \qquad (2.10)$$

and the relevant boundary conditions. From these, expressions were sought for the height of the water table along the arch shaped water table profile.

The boundary conditions for the stream function Ψ were formulated along the following observations:

1. From E to C the stream function Ψ rises linearly from zero at E to a maximum value Ψ_o at C.
2. The extreme streamline is CBAF; entering the soil midway between the ditches and leaving it at the bottom of the ditch, F. The stream function is therefore constant along CB, BA, AF, and is equal to Ψ_o.

3. From F to E, the stream function ψ decreases linearly from the value ψ_o at F to zero at E.

By inspection, expressions for ψ and ϕ which satisfied these boundary conditions along with the laplace equations were written in the form of infinite Fourier series, for a number of different types of drainage outlets. From the expression of the potential function, formulae for the hydraulic head were deduced. Kirkham's final expression for the maximum level of water table midway between the drains was written as

$$m = \frac{2sR}{K} F_k \left(\frac{2r}{2s}, \frac{h}{2s}\right) \qquad (2.11)$$

= maximum level of water table above the drain axes, in which

s = semi-spacing of the drains

= ½ the drain spacing, S

R = rate of steady precipitation

K = hydraulic conductivity of the soil

F_k is a function of $(\frac{2r}{2s})$ and $(\frac{h}{2s})$, given by the expression

$$F_k = \frac{1}{\pi}\left[\ln \frac{2s}{\pi r_o} + \sum_{m=1}^{\infty} \frac{1}{m}\left(\cos \frac{m\pi r}{s} - \cos m\pi\right)\left(\coth \frac{m\pi h}{s} - 1\right)\right] \cdots (2.1$$

in which

h = depth of impervious layer below the axes of the tile drains (or below water level in ditch drains).

The resulting equation is also applicable for ditch drainage systems (Kirkham et al, 1974) if the width of the ditch bottom is substituted for 2r, and the depth of the impervious layer below the ditch water level for h.

If, however, the hydraulic head loss along the arched region EDCE is significant, then m is no longer negligible compared to h. To correct for this possible deviation from his original assumption, Kirkham in a subsequent study (Kirkham, 1961) proposed a correction factor of $(1-R/k)^{-1}$, to be applied to m obtained in the equation (2.12), in order to obtain the expected upper limit of m under such conditions.

For ease of determination of the function F_k, charts were subsequently prepared by Toksoz and Kirkham (1961), based on the earlier works of Kirkham, relating F_k with the various values of $(\frac{2r}{2s})$ and $(\frac{h}{2s})$.

The mathematically exact drainage equations, due to their complexity are only used occasionally, in evaluating the validity of simpler, more approximate methods. As noted by Van Schilfgaarde (1970) approximate solutions are frequently preferred as long as their limitations are clearly understood. Some of these approximate solutions are presented below:

2.5.3. Dupuit-Forchheimer (D-F) Theory Solutions:

One peculiar difficulty in the analyses of drainage in unconfined flow systems is the presence of an upper boundary, the free surface, along which pressure is constant, the shape of which is nonlinear and unknown prior to analysis. In addition the exit of the free surface normally occurs at a slightly higher level than the water level in the ditch thus creating a surface of seepage along the exit face which itself is another

boundary (Muskat, 1937). It then becomes extremely difficult and tedious to find analytical solutions comforming to the above boundary conditions.

The D-F Theory:

About the only method by means of which an exact analytical solution can be derived for these conditions is the hodograph method (Bear, 1972). Employing the hodograph method in the analysis of drainage flow problems, however, leads to extremely complex analyses. This therefore necessitates the use of simplifying assumptions which lead to approximate solutions. The results from these approximations are widely accepted as good enough for practical field conditions where, after all, the various differential equations and boundary conditions which are applied, the assumptions of homogeneity, isotropy, uniformity of recharge, etc., are all in themselves approximate in nature.

The chief and most widely used of such approximations in the treatment of problems of unconfined flow are the Dupuit approximations. These were first used by Dupuit in 1865 resulting from an observation that in most groundwater flows, the slope of the free surface is very small. The Dupuit approximations have been extensively used by numerous authors and have come to be known as the Dupuit-Forchheimer (D-F) theory.

The two basic assumptions in the Dupuit approximation are:

1. For small inclinations of the free surface of a flow system, the streamlines can be taken as horizontal

everywhere in a vertical section.

2. Flow velocity along any vertical section is constant, i.e. independent of the depth, but is proportional to the slope of the free water table.

The D-F theory was also referred to as the "Hydraulic theory" by Polubarinova - Kochina (1962) because the approximation effectively converts the analysis into that of hydraulic flow - defined by analogy with flow in open channels as a mainly 1-dimensional free surface flow. In the hydraulic flow, transversal flow components are considered negligible and streamlines are hence almost parallel to each other. Polubarinova - Kochina used the theory in the analysis of, among others, free surface with infiltration or evaporation.

Muskat (1937) has shown that remarkably accurate results are obtained when the D-F theory is used to determine the flux of seepage, i.e. macroscopic velocity, but that the shape of the free surface, the flow net, and the velocity distribution are generally greatly in error as determined by comparison with more exact theoretical solutions. In this regard, he therefore rejected the theory in its entirely and credited the success of the flux determination to fortuitous coincidence.

Numerous authors have noted how strict application of the Dupuit conditions lead to erronous implications. Kirkham (1967) examined the paradoxes inherent in the theory. Referring to Figure 2.3 which shows a model of rainfall draining through soil into drainage ditches, he noted that if the assumptions in the D-F theory are applied

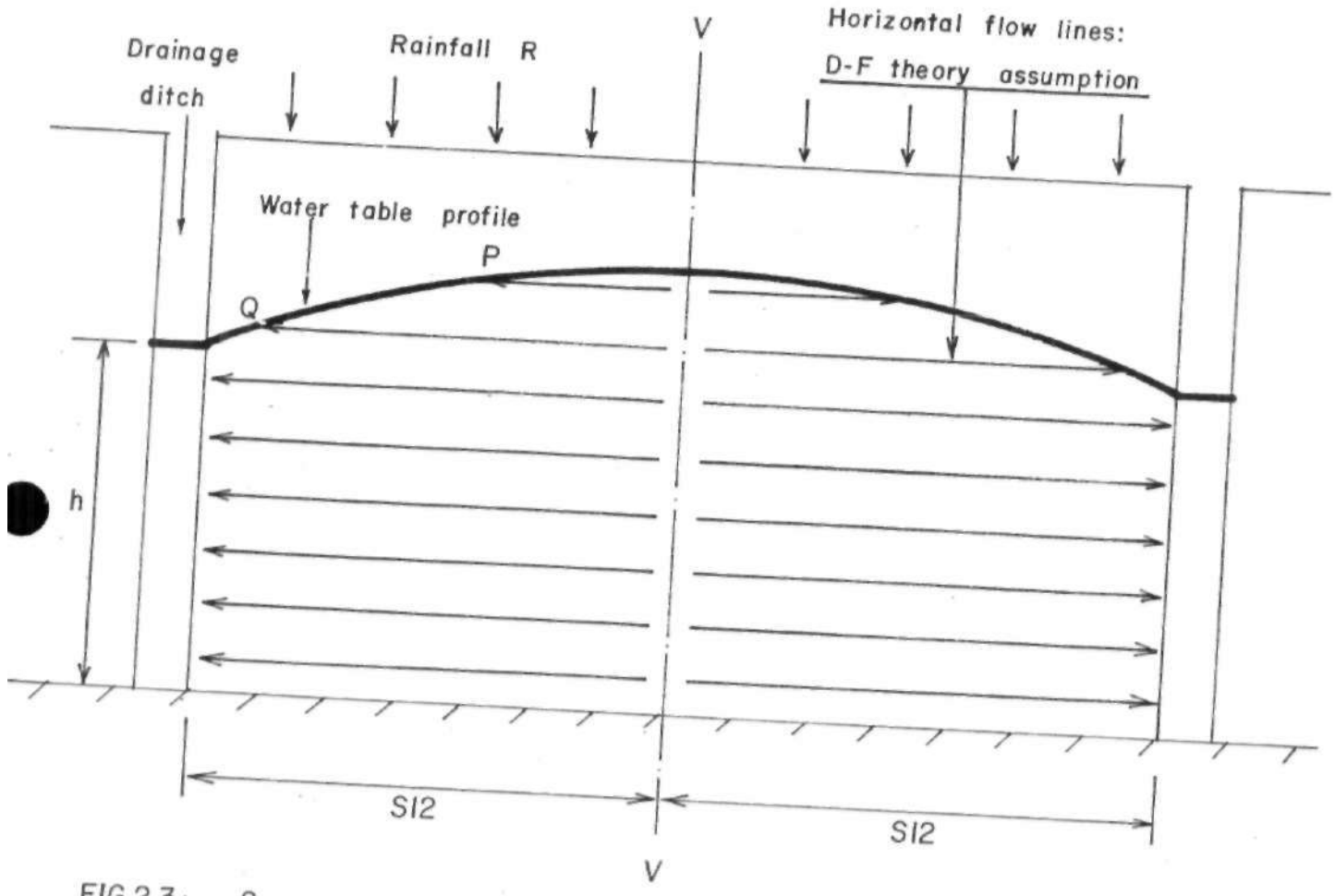


FIG.2.3: Seepage flow towards drains from D-F theory

then streamlines become horizontal everywhere. Two difficulties consequently result, viz:

1. Part of the discharge, e.g. at points P,Q, outlets into the soil rather than the ditches.
2. If the model conditions are strictly applied then the source of the drainage water becomes the vertical plan VV rather than the horizontal plane on the ground surface.

Furthermore, the model based on the D-F theory does not provide for the surface of seepage which should exist at the exit face of the flow above the water level in the ditch.

To explain these paradoxes, Kirkham (1967) proposed a fictitious "slab-slot" or "D-F" model of a soil that contains a large number of vertical, parallel, infinitely permeable, equally spaced, infinitessimally thin slots cut into the soil down to the impervious barrier. He showed that using this model the D-F theory gives correct flux as well as streamlines. However, not all practical soil conditions can be approximated to the fictitious D-F soil. For actual field conditions Kirkham, among other conclusions, noted that:

(i) the D-F theory gives nearly correct streamlines.

(ii) For great values of h, i.e. depth to impervious barrier, the D-F theory gives slightly lower water table heights, i.e. drain spacings must be slightly less than spacings given by the D-F theory in order to establish given water table heights.

(iii) The D-F theory fails completely (gives infinite spacing) when the impervious layer is at infinite depth.

(iv) Equipotential lines in the D-F theory are vertical for conditions of drainage flow.

(v) The D-F theory results in a non-orthogonal flow net.

Kirkham (1958) had, however, shown that theoretical analyses based on a more exact mathematical method free of the D-F theory assumptions reduce, under special conditions of very small free surface inclinations to the results of the D-F theory, and that accordingly, the D-F theory is justified for these conditions. Similarly, Charnii, as reported by Polubarinova - Kochina (1962), avoided the use of the Dupuit-approximations and established the necessary boundary conditions for seepage through an embankment including existence of a surface of seepage. Charnii's result for discharge was identical to that obtained from the D-F theory.

Various other authors (Scheidegger, 1960; Bear, 1972; Glover, 1978) have acknowledged the value of the D-F theory as a helpful tool in the solution of most field problems of unconfined flow. The general consensus so far as the D-F theory is concerned is that its application should be restricted to flow systems that are shallow relative to their aereal extent and that exhibit relatively small curvature of the free surface.

The D-F Theory Solutions:

Analyses of steady state seepage towards drains based

on the D-F theory have been carried out by various authors. Most notable among these is the analysis by Hooghoudt, a Dutch Drainage Engineer, in 1940. Hooghoudt's analysis (see Van Schilfgaarde, 1957; Luthin, 1973) is based on the condition of Figure 2.4, showing a homogeneous soil of known hydraulic conductivity k with an impermeable horizontal barrier underlying it. Apart from the D-F theory assumptions, Hooghoudt made the following further assumptions:

1. Darcy's law is valid for flow through the soil.
2. Soil is homogeneous and of uniform hydraulic conductivity K;
3. The drains are parallel and evenly spaced at distances S apart.

From the Figure 2.4, it is evident that a plane at the centre line between the two drains is a diversion plane for the flow system, across which no horizontal flow occurs. All the water entering the soil to the right of this plane flows into the right drain and similarly all the water on the left goes to the left drain. Effectively, therefore, the centre line can be represented as an impervious boundary for each of the two symmetrical halves.

From continuity of flow, the quantity of per unit length of drain moving horizontally across a vertical plane EB located at distance x from the origin is:

$$q = K(\frac{S}{2} - x) \qquad (2.13)$$

If V = macroscopic velocity, here for incompressible porous media, and from Fig. 2.4,

$$q = V.y \qquad (2.14)$$

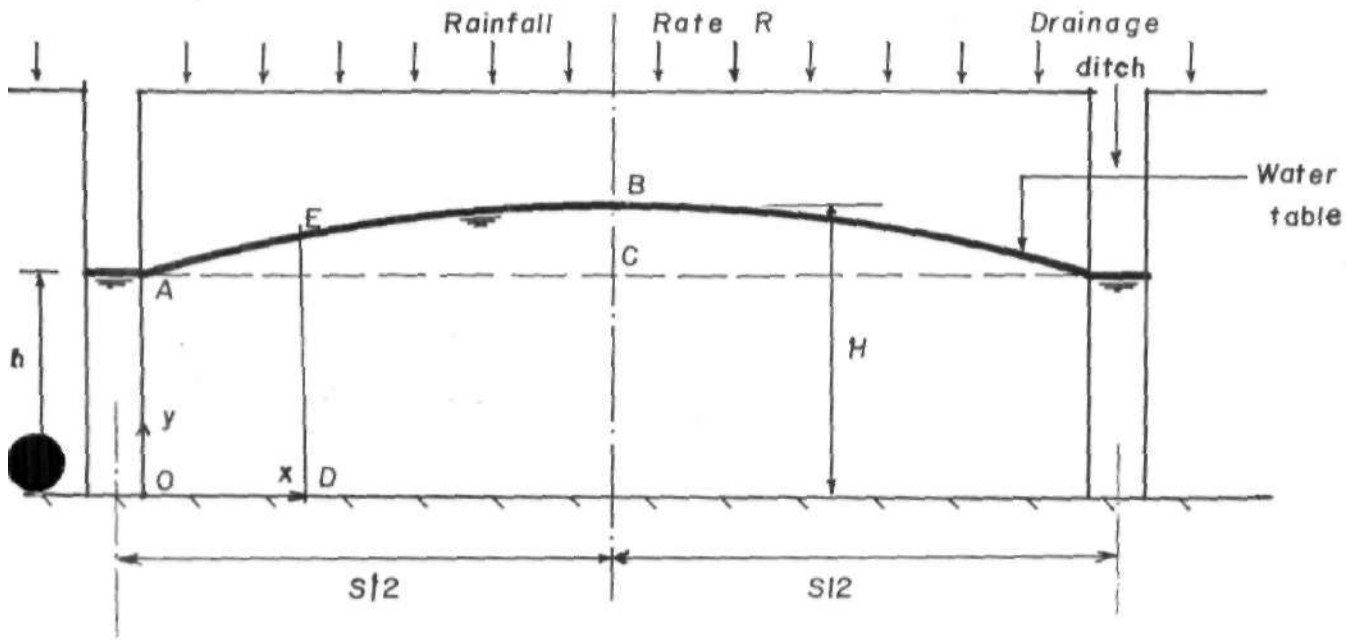


FIG 2.4: Seepage of steady rainfall into parallel ditch drains.

which from Darcy's law and the D-F assumptions, becomes

$$q = y.k.\frac{dy}{dx} \qquad (2.15)$$

Combining equations (2.13) and (2.15)

$$(\frac{S}{2} - x)R = ky.\frac{dy}{dx}$$

and rearranging

$$(\frac{S}{2} - x)Rdx = kydy \qquad (2.16)$$

Integration of equation (2.16) gives

$$R.\frac{S}{2}x - R\frac{x^2}{2} = k\frac{y^2}{2} + C \qquad (2.17)$$

Applying the boundary condition

$$y = h \text{ at } x = 0$$

gives finally the equation

$$RSx - Rx^2 = k(y^2 - h^2) \qquad (2.18)$$

which is the equation of an ellipse. The same equation was also derived by Aronovici and Donnan (1946).

Similarly, applying the second boundary condition, $y = H$ at $x = s/2$; gives the equation:

$$S^2 = \frac{4k}{R}(H^2 - h^2) \qquad (2.19)$$

Equation (2.19) is the drain spacing formula for S. H is the maximum water table height occurring midway between drains. A similar expression was also obtained by Kirkham (1958) for the case when $\frac{h}{S} \to \infty$.

It is customary for the equation (2.19) to be rearranged as follows:

$$S^2 = \frac{4k}{R}(H + h)(H - h)$$

recognising that $H - h = m$ and $H + h = 2h + m$; the expression becomes

$$S^2 = \frac{4k}{R}(2h + m)m, \text{ or } S^2 = \frac{4km}{R}(2h + m) \qquad (2.20)$$

The drain spacing formula is used in a form similar to equation (2.20) in drainage design using the drainage coefficient method (Bouwer, 1974).

It has been noted by a number of authors (Van Schilfgaarde, 1957) that the application of the ellipse equation to tile rather than open ditch drains introduces little or no error especially if drains are installed near the impervious layer. Often the back filled trenches retain a higher permeability than the undisturbed material so that tile drains act essentially as open ditches.

2.5.4. Hooghoudt's Correction Solution:

Hooghoudt developed a correction solution for cases when the drain is not on the impervious layer or when the depth h in Figure 2.4 is great.

When the drain lies above the impervious layer, flow occurs into the drain from below the drain axis which is radial in nature similar to the radial flow into a well. This flow is neglected by the D-F theory.

The pressure head potential ϕ of a point about a well axis in a homogeneous medium is written (Todd, 1959) as:

$$\phi = \frac{Q}{2\pi k} \ln r$$

and hence for a semi-circular flow region below the drain axis,

$$\phi = \frac{Q}{\pi k} \ln r$$

where

Q = uniform flow into drain per unit length of drain

r = distance of point from the drain axis; and

k = hydraulic conductivity;

and for N parallel tiles:

$$\phi = \frac{Q}{\pi k} \sum_{1}^{N} \ln r_n \qquad (2.21)$$

It is thus possible to determine in this way the potential difference $\Delta\phi$ between two points A and B, with A on the drain surface and B midway between two drains. (See Figure 2.5) as:

$$\Delta\phi = \phi_B - \phi_A$$

$$= \frac{Q}{\pi k}\left(\sum_{1}^{N} \ln r_{BN} - \sum_{1}^{N} \ln r_{AN}\right) \qquad (2.22)$$

in which r_{AN} and r_{BN} are the distances from points A and B respectively to the various tiles (N in number).

Hooghoudt used this approach to consider the case of uniform rainfall removed by parallel drains. Uniform rainfall was represented as an indefinite number M of line sources in the plane through the drain axis spaced evenly apart, each of equal strength Q/M. The expression for the potential difference between the drain surface and the centre line between drains was determined in the form of equation (2.22), which was subsequently reduced to the form:

$$\Delta\phi = \frac{Q}{\pi k}\left[\ln\left(\frac{S}{r_o}\right) - 0.454\right] = \frac{Q}{k}.A \qquad (2.23)$$

where A was a constant whose value for various drainage conditions was tabulated by Hooghoudt.

However, assumptions of radial flow towards drains as illustrated above, fail progressively in error with decreasing h, and for the extreme case when the drain lies on the impervious base (h = o) the analysis fails completely

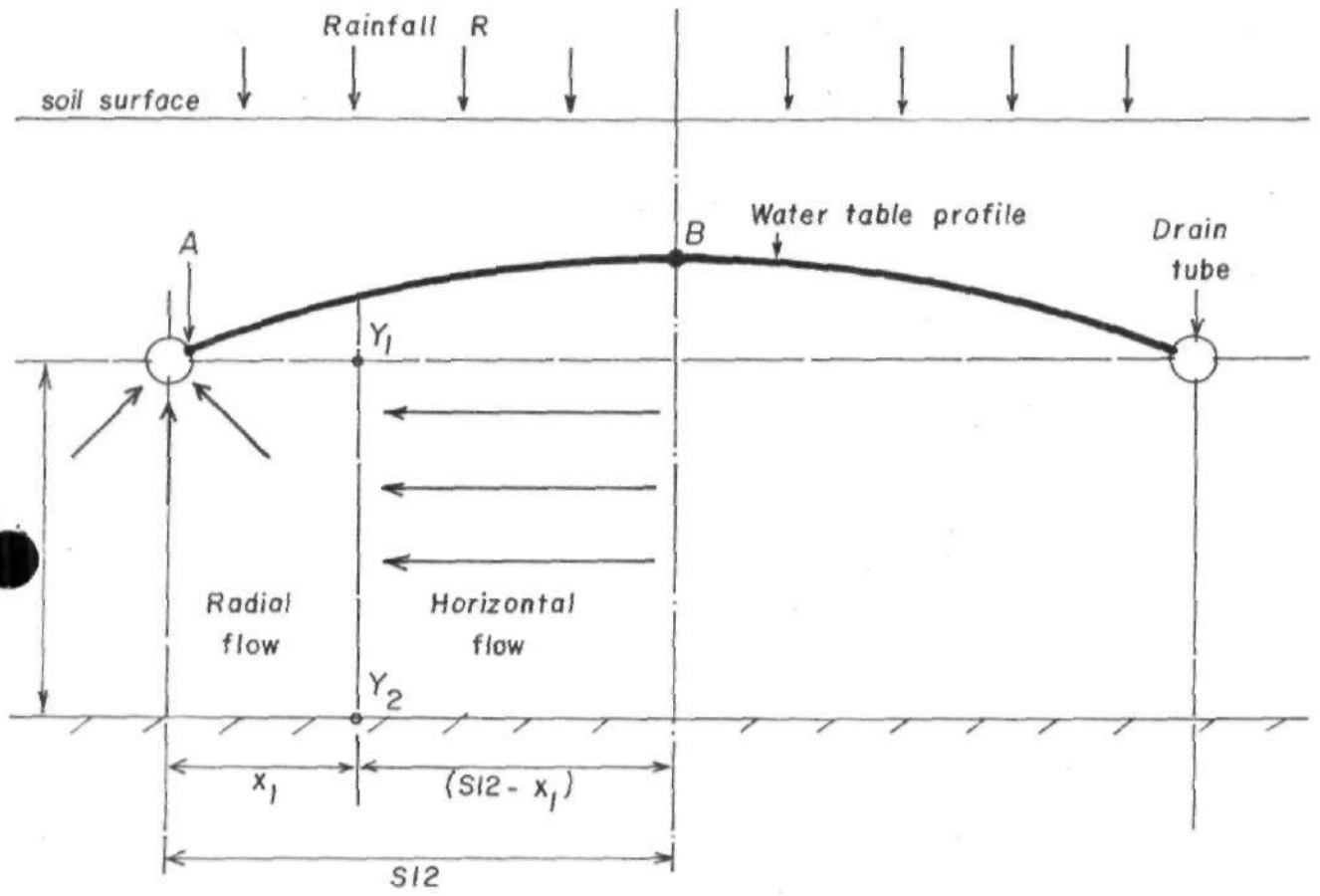


FIG 2.5: Combining radial and horizontal (D-F) flow assumptions (Hooghoudt, 1940).

In other words, both the D-F theory assumption of horizontal flow and the radial flow assumption fail completely at two opposite extremes (of small h and large h) and neither of the two yields satisfactory results for intermediate depths. Hooghoudt sought a correction solution by combining the two assumptions. He assumed that the flow in the region near the midpoint between drains is horizontal, and that in the region near the drain is radial and the two regions are separated by a vertical plane YY at a distance X_1 selected such that the potential difference $\Delta\phi$ between the upper and the lower points of the plane (Y_1 and Y_2 in Fig. 2.5) is a minimum, i.e. causing the plane to be nearly an equipotential, as it should be for the D-F assumptions to apply. This turned out to be the plane $X_1 = \frac{h\sqrt{2}}{2}$

Determining the potential differences through the two regions using the relevant equations and summing together the difference in potential between the drain surface and the centre line, the result was written in terms of an infinite series and then simplified in terms of two constants B and C as follows:

$$\Delta\phi = \frac{Q}{k} (B + C) \qquad (2.24)$$

However, instead of working with equations (2.21) - (2.24) above, Hooghoudt considered it more practical to have a formula similar to the ellipse equation (2.20). To account for the extra resistance caused by the radial flow near the drains, he introduced a reduction of the depth h to a smaller equivalent depth d and equation (2.20) then reads:

$$S^2 = \frac{4km}{R}(2d + m) \qquad (2.25)$$

In design based on steady state, R is taken as the drainage coefficient.

The values of d depend on the depth h, the spacing S, and drain radius r_o (or width of drainage ditch $2r_o$). Various values of d for different values of h, S, r_o have been presented in extensive tables originally due to Hooghoudt in 1940. To further simplify the determination of d, graphical and/or analytical methods have been presented (Moody, 1966).

Wesseling (1964) has compared the Hooghoudt solution with that of Toksoz and Kirkham (1961) and found that for practical field conditions, the two never differed by more than 5%.

2.5.5. Dagan's Solution:

Dagan (1964) in an analysis of flow to different types of drains located at finite depths combined two methods of approximate solution, viz:

1. The D-F theory assumptions, which he applied in the region near the centre line between drain. The drawdown in this region was thus calculated using the ellipse equation.
2. Linearization of the non-linear flow differential equation (2.26) which is applicable to the free surface of the groundwater table, by neglecting the quadratic terms against the remaining ones. The non-linear equation is:

$$\left(\frac{\partial \phi}{\partial x}\right)^2 + \left(\frac{\partial \phi}{\partial y}\right)^2 - (R + K)\frac{\partial \phi}{\partial y} + KR = 0 \qquad (2.26)$$

The quadratic terms neglected are:

$$(\frac{\partial \phi}{\partial x})^2, \ (\frac{\partial \phi}{\partial y})^2 \text{ and } R(\frac{\partial \phi}{\partial y})$$

where ϕ is the velocity potential.

The equation (2.26) was consequently transformed into:

$$\frac{\partial \phi}{\partial y} = R \qquad (2.27)$$

This approximation is valid for small water table drops. Its solution was used in the calculation of the drawdown in the region near the drains.

Dagan then used the combination of the results of the two methods, for both isotropic and anisotropic soils, in a manner similar to the combination of radial and horizontal flows used by Hooghoudt. His solution was of the general form:

$$\frac{S}{2} \ (\frac{S}{2} - 2\alpha h) = \frac{K}{R} \ (H^2 - h^2) \qquad (2.28)$$

in which α is a parameter which differs from case to case and is dependent on the depth h. Values of α for various conditions were prepared by Dagan.

Dagan's solution generallizes the ellipse equation ($\alpha = 0$) and unlike other solutions, can be adapted, by selecting appropriate values of α, to different cases including non-isotropic soil conditions and drains located below the free surface.

2.6. SOLUTIONS FOR NON-LINEAR FLOWS

Because of results of various research data over the years indicating that laminar flows do exist in numerous soil conditions which do not obey Darcy's law, it now seems to be very desireable to have solutions

of problems of percolation through porous media incorporating velocity gradient relationships representing the Non-Darcy flow zones. Such solutions are, however, relatively few in available literature. A characteristic sample of some solutions based on non-linear infiltration or seepage flows is presented below.

2.6.1. Vertical Infiltration:

Gill (1976) presented an analysis of one-dimensional vertical infiltration using the Forchheimer non-linear velocity - gradient relationship. (equation 2.5). He considered infiltration under constant head as well as falling head of water through a homogeneous isotropic medium with constant hydraulic resistivity.

Under constant head H_o, the hydraulic gradient (dh/dy) at any location y_o of the infiltrated front of water (see Fig. 2.6) can be written as:

$$\frac{dh}{dy} = - \frac{H_o + y_o + h_k}{y_o} \qquad (2.29)$$

in which h_k = capillary head, which also remains constant.

The infiltration velocity V is given as

$$V = m \cdot \frac{dy_o}{dt} \qquad (2.30)$$

where m = porosity of the medium.

Gill combined the above expressions with the Forchheimer head loss equation as:

$$- \frac{dh}{dy} = aV + bV^2$$

to obtain the equation:

$$am\left(\frac{dy_o}{dt}\right) + bm^2 \left(\frac{dy_o}{dt}\right)^2 = \frac{H_o + h_k + y_o}{y_o} \qquad (2.31)$$

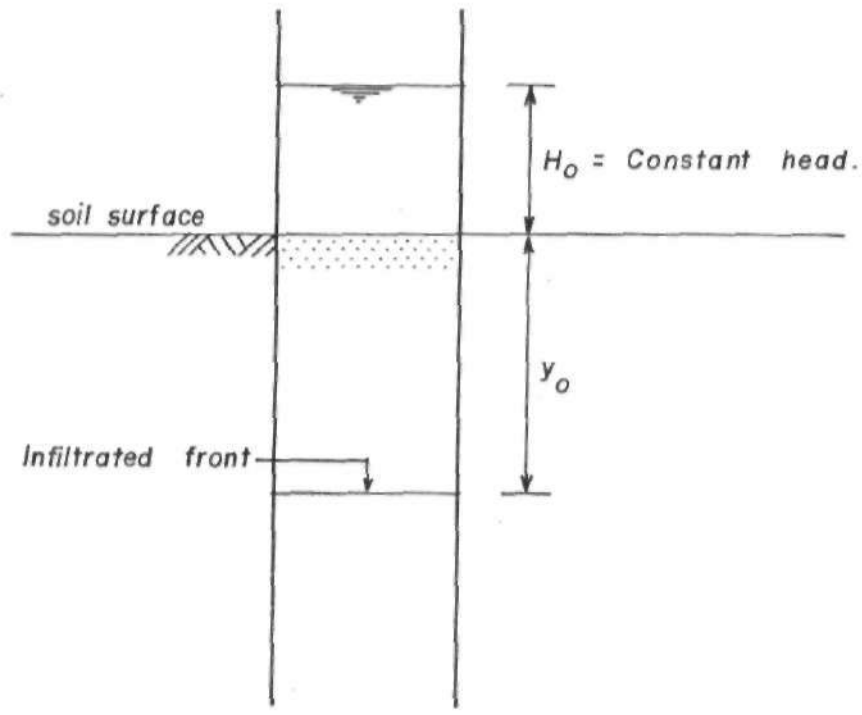


FIG 2.6: One dimensional vertical infiltration (non Darcy flow; Gill, 1976)

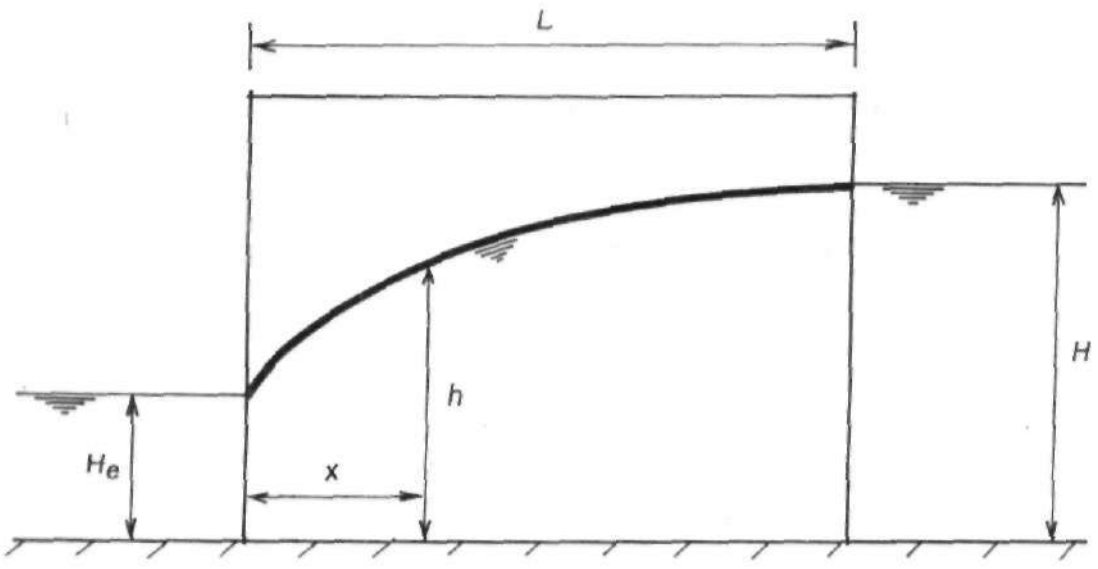


FIG 2.7: Steady non-Darcian seepage through embankment (Basak, 1976)

The derived solutions for non-linear flow, i.e. equations (2.32) and (2.33) showed that lesser time is required for infiltration to equal depths through a material characteristic of non-Darcy flow (e.g. gravel) than for materials characteristic of Darcian flow. Similar trends were established for infiltration under falling head conditions.

2.6.2. Seepage Through Embankments:

Basak (1976) presented a steady state analytical solution for unconfined flow through embankments. He used the Forchheimer non-linear velocity-gradient relationship. The embankment analysed has vertical faces with a horizontal impervious boundary and has dimensions as shown in Figure 2.7.

Combining the continuity equation

$$V = q/h,$$

and the Forchheimer equation

$$\frac{dh}{dx} = aV + bV^2$$

and applying the D-F assumptions, Basak arrived at the equation:

$$\frac{H}{L}\frac{dy}{dx} = \frac{q_*}{y} + C\left(\frac{q_*}{y}\right)^2 \qquad (2.35)$$

in which

V = macroscopic velocity

q = discharge per unit width of embankment

X = x/L

y = h_*/H, and $H_e/H = y_o$

$q_* = aq/H$ and

C = b/a^2

C is a dimensionless non-linear parameter which gives a measure of non-linearity of flow.

Inserting the boundary conditions:

$$X = 0;\ h_* = H_e \text{ and } y = y_o; \qquad X = L;\ h_* = H \text{ and } y = 1 \tag{2.36}$$

the solution to the equation (2.35) gave

$$1 = \frac{H}{L}\left[\left(\frac{1-y_o^2}{2q}\right) - C(1-y_o) + C^2 q \ln\frac{(1+Cq_*)}{(y_o+Cq_*)}\right] \tag{2.37}$$

For Darcian flow, (C = 0) the corresponding equation becomes parabolic, i.e.

$$X = \frac{H}{L}\left(\frac{y^2 - y_o^2}{2q_*}\right) \tag{2.38}$$

The derived solution, i.e. equation (2.37) showed that for the same steady discharge the free surface is higher for non-Darcian flow compared to Darcian flow, and that the non-linear flow solution always predicts lower (and more accurate) discharge for the same drawdown than the corresponding discharge predicted on the basis of Darcian flow. Furthermore, for non-linear flow conditions, the variation of discharge with y_o is no longer parabolic as in the linear flow case. Basak compared the results of his analytical solution with a numerical solution to the same problem, using the finite elements approach used by Volker (1969). There was found to be a close agreement between the two solutions.

2.6.3. Seepage Into Drains:

Basak (1977) presented an analysis of a ditch drainage system with steady precipitation, based on a non-linear seepage law. He used the Izbash non-linear flow

equation (i.e. equation 2.4),

$$V = M(\frac{dy}{dx})^n$$

The continuity equation from Fig. 2.4 was written down as:

$$q = R(S/2 - x)$$

$$= V.y$$

using the D-F assumption, the following equation was derived:

$$Y(\frac{dY}{dX}) = \{\frac{S/2}{H}\}^{n+1}(\frac{R}{M})(1 - X) \qquad (2.39)$$

in which

$$Y = \frac{y}{H} \; ; \; X = \frac{x}{S/2}$$

Inserting the boundary conditions

At $y = h$; $x = 0$

At $y = H$; $x = S/2$

The solution to the equation (2.39) gave the equations for water table profile and drainage spacing respectively as follows:

$$Y^{1+1/n} - Y_o^{1+1/n} = (\frac{R}{M})^{1/n}\{\frac{S/2}{H}\}^{1+1/n}[1-(1-x)^{1+1/n}] \qquad (2.40)$$

$$\frac{S}{H} = (2^{(1-1/n)/(1+1/n)})(\frac{4M}{R})^{1/[n(1+1/n)]}$$

$$* \; (1-(\frac{h}{H})^{1+1/n})^{1/1+1/n)} \qquad (2.41)$$

where $Y_o = \frac{h}{H}$

Thus, it is seen that for Darcy flow ($n = 1$, $M = k$) the equation (2.41) reduces to the ellipse equation for drain spacing, i.e.

$$S/H = (\frac{4M}{R})^{\frac{1}{2}}(1 - (\frac{h}{H})^2)^{\frac{1}{2}}$$

The solution derived by Basak showed that:

- For non-Darcy flow, the shape of the water table between the two ditches no longer remains elliptic.
- In the transitional zone (n < 1) the water table lies above the water table based on Darcian flow assumption.
- For post linear flow regimes (n < 1) drainage spacing would always be greater than that predicted by the equation based on Darcian flow assumption.

2.7. SEEPAGE FLOW MODELS AND ANALOGUES

The use of models and analogues in the study of groundwater flow has been widely practised, as a technique in which the behaviour of fluid flow in a porous medium is reproduced on a different and more convenient scale or form.

2.7.1. Analogues:

Two systems are said to be analogous to each other if there is a one-to-one correspondence between each element in the two systems as well as between the excitation and response functions of these elements and the system as a whole (Boer and Van der Molen, 1972). An analogue and a prototype normally belong to entirely different physical systems. The analogy is based on the similarities between the laws which apply to the two systems. Analogues typically used for seepage flow studies include:

(i) Viscous flow analogues: which are based on the similarity between Darcy's law governing saturated seepage flow and the equation

governing the flow of viscous liquids in the narrow space between two parallel smooth plates (Guitjens, 1974).

(ii) Electric analogues: based on the similarity between Darcy's linear law for flow in porous media and ohm's law, which postulates a linear relationship between the electric current and the voltage gradient.

(iii) Membrane analogues: based on the similarity between Darcy's linear seepage law and the linear stress-strain relationships in an electric membrane (Bear, 1972).

2.7.2. Sand Tank Models:

Models are physical analogues which involve the same physical phenomena as those in the prototype. In a model, every prototype element is reproduced, different only in scale.

The reduced scale models used in groundwater flow studies are known as sand tank or sand box models. The sand tank models, are replications of field conditions, consisting usually of a rigid container filled with a porous medium such as sand, with the geometry of the container corresponding to that of the prototype flow domain. For one-dimensional flow studies such as vertical infiltration, sand columns are most commonly used, consisting of a vertical cylindrical pipe packed with sand. The most common shape for two-dimensional flow models is rectangular. Sometimes symmetry properties of the

to verify theoretical streamlines, using tracer dyes, of flow of water from an artesian basin into horizontal equally spaced circular drains.

Sand tank models are also very valuable in studies of flow situations involving high velocities, where energy losses due to prominence of inertial forces and turbulence create non-Darcy flow conditions. Since all other drainage analogues depend for their analogy with groundwater flow on linear response laws similar to Darcy's law they obviously cannot be used to simulate non-Darcy flow conditions. Thus, Luthin and Haig (1971) performed sandbox model experiments to study conditions in the immediate vicinity of a drain tube where high velocities of flow cause turbulence losses in energy that could not otherwise be predicted. Similarly, Volker (1975) used sand box model for the study of two dimensional as well as axisymmetric flows involving non-Darcy flow regimes.

Sand box models can be used for the study of a variety of other cases involving, among others, steady and unsteady state flows, anisotropic media, inhomogeneous media, hydrodynamic dispersion (miscible displacement) and leaky formations (Bear, 1972).

2.8. SUMMARY

The preceding discussions in this chapter have pointed out the wide possibility of the existence of laminar flows in porous media which do not obey Darcy's law. So far as flows through coarse sand under medium to high gradient goes, published experimental results for the last few decades have indicated that the flow is initially

linear up to a Reynold's number around unity and then enters into the post-linear regime. It therefore seems necessary to have solutions of subsurface drainage flow problems incorporating a velocity-gradient response that is non-linear. Such treatments have been comparatively lacking in the literature.

Accordingly, the next chapter presents an analysis of steady state seepage flow into drains incorporating a non-linear flow equation. Subsequent chapters will present results from sand tank model experiments investigating the validity of the analysis.

CHAPTER THREE

ANALYSIS OF STEADY NONLINEAR SEEPAGE INTO DRAINS

3.1. INTRODUCTION AND ASSUMPTIONS

In this chapter, approximate theoretical formulae are derived for the height of all points of the arch-shaped water-table established by steady non-Darcian seepage through a homogeneous soil into parallel ditch drains. The soil is underlain by an impervious layer at the bottom of the ditch, and the depth of the ditch is shallow in comparison with the horizontal spacing between the drains. The drains are equally deep with equal water levels in them. Figure 2.4 shows a definition sketch of the problem.

In the figure, parallel ditch drains in the soil remove ground water at a steady rate equal to that of a steady precipitation. The ditches have water in them up to the level A where the water table AB intercepts them. A surface of seepage at A is neglected. The slope of the ground water table is zero at the centre-line, about which the flow system is symmetrical. Consequently, the velocity component perpendicular to the centre line is zero, and the centre line becomes analogous to a vertical impervious boundry. The following further assumptions are made:

(1) The non-Darcy flow regime follows the Forchheimer head loss equation, i.e.

$$I = av + bv^2 \quad \frac{dy}{dx}, \qquad \text{----------(3.1)}$$

where v = microscopic velocity, and the coefficients of flow resistivity a and b remain constant.

(2) The water table has small curvature, the distance BC is very small in relation to AC and hence the D-F assumptions are approximately true.

(3) The porous medium is homogeneous and isotropic and the precipitation rate, R m/s is steady and uniform.

These assumptions have been most frequently used for analyses of Darcian seepage to drains and found to yield valid results for practical purposes. It is believed that they will hold good for non-Darcy flows as well.

The x-axis as shown in Figure 2.4 shall be the reference level for hydraulic head.

3.2. CONTINUITY OF FLOW

With reference to the Figure 2.4 and from the continuity of flow, the quantity of flow q per unit length of ditch moving horizontally across a vertical plane DE located at a distance x from the origin is:

$$q = R(S/2 - x) \qquad \text{----------(3.2)}$$

Similarly, for incompressible porous media,

$$q = vy, \qquad \text{----------(3.3)}$$

where y = the vertical distance ED.

Combining the above two equations (3.2) and (3.3) gives

$$v = \frac{R}{y}(S/2 - x), \qquad \text{----------(3.3a)}$$

Substituting equation (3.3a) into equation (3.1) gives

$$\frac{aR(S/2 - x)}{y} + \frac{bR^2(S/2 - x)^2}{y^2} = \frac{dy}{dx}$$

thus yielding the homogeneous equation

$$-\frac{dy}{dX} = P\frac{X^2}{y^2} + Q\frac{X}{y}\ , \qquad \text{----------(3.4)}$$

in which

$$X = (S/2 - x) \qquad \text{----------(3.4a)}$$

and hence dx = - dX and P and Q are the dimensionless coefficients of quadratic and linear resistivity respectively, i.e.

$$\left.\begin{aligned} P &= bR^2 \\ Q &= aR \end{aligned}\right\}\ , \qquad \text{----------(3.4b)}$$

The equation (3.4) is nonlinear but due to its homogeneous nature, its solution can be sought analytically.

If we put $u = y/X$; or $y = uX$, ----------(3.5a)

i.e. $\frac{dy}{dX} = u + X\frac{du}{dX}$, ----------(3.5b)

then equation (3.4) becomes

$$-\frac{dy}{dX} = \frac{P}{u^2} + \frac{Q}{u}$$

or $$\frac{dy}{dX} = \frac{-(P + Qu)}{u^2}\ , \qquad \text{----------(3.6)}$$

Combining equations (3.5b) and (3.6) gives

$$\frac{-(P + Qu)}{u^2} - u = X\frac{du}{dX}\ , \qquad \text{----------(3.7a)}$$

Rearranging the above equation gives

$$\frac{-(P + Qu + u^3)}{u^2} = X\frac{du}{dX}, \qquad \text{----------(3.7b)}$$

or

$$\int \frac{u^2\,du}{(P + Qu + u^3)} = -\int \frac{dX}{X}\ , \qquad \text{----------(3.7c)}$$

The integral on the LHS of equation (3.7c) can be evaluated by resolving into partial fractions. For this

the conditions.

Thus we can now resolve the LHS of the equation (3.7c) into partial fractions as follows:

$$\int \frac{u^2\,du}{(Q + Qu + u^3)} = \int \frac{udu}{(Q + u^2)}$$

$$= \int \frac{A\,du}{u + i\sqrt{Q}} + \int \frac{B\,du}{u - i\sqrt{Q}}$$

$$= \int \frac{udu}{(u + i\sqrt{Q})(u - i\sqrt{Q})}\,, \qquad \text{----------(3.9a)}$$

The constants A and B are determined from

$$u = A(u - i\sqrt{Q}) + B(u + i\sqrt{Q}), \qquad \text{----------(3.9b)}$$

giving $A + B = 1;$ ----------(3.9c)

and $-Ai\sqrt{Q} + Bi\sqrt{Q} = 0,$ ----------(3.9d)

equation (3.9d) => A = B

and therefore from equation (3.9c)

$A = \frac{1}{2}$ and $B = \frac{1}{2}$

Substituting these values into (3.9a) and reverting back to equation (3.7c) gives

$$\tfrac{1}{2}\int \frac{du}{(u + i\sqrt{Q})} + \tfrac{1}{2}\int \frac{du}{(u - i\sqrt{Q})} = -\int\frac{dX}{X}, \qquad \text{-----(3.9e)}$$

Integration gives

$$\tfrac{1}{2}\log(u + i\sqrt{Q}) + \tfrac{1}{2}\log(u - i\sqrt{Q}) = -\log X + C_1$$

Rearranging the above expression gives successively the following:

$$(u^2 + Q)^{\frac{1}{2}} = C_2/X$$

$$u^2 + Q = C_3/X^2$$

$$u^2X^2 + QX^2 = C_3, \qquad \text{----------(3.9f)}$$

C_1, C_2, C_3, are all various constants assuming different values.

Substituting the expression u = y/X of equation (3.5a); equation (3.9f) becomes

$$y^2 + QX^2 = C_3, \quad \text{----------(3.9g)}$$

Equation (3.9g) is an equation of an ellipse, and since X = (S/2 - x), then it represents an ellipse with an axis of summetry at x = S/2, i.e. the centre line. According to Van Schilfgaarde (1970), it was first derived, albeit in a somewhat different manner by Colding in 1872 and later, apparently independently by a number of other workers including Hooghoudt in 1937.

Returning to equation (3.9g) and substituting back the expression (3.4a) we obtain

$$y^2 + Q(S/2 - x)^2 = C_3, \quad \text{----------(3.10a)}$$

To obtain C_3 we substitute the boundary condition

$$y = h \text{ at } x = 0$$

$$\therefore \quad C_3 = h^2 + Q(S/2)^2$$

and hence (3.10a) becomes

$$y^2 + Q(S/2 - x)^2 = h^2 + Q(S/2)^2, \quad \text{-------(3.10b)}$$

Rearranging, we obtain

$$y^2 - h^2 = Q(Sx - x^2), \quad \text{----------(3.10c)}$$

Inserting the second boundary condition;

$$y = H \text{ at } x = S/2$$

and simplifying, the expression for drainage spacing is obtabined as:

$$S^2 = \frac{4}{Q}(H^2 - h^2), \quad \text{----------(3.11)}$$

In Darcy flow literature the above expression is

encountered as

$$S^2 = \frac{4k}{R}(H^2 - h^2), \qquad \text{---------(3.11a)}$$

where k = hydraulic conductivity

= 1/a

Equations (3.10c) and (3.11) are also written as:

$$(\frac{y}{h})^2 - 1 = Q.(S/h)(x/h) - Q\,(x/h)^2, \qquad \text{---(3.10d)}$$

$$(\frac{S}{h})^2 = \frac{4}{Q}[(H/h)^2 - 1], \qquad \text{----------(3.11b)}$$

$$(\frac{S}{H})^2 = \frac{4}{Q}[1 - (h/H)^2], \qquad \text{----------(3.11c)}$$

3.4. TRANSITIONAL NON-DARCY FLOW

For transitional non-Darcy flow regimes, $a \neq o$; and $b \neq o$ and hence $P \neq o$.

Recall from (3.4b) that $P = bR^2$ in which R = precipitation or drainage rate in metre depth per second.

Typical values of R(m/sec) are normally extremely small. For instance, a 5 cm rainfall storm of 1 hour duration gives

$$R = \frac{5/100}{3,600} = 1.39 \times 10^{-5} \text{ m/sec.}$$

Reported values of b range from the high range of about 7450 $(s/m)^2$ for sandy material to the lower ranges around 10 - 20 $(s.m)^2$ for gravel material (Basak, 1976; Arbhabhirama and Dinoy, 1973). Values of a on the other hand range between about 700 s/m for sand to below 10 (s/m) for coarse gravel. Values of $P = bR^2$ would therefore normally be very small in relation to the values of Q and the distance measures of x and y.

It would therefore be possible to determine a first order approximation of the roots of the polynomial f(u) in equation (3.7d). We base the approximation on the three roots of f(u) for the case P = 0 (see (3.9)) which were 0, $\pm i\sqrt{Q}$.

When $P \neq 0$, but is small, it induces small changes in the values of the roots as they existed for P = 0. They would now become

$$\alpha, \beta \pm i\sqrt{Q}$$

where α and β are also small, perhaps of the order of P (or Q). Thus we assume

$$\left.\begin{aligned} u_1 &= \alpha \\ u_2 &= \beta + i\sqrt{Q} \\ u_3 &= \beta - i\sqrt{Q} \end{aligned}\right\}, \quad \text{----------(3.12)}$$

If these roots are to satisfy the equations (3.8a) and (3.8b), then:

(a) $u_1 + u_2 + u_3 = 0$, i.e.

$$\alpha + 2\beta = 0$$

$$\Rightarrow \beta = -\alpha/2.$$

(b) $u_1u_2u_3 = P$, i.e.

$$\alpha(\beta + i\sqrt{Q})(\beta - i\sqrt{Q}) = P$$

$$\Rightarrow \alpha(\beta^2 + Q) = P$$

Neglecting higher orders (of α, β), this gives

$$\alpha Q = P \Rightarrow \alpha = P/Q$$

and therefore

$$\beta = -\alpha/2$$

$$= -P/2Q.$$

(c) Substituting into the third condition of equation (3.8b) in order to check; LHS of equation 3.8b (iii) is

$$u_2u_3 + u_1u_3 + u_1u_2$$
$$= (\beta + i\sqrt{Q})(\beta - i\sqrt{Q}) + \alpha(\beta - i\sqrt{Q}) + \alpha(\beta + i\sqrt{Q})$$
$$= (\beta^2 + Q) + (\alpha\beta - i\alpha\sqrt{Q}) + (\alpha\beta + i\alpha\sqrt{Q})$$
$$= Q + - i\alpha\sqrt{Q} + i\alpha\sqrt{Q}$$
$$= Q$$

i.e. neglecting β^2, $\alpha\beta$.

Thus, the third condition of (3.8b) is also satisfied. Therefore the three roots of f(u) in (3.7d) have been determined as:

$$u_1 = P/Q$$
$$u_2 = -P/2Q + i\sqrt{Q} \quad \}, \quad \text{----------(3.13)}$$
$$u_3 = -P/2Q - i\sqrt{Q}$$

Thus we can now resolve the LHS of equation (3.7c) for this case into partial fractions as follows:

$$\int \frac{u^2\,du}{P + Qu + u^3} = \int \frac{A\,du}{(u + \frac{P}{2Q}) + i\sqrt{Q}}$$

$$+ \int \frac{B\,du}{(u + \frac{P}{2Q}) - i\sqrt{Q}} + \int \frac{Cdu}{(u - \frac{P}{Q})} \quad \text{----------(3.14)}$$

Expanding and rearranging,

$$u^2 = A\{(u + \frac{P}{2Q}) - i\sqrt{Q}\}(u - \frac{P}{Q})$$

$$+ B\{(u + \frac{P}{2Q}) + i\sqrt{Q}\}(u - \frac{P}{Q})$$

$$+ C\{(u + \frac{P}{2Q}) + i\sqrt{Q}\}\{(u + \frac{P}{2Q}) - i\sqrt{Q}\}$$

$$u^2 = A\{(u - \frac{P}{Q})(u + \frac{P}{2Q}) - i(u - \frac{P}{Q})\sqrt{Q}\}$$

$$+ B\{(u - \frac{P}{Q})(u + \frac{P}{2Q}) + i(u - \frac{P}{Q})\sqrt{Q}\}$$

$$+ C\{(u + \frac{P}{2Q})^2 + Q\}.$$

The constants A, B, C, are determined, by comparison of coefficients of similar powers of u, in the following equations:

(i) $A + B + C = 1$, ----------(3.15)

(ii) $A(\frac{-P}{2Q} - i\sqrt{Q}) + B(\frac{-P}{2Q} + i\sqrt{Q}) + C\frac{P}{Q} = 0$

$$\Rightarrow \frac{P}{2Q}(-A-B+2C) + i\sqrt{Q}(-A+B) = 0, \text{------(3.16)}$$

(iii) $A(\frac{-P^2}{2Q^2} + i\frac{P}{Q}\sqrt{Q}) + B(\frac{-P^2}{2Q} - i\frac{P}{Q}\sqrt{Q}) + C(\frac{P^2}{4Q^2} + Q)$

$$\Rightarrow \frac{P^2}{4Q^2}(-2A-2B+C) + CQ + i\frac{P}{Q}\sqrt{Q}(A-B) = 0, \text{----(3.17)}$$

For both equations (3.16) and (3.17), equating the coefficients of i gives

$$A = B.$$

Further, multiplying (3.16) by P/Q and adding the result to equation (3.17) gives

$$\frac{P^2}{4Q^2}(-4A-4B+5C) + CQ = 0, \text{----------(3.18)}$$

Putting A = B, from (3.18) gives,

$$\frac{P^2}{4Q^2}(-8B+5C) + CQ = 0, \text{----------(3.19)}$$

and from (3.15),

$$2B + C = 1, \text{----------(3.20)}$$

(Equation (3.19) x $\frac{P^2}{Q^2}$) - CQ:

$$\frac{P^2}{4Q^2}(8B + 4C) - CQ = \frac{P^2}{4Q^2} - CQ, \text{----------(3.21)}$$

(Equation 3.19) + (Equation 3.21):

$$\frac{P^2}{4Q^2}.9C = \frac{P^2}{Q^2} - CQ$$

Rearranging the above expression gives

$$C(\frac{9P^2}{4Q^2} + Q) = \frac{P^2}{Q^2}$$

or

$$C(\frac{9P2 + 4Q^3}{4Q^2}) = \frac{P^2}{Q^2}, \text{ ----------(3.21a)}$$

giving

$$C = \frac{4P^2}{9P^2 + 4Q^3}, \text{ ----------(3.21b)}$$

C could also be expressed as

$$C = \frac{4P^2/Q^2}{9P^2/Q^2 + 4Q} = \frac{4\alpha^2}{9\alpha^2 + 4Q}$$

If, as assumed earlier we could neglect higher orders of α, then it turns out that $C \equiv 0$.

We are thus left, from equation (3.20) with

$$2B = 1; \text{ i.e. } B = \tfrac{1}{2}$$

and, from equation (3.15),

$$A = \tfrac{1}{2}.$$

If we substitute these values of A, B and C into equation (3.14) and write down in full the equation (3.7c), we obtain

$$\int \frac{u^2\,du}{P+Qu+u^3} = \tfrac{1}{2}\int \frac{du}{(u+\frac{P}{2Q}) + i\sqrt{Q}} + \tfrac{1}{2}\int \frac{du}{(u+\frac{P}{2Q}) - i\sqrt{Q}}$$

$$= -\int \frac{dX}{X}, \text{ ----------(3.22)}$$

Integrating the above equation and simplifying gives

$$\tfrac{1}{2}\log\{(u + \frac{P}{2Q})^2 + Q\} = \log\frac{C_1}{X}$$

and therefore,

$$(u + \frac{P}{2Q})^2 + Q = \frac{C_2}{X^2}, \quad \text{----------(3.22a)}$$

Substituting back the expression (3.5a), i.e.

$$u = y/X$$

and rearranging, gives

$$(y + \frac{P}{2Q} X)^2 + QX^2 = C_2, \quad \text{----------(3.22b)}$$

C_1 and C_2 are both constants assuming different values.

It is seen that equation (3.22b) above is not an equation of an ellipse.

To obtain the constant C_2 in equation (3.22b) above, we substitute back equation (3.4a) for X, i.e.

$$\{y + \frac{P}{2Q}(S/2 - x)\}^2 + Q(S/2 - x)^2 = C_2, \quad \text{---(3.22c)}$$

and insert the boundary condition

$$y = h \text{ at } x = 0$$

giving

$$C_2 = \{h + \frac{P}{2Q}.S/2\}^2 + Q(S/2)^2, \quad \text{----------(3.22d)}$$

Equation (3.22c) thus becomes

$$\{y + \frac{P}{2Q}(S/2 - x\}^2 + Q(S/2 - x)^2$$

$$= \{h + \frac{P}{2Q}.S/2\}^2 + Q(S/2)^2, \quad \text{----------(3.23a)}$$

Rearranging, (3.23a) gives

$$\{y + \frac{P}{2Q}(S/2 - x)\}^2 - \{h + \frac{P}{2Q} S/2\}^2$$

$$= Q(Sx - x^2), \quad \text{----------(3.23b)}$$

Inserting the second boundary condition, i.e.

$$y = H \text{ at } x = S/2$$

and simplifying, the expression for drainage spacing is

obtained as:

$$S^2 = \frac{4}{Q}\{H^2 - (h + \frac{P}{2Q}.S/2)^2\}, \text{ ----------(3.24)}$$

It is seen that equation (3.23b) which gives the water table profile and the equation (3.24) which gives an expression for drainage spacing are generalizations for the case of non-Darcian seepage, of the corresponding equations, 3.10c and 3.11 for the Darcian seepage ($P = 0$).

Equations (3.23b) and (3.24) are also written as:

$$\{\frac{Y}{h} + \frac{P}{2Q}(\frac{S/2}{h} - \frac{x}{h})\}^2 - \{1 - \frac{P}{2Q}\frac{S/2}{h}\}^2$$

$$= Q(\frac{S}{h})(\frac{x}{h}) - Q(\frac{x}{h})^2, \text{ ----------(3.23c)}$$

$$(\frac{S}{h})^2 = \frac{4}{Q}\{(\frac{H}{h})^2 - (1 + \frac{P}{2Q}\frac{S/2}{h})^2\}, \text{ ------(3.24a)}$$

$$(\frac{S}{H})^2 = \frac{4}{Q}\{1 - (\frac{h}{H} + \frac{P}{2Q}\frac{S/2}{H})^2\}, \text{ ---------(3.24b)}$$

3.5. FULLY TURBULENT FLOW

For fully turbulent non-Darcy flow regimes $a = 0$; and $b \neq 0$ and hence $Q = 0$; and $P \neq 0$.

Equation (3.7c) then becomes

$$\int \frac{u^2\,du}{P + u^3} = -\int \frac{dX}{X}, \text{ ----------(3.25a)}$$

or, rearranging:

$$\tfrac{1}{3}\int \frac{3u^2}{(P + u^3)} = -\int \frac{dX}{X}, \text{ ----------(3.25b)}$$

Integration gives:

$$\tfrac{1}{3}\log(P + u^3) = -\log X + C_1$$

and therefore,

$$(P + u^3) = \frac{C_2}{X^3}, \text{ ----------(3.26)}$$

The above expression gives

$$PX^3 + u^3X^3 = C_2, \text{ ---------- (3.26a)}$$

Substituting back the expression (3.5a), i.e.

$$u = y/X$$

gives

$$y^3 + PX^3 = C_2, \text{ ---------- (3.27)}$$

C_1 and C_2 are both constants assuming different values. It is seen that equation (3.27) is also not an equation of an ellipse.

Substituting back the expression for X in equation (3.4a) gives

$$y^3 + P(S/2 - x)^3 = C_2, \text{ ---------- (3.27a)}$$

To obtain the constant C_2, we insert the boundary condition

$$y = h \quad \text{at } x = 0$$

giving

$$C_2 = h^3 + P(S/2)^3$$

Equation (3.27a) thus becomes

$$y^3 + P(S/2 - x)^3 = h^3 + P(S/2)^3$$

Rearranging

$$y^3 - h^3 = P\{(S/2)^3 - (S/2 - x)^3\}, \text{ ------ (3.28)}$$

Inserting the second boundary condition, i.e.

$$y = H \text{ at } x = S/2$$

and simplifying, the expression for drainage spacing S is obtained as:

$$S^3 = \frac{8}{P}(H^3 - h^3), \text{ ---------- (3.29)}$$

Equation (3.28) is for the water table profile. It represents a cubic curve whose shape is markedly different from those represented by equations (3.10c) and (3.23b); as is seen from the Figure 3.2. It is, however, recognized that the occurrence of turbulent flow through porous media is an extreme limiting case which would not normally be found in natural soils and rocks.

The equations (3.28) and (3.29) can also be written as:

$$(\frac{Y}{H})^3 - 1 = P\{(\frac{S/2}{h})^3 - (\frac{S/2}{h} - \frac{x}{h})^3\}, \text{ -------(3.28a)}$$

$$(\frac{S}{h})^3 = \frac{8}{P}\{(\frac{H}{h})^3 - 1\}, \text{ ----------(3.29a)}$$

$$(\frac{S}{H})^3 = \frac{8}{P}(1 - (\frac{h}{H})^3), \text{ ----------(3.29b)}$$

3.6. EVAPORATION (NEGATIVE RECHARGE)

The concept of evaporation as negative recharge can be applied for a case of a water table profile that is maintained between two ditches or supply canals containing water in them and with evaporation or evapotranspiration occurring in the adjoining soil block instead of precipitation. Negative recharge might also be considered as the uniform occurrence of deep seepage below the drainage ditch levels.

In negative recharge or evaporation, the quantity R becomes negative. Thus Q, which = aR also becomes negative. P, which = bR^2, however, retains its sign.

Equations(3.10c) and (3.23b) for the water table profiles under Darcy and non-Darcy transitional flow regimes respectively, would hence become:

$$y^2 - h^2 = Q_E\,(x^2 - Sx), \quad \text{----------(3.30)}$$

$$\{y - \frac{P}{2Q_E}(S/2 - x)\}^2 - \{h - \frac{P}{2Q_E}.S/2\}^2 = Q_E(x^2 - Sx) \text{--(3.31)}$$

where

$$Q_E = aE$$

and E = Evaporation rate (negative precipitation).

Effectively, results of water table profiles obtained using equations (3.30) and (3.31) above can be superimposed on the results obtained from equations (3.10c) and (3.23b); which consider uniform positive recharge and in effect assumed the absence of evaporation and deep seepage. The consideration of evaporation in the design of a drain spacing would result in increased spacing and hence greater cost savings.

Typical theoretical water table profiles as given by equations (3.10c), (3.23b), 3.28) for positive recharge and (3.30) and 3.31) for evaporation, are shown in Figures 3.1 and 3.2. It is seen that for non-Darcian transitional flow regimes, the shape of the water table profile in equilibrium with steady precipitation between two drains no longer remains elliptic (Figure 3.1). The water table profile would lie above the Darcian water table.

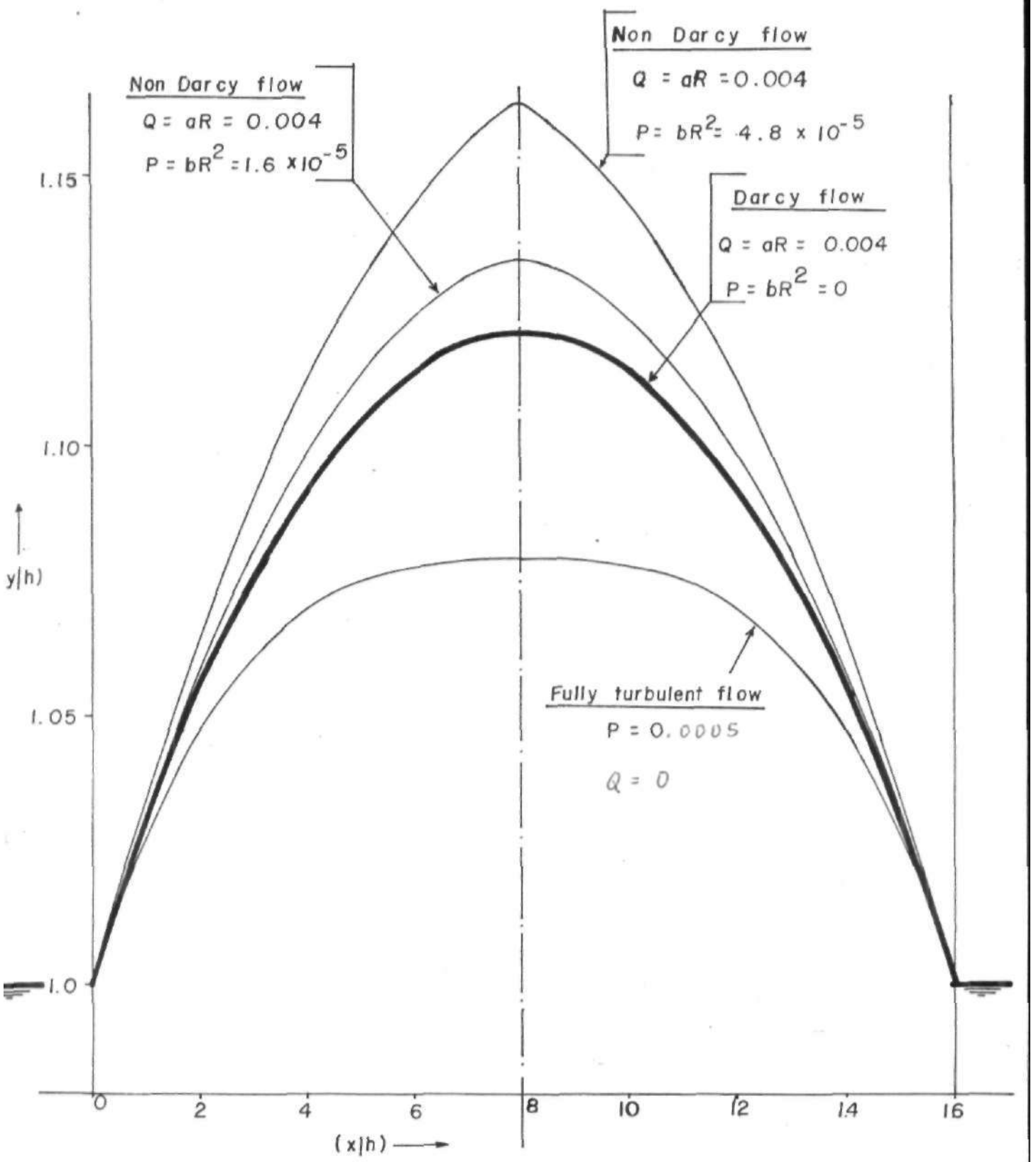


FIG 3.1 : Typical water table profiles for various values of dimensionless parameters P and Q ; S/h = 16

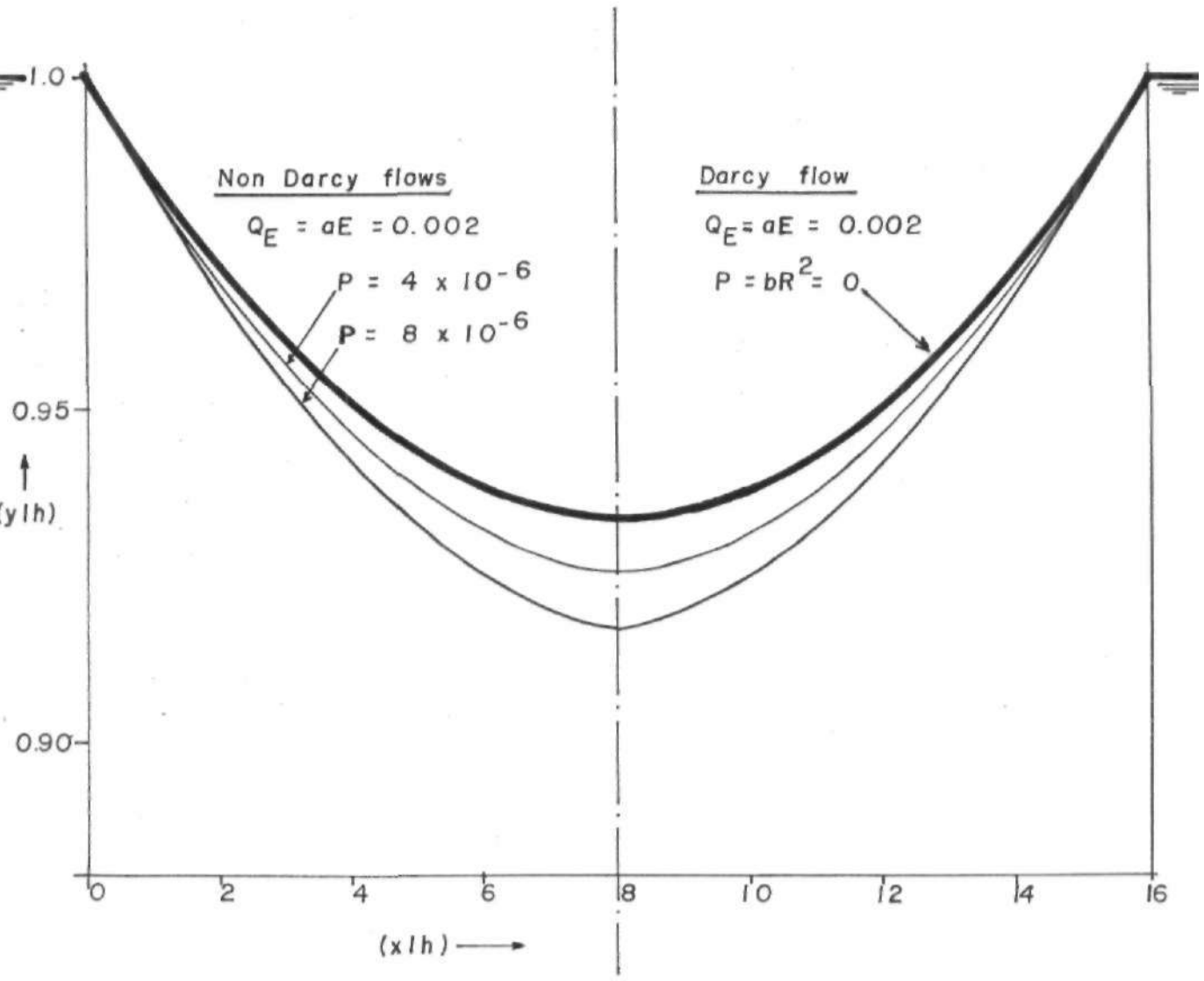


FIG 3.2: Typical water table profiles under evaporation

$S/h = 16$

3.7. SUMMARY

The presentation in this chapter has provided an approximate analytical solution to the problem of steady seepage into parallel drains which does not obey Darcy's linear seepage law. The effect of surface evaporation considered as negative precipitation has also been briefly discussed. The assumptions made therein are identical to those most often made in the treatment of the corresponding seepage flow problems incorporating Darcy's law; namely that the D-F theory is valid, the porous medium is homogeneous and isotropic and horizontal. These assumptions are expected to give reasonable agreement with actual field conditions.

The next chapter shall present the details of sand tank seepage flow model experiments maintaining seepage flow rates which fall in the non-Darcy transitional regimes, in order to investigate the extents of the validity of the solution presented in this chapter and the assumptions contained therein.

CHAPTER FOUR

EXPERIMENTAL SET UP AND PROCEDURE

4.1. INTRODUCTION

The purpose of the experimental aspect of this project is to employ a sand tank model for the study of the water table profile in the seepage of steady precipitation through a porous medium into drainage ditches. The studies are, among other things, intended to ascertain the validity of the equations (3.23b) and (3.24) for seepage in the non-Darcy transitional flow regimes.

The porous medium used is of such size and conductivity as would be expected to maintain a steady state seepage under the high precipitation rates that are created. It consists of coarse sand of effective size 2.86 mm. The main components of the sand tank experimental model used in the study are described in the following sections.

4.2. THE RAINFALL SIMULATOR

To produce a rainfall simulator, a rectangular metal box was constructed from galvanized iron sheets of 1.6 mm gauge thickness. The sheets were obtained in the form of flat rectangular mild steel sheets 2.438 metres (8 feet) in length and 1.219 metres (4 feet) in width. These were then cut into smaller pieces of 1.219 metre length and one metre width. Each of these smaller pieces was then made to form open ended metal boxes of 1.219 m length, 0.6 m base width and 0.2 m depth.

Four of such small metal boxes were then welded together, end to end, to form a metal box of total length 4.87 m and same base width and depth as the smaller metal boxes. Finally, the open ended box was sealed at both ends by welding mild steel sheets of 0.6 m length and 0.2 m depth to the end edges of the metal box. This metal box forms the container of the rainfall simulator.

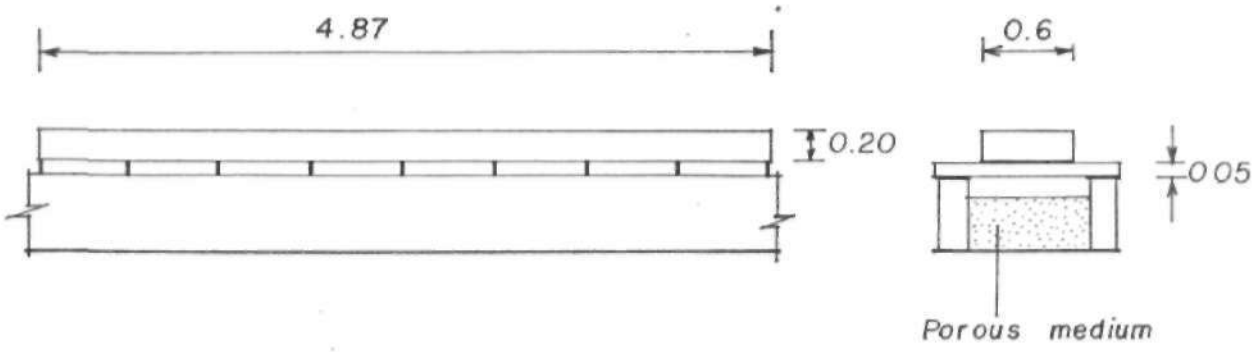
The base of the constructed metal box was then perforated to enable the uniform drip of water through the container. The perforation was made by drilling 2 mm diameter holes through the base using electric drills of 2 mm diameter at spacings of 5 mm in both directions. The rainfall simulator container was then provided with supports consisting of 50 mm x 6 mm structural steel flat bars, welded to its base as shown in Figure 4.1. Flat bars were preferred to angle bars or flanged sections so as to ensure that no holes were blocked by the flanges welded to the base. The flat bars were in turn to be supported by the walls of the sand tank model.

Figure 4.1 shows the details of the rainfall simulator construction.

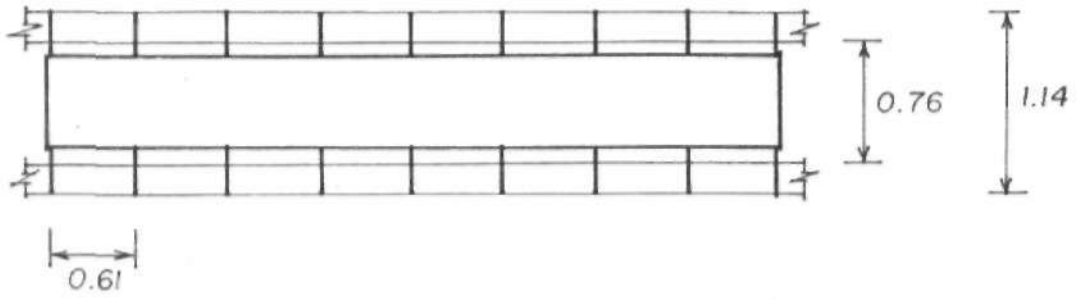
4.3. THE SAND TANK

The sand tank used for the experimental model was of cement block masonry construction and consists of two parallel walls, with their internal surfaces 0.76 m apart, and a concrete slab floor, representing a horizontal impervious barrier. The length of the model

(a) Elevations:



(b) Plan:



(c) Isometric view:

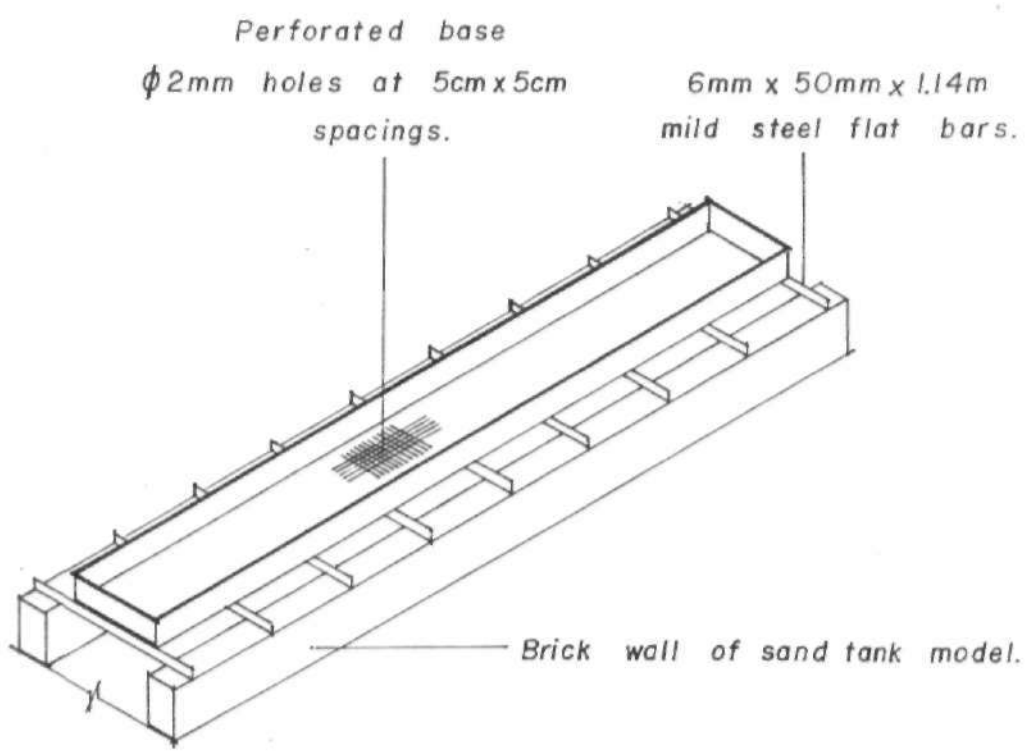


FIG. 4.1: Rainfall simulator — Plan and views.
(Dimensions in metres)

along the direction of flow is the same as the length of the rainfall simulator, i.e. 4.87 m. The depth of the sand tank = 0.50 m. The porous medium was placed in the tank to a depth of 40 cm, and the surface was levelled using a mason's spirit level, to ensure its horizontality.

On one end the vertical boundary of the porous medium was in the form of a vertical perforated metal sheet of 3 mm gauge thickness, representing the vertical surface of a drainage ditch. About 40 cm away from this boundary, a 15 cm thick wall was constructed to a height of 17.5 cm to establish a constant water level in the ditch. Thus, with this arrangement, a drainage ditch is created during the experiment, of 40 cm width, with its base at the impervious boundary (the concrete slab floor) and its water level established at a constant height slightly above 17.5 cm, being the height of the wall boundary over which excess water flows.

On the other end of the tank, the vertical boundary of the porous medium was in the form of a vertical wall of 150 mm thickness, constructed to the full height of the sand tank, i.e. 0.50 m; representing the centre-line between two ditches, which is equivalent to an impervious boundary. In this way, seepage flow in the sand tank model represents one symmetrical half of the seepage flow between two parallel ditches in actual prototype field conditions, because in seepage flow towards parallel drains, flow conditions on both sides of the

centreline are identical to each other. It would therefore suffice to concentrate study on only one of the two identical conditions.

Representation of the centreline with an impervious boundary in the model provides two advantages for the model study of seepage flow:

1. It leads to an enlarged scale representation of the prototype field, i.e. instead of the length of the model representing a spacing between two ditches, it represents only a half spacing. This leads to more tangible readings of the water table variations in the vertical direction, which are normally of very small order in relation to the horizontal distances.

2. It saves the extra precaution of ensuring that the water level is exactly the same in the two parallel ditches. If two ditches were provided in the model then it would have been rather difficult to ensure that the discharges to and water levels in the two ditches remained exactly the same. Experimental variations in the two levels would then lead to resultant inaccuracies in the determination of the water table profiles.

4.4. WATER SUPPLY TO THE MODEL

The supply of water to the rainfall simulator was tapped from a 75 mm mains pipe delivering water from an overhead tank in the hydraulics laboratory. A 31.75 mm G.I. pipe was used for this purpose. The tapped supply was then made to deliver water to the

container of the rainfall simulator via a constant head reservoir in the form of a drum.

The head and discharge of the water supplied directly from the mains could be subject to wide variations with time and hence would not ensure a steady rate of discharge and precipitation. By conducting the supply through the constant head reservoir, however, the two valves V_1 and V_2 (Figure 4.2) are adjusted until the discharge through V_1 (inflow) is only slightly greater than the discharge through V_2 (out flow) and the water level in the constant head reservoir is kept at the level of the overflow pipe (see Figure 4.2). Thus the constant head reservoir in effect absorbs the minor fluctuations in discharge quantities and provides a steady rate of discharge into the rainfall simulator container.

A preliminary estimate of the order of the precipitation rate that could be produced by the rainfall simulator was carried out as follows:

The discharge Q_d through each hole is given as:

$$Q_d = C_d \cdot A.V. \quad \text{----------(4.1)}$$

where

A = area of each hole, diameter 2 mm

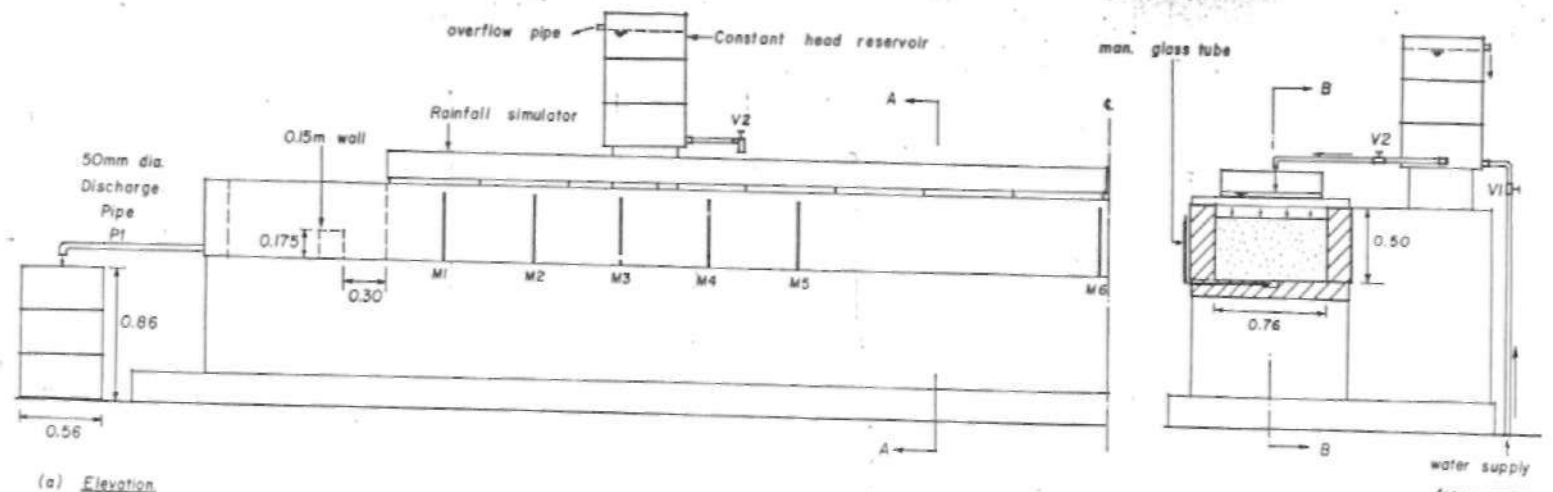
$= \frac{\pi}{4} (0.002)^2 \ m^2$

$= 3.1416 \times 10^{-6} \ m^2$;

V = macroscopic velocity through the hole

$= \sqrt{(2gd)}$

in which $g = 9.81 \ m/s^2$ and d = depth of water in the container:



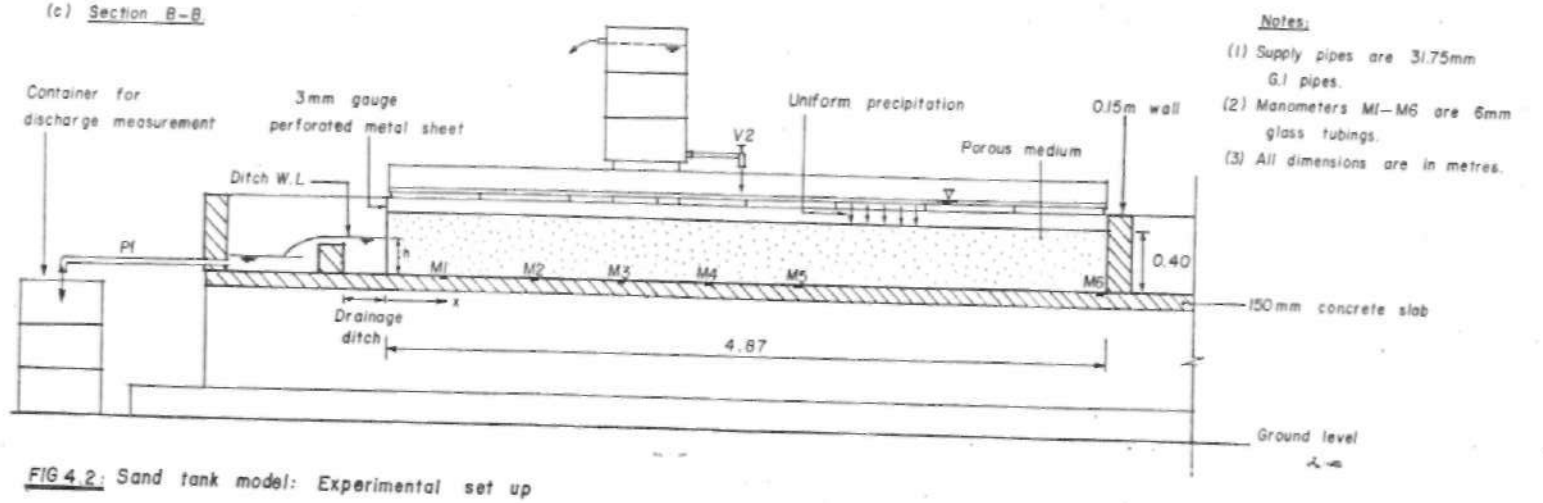
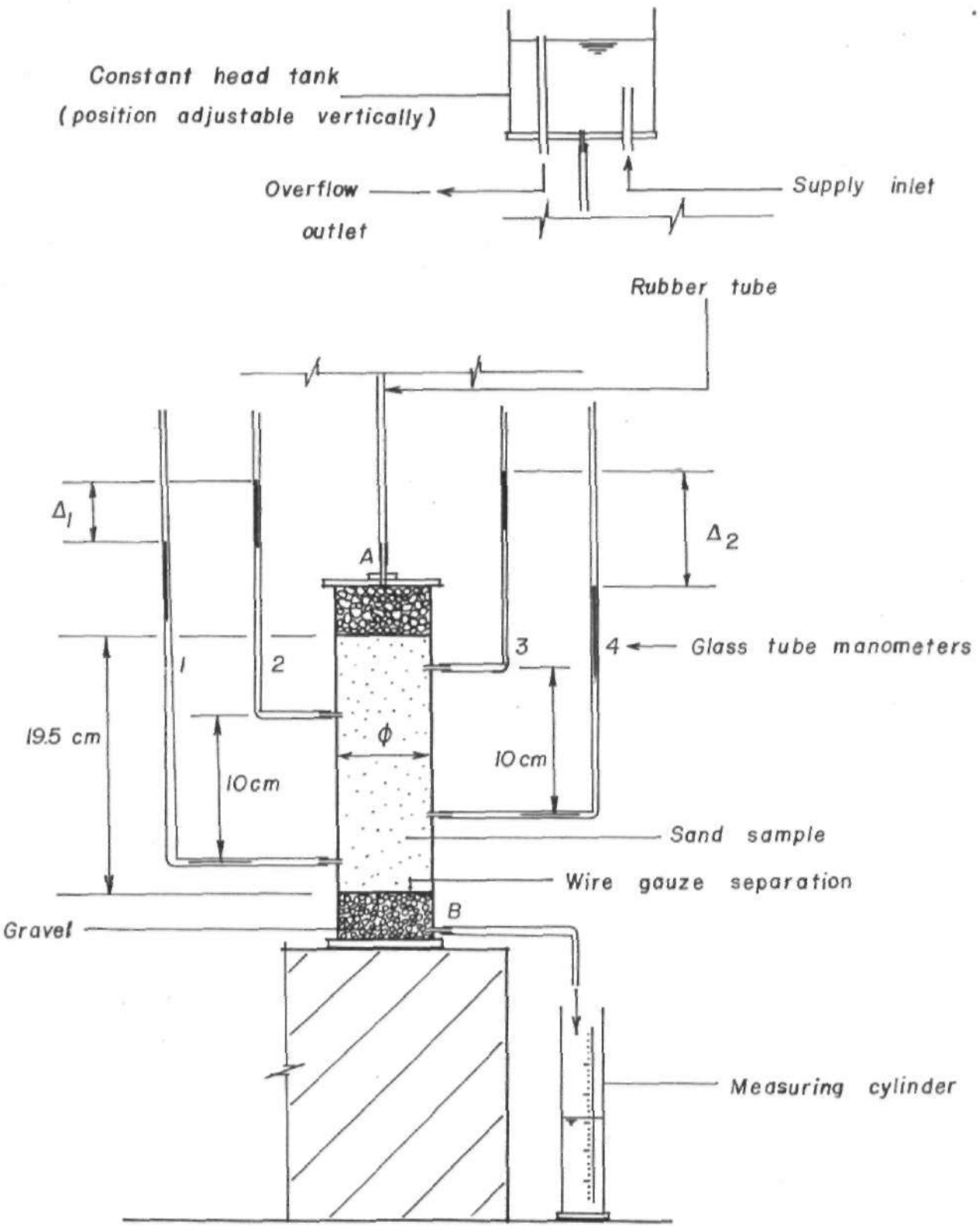


FIG 4.2: Sand tank model: Experimental set up



A : Inlet into permeameter

B : Outlet from permeameter

ϕ : Internal diameter of permeameter = 7.57 cm

FIG. 4.3 : Schematic diagram of the constant head permeameter experiment.

C_d = coefficient of discharge through the holes. In reality, C_d varies with the holes depending on the individual smoothness of the hole surfaces. An average value can, however, be assumed for the overall coefficient C_d.

With the given spacing of the holes, (2.5 cm x 2.5 cm), the number of holes per square metre is

$$(\frac{100}{2.5})^2 = 1600$$

and in the total container area (4.87 m x 0.76 m) is:

$$1600 \times 4.87 \times 0.76 = 5922.$$

Applying equation (4.1) for each hole the total discharge Q_D through all the holes is given as:

$$Q_D = 5922 \times C_d \times 3.1416 \times 10^{-6} \times \sqrt{(2gd)}$$

which becomes:

$$Q_D = C_d.(82.4077)\sqrt{d} \times 10^{-3} \text{ m}^3/\text{sec}$$

An approximate upper value for C_d for the holes (considered as small sharp edged orifices with diameter << d) can be assumed to be 0.63 (Fox, 1974); and hence,

$$Q_D = 51.917 \sqrt{d} \times 10^{-3} \text{ m/sec.}$$

Thus, for instance, for d = 5 cm (0.05 m), then the container precipitates

$$Q_D = 51.917 \times \sqrt{0.05} \times 10^{-3} \text{ m/sec}$$
$$= 11.609 \times 10^{-3} \text{ m}^3/\text{sec}$$

giving a uniform precipitation rate R of

$$R = \frac{11.609 \times 10^{-3}}{4.87 \times 0.76} = 31.137 \times 10^{-4} \text{ m/sec.}$$

The above estimate of R was only a rough check on the estimated R, carried out in determining the size and spacing of the perforation holes on the rainfall simulator container base. It does not indicate the method that was used in the experiment for determining R.

The seepage out of the porous medium flows into and out of the ditch and eventually out of the model through pipe P_1 shown in Figure 4.3. This flow out of pipe P_1 is equal to the discharge precipitated unto the porous medium when the steady state is attained and is therefore measured using a container of known dimensions and a timer. Details of the sand tank model experimental set up is shown in Figure 4.2; and also in Plates I to V

4.5. MODEL EXPERIMENT: PROCEDURE

In the sand tank model experiments the model is set up as described in the preceding sections and also in Figure 4.2 and Plates I - V. First, the two valves, V_1 and V_2, are opened for inlet and outlet of water into and out of the constant head reservoir. The two valves are adjusted for a particular selected discharge such that a little amount of overflow is maintained from the constant head reservoir. This ensures that the level of water in the reservoir remains constant at the level of the overflow pipe and consequently, a steady discharge is maintained into the perforated rainfall simulator container.

Next, small adjustments are made on the level of the rainfall simulator at the supports in order to ensure

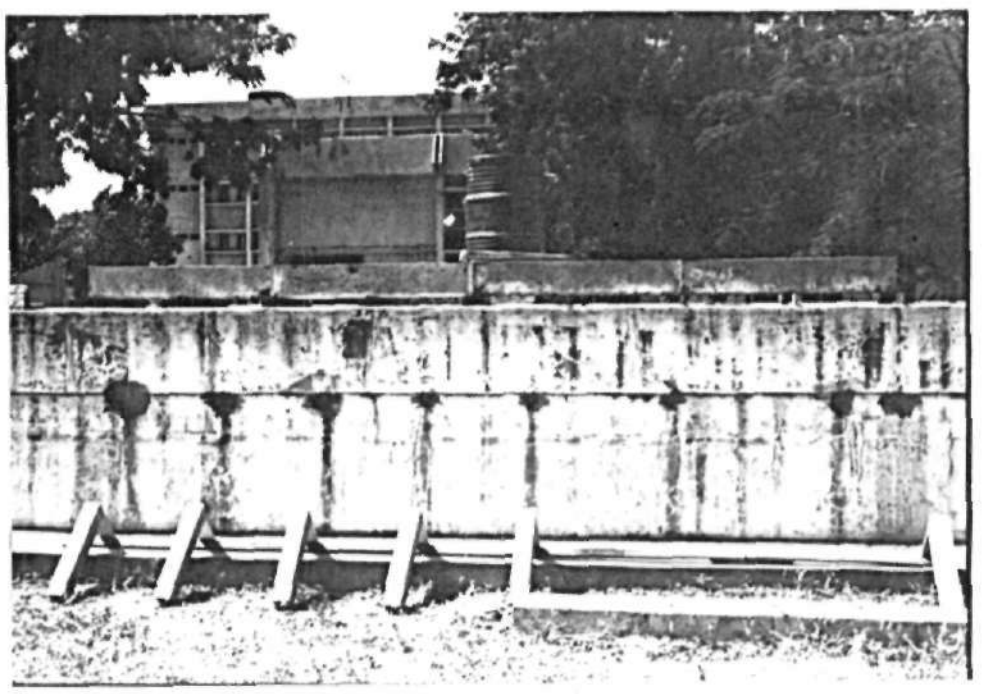


PLATE I: FRONT VIEW OF SAND TANK MODEL

305014

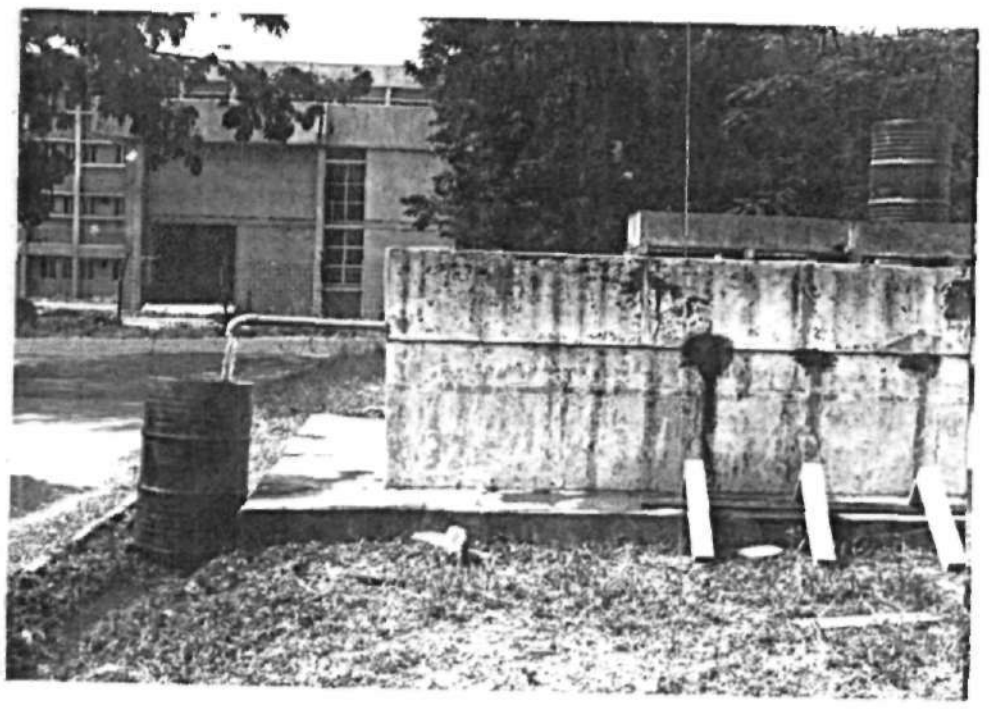


PLATE II: DISCHARGE PIPE P_1 WITH MEASURING CONTAINER

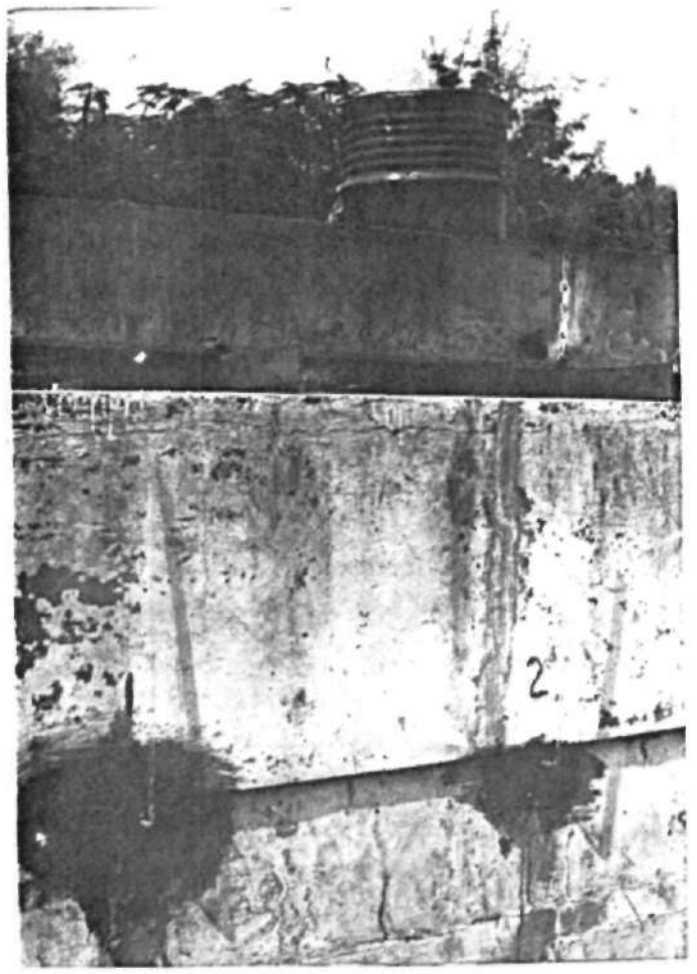


PLATE III: MANOMETRIC GLASS TUBES, AND PRECIPITATION FROM RAINFALL SIMULATOR

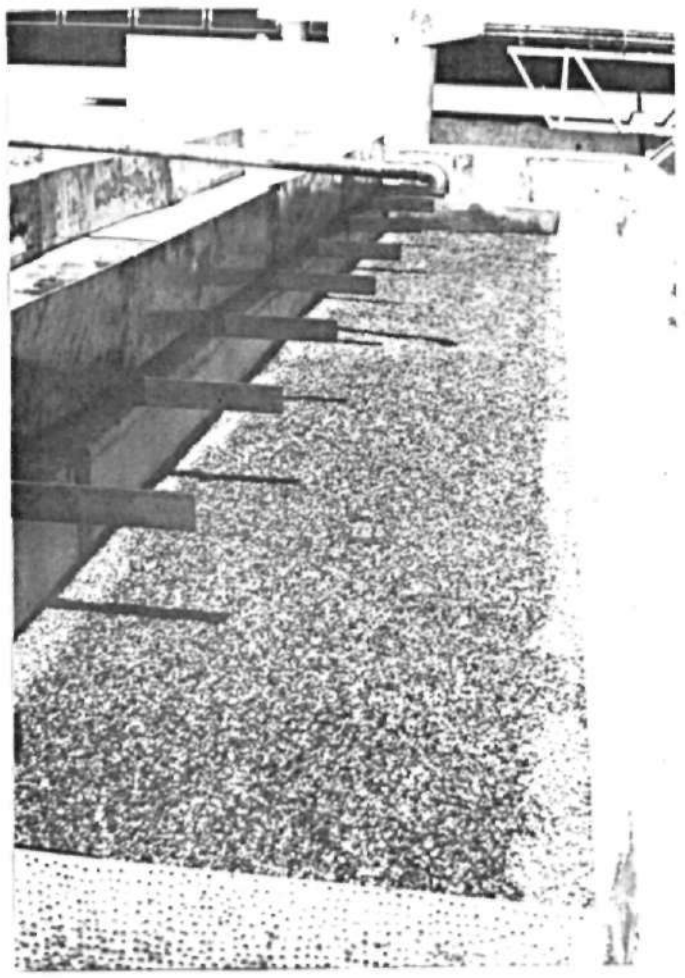


PLATE IV: POROUS MATRIX BED AFTER APPLICATION OF PRECIPITATION

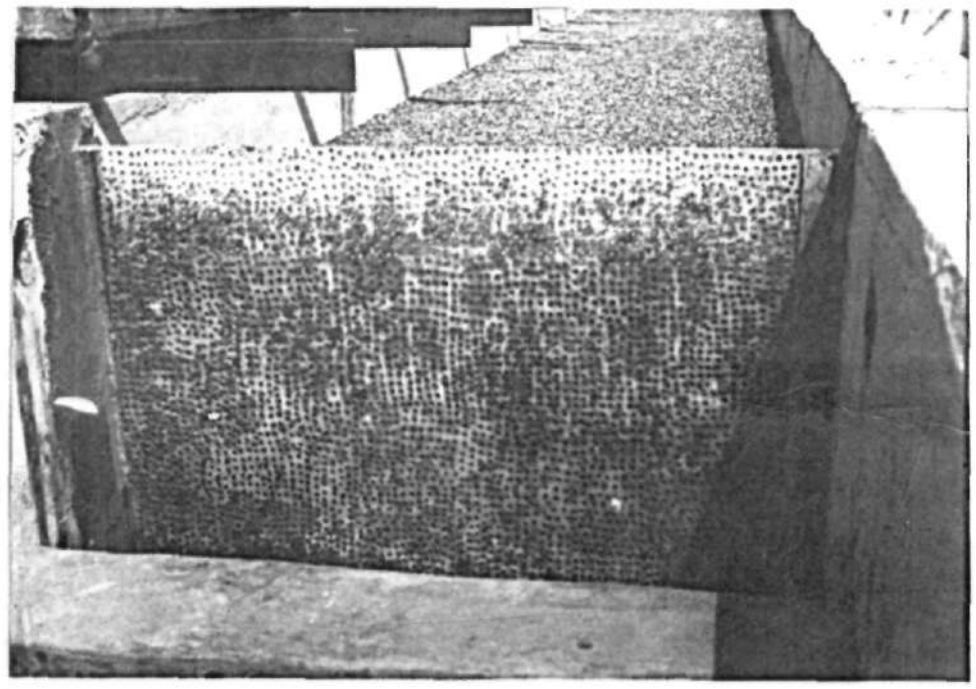


PLATE V: POROUS MATRIX BED BOUNDED BY PERFORATED METAL SHEET AS VERTICAL DITCH SURFACE

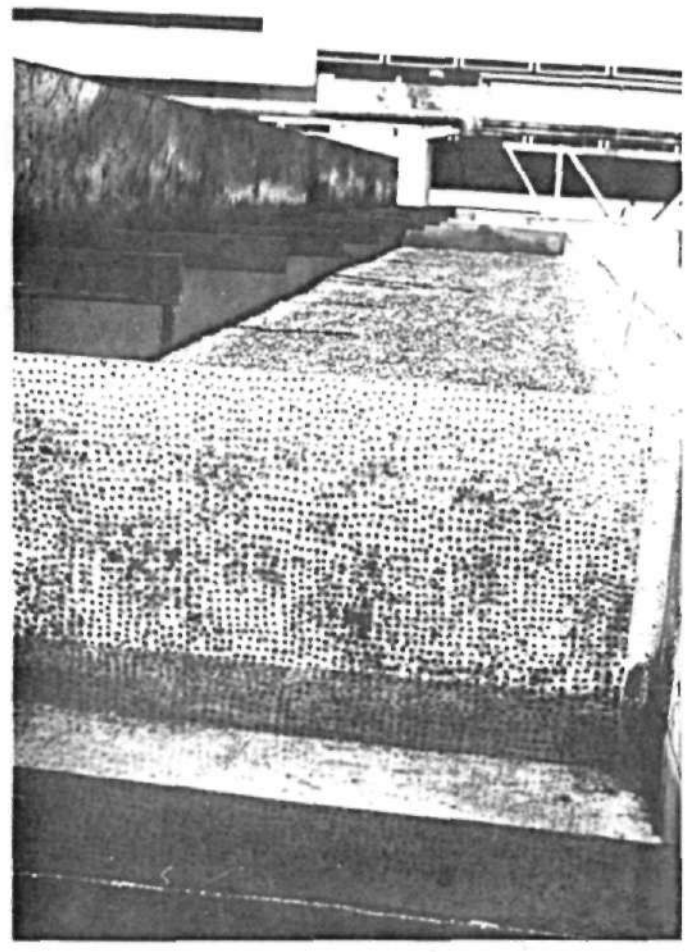


PLATE VI: DITCH WATER LEVEL AND OVERFLOW FROM DITCH,
TO BE DISCHARGED OUT THROUGH PIPE P_1

its complete horizontality, and the levels of water in the simulator are equal at the two ends. This ensures, within the range of experimental possibilities, a uniform water level in the simulator and hence a uniform precipitation rate unto the porous matric bed. Even this procedure, however, did not rule out the effects of small undulations which existed along the perforated bottom of the simulator making the depth in some areas to be slightly more than in others.

Having thus established a steady and fairly uniform precipitation rate unto the bed of the porous matrix, the rise of the water level, as observed in the manometric glass tubes is monitored until it reaches a steady level at which a steady state is then assumed to exist. At this steady state, the water table profile does not change with time, and the total quantity of precipitation over a given period of time is equal to the quantity of discharge out of the model through the pipe P_1 in Figure 4.2, for the same period of time.

Measurements are then taken of the various water table elevations from the glass tube manometers. The depth of water in the ditch is also measured. Finally, the time taken to fill the measuring container, (a drum of measured dimensions) with discharge from P_1 is measured two or three times and the average value is calculated.

4.6. THE PERMEAMETER EXPERIMENT

The constant head permeameter is a standard equipment in the conducting of permeability tests on

porous media samples. Figure 4.4 shows details of its arrangement. The constant head tank is mounted and fixed on a vertical wodden board and its fixed position can be adjusted to vary its relative height above the permeameter. It also contains an overflow outlet pipe to maintain its constant water level. Water flows from the constant head tank to the permeameter through a flexible rubber tubing.

The four manometric glass tubes 1, 2, 3 and 4 are all mounted on a vertical wooden board which has been graduated to permit easy recording of the heights. To obtain a set of readings for a given position of the constant head tank, the hydraulic heads Δ_1 and Δ_2 and the average of their values are recorded and the discharge out of the permeameter is measured by determining the average time it takes for a 250 ml measuring cylinder to get filled up.

The important sources of experimental error in a permeameter test are the formation of a filter skin of fine material on the surface of the sample and the segregation of air in the form of bubbles within the sample. Both of this phenomenon increase the resistivities of the sample (Terzaghi and Peck, 1967). Further, for these experiments, time readings of 5 seconds and less obtained for hydraulic gradients of 0.23 and more created a high error potential. This error was minimized by ensuring that a minimum of five consistent readings were obtained for which the average value was determined. The error due to formation of a filter skin was eliminated by

measuring the losses of hydraulic head between two pairs of points located in the interior of the sample and the average value determined. The error due to the segregation of the air bubbles within the sample can be substantially reduced by reversing the flow of water through the permeameter so that it entered through B in Figure 4.4 and exits through the inlet A. The consequent upward flow of water in the sample displaces air upwards and thus minimizes the entrapment of air bubbles within the sample. This was the procedure adopted in the experiment.

CHAPTER FIVE

EXPERIMENTAL RESULTS AND ANALYSIS

5.1. THE POROUS MEDIUM

The porous matrix used in the sand tank experiment consisted of fine gravel with average particle size of 3.4 mm and a uniform gradation. Figure 5.1 shows the grain size distribution curve for the porous matrix.

The characteristic grain sizes for the sample are:

Medium size, D_{50} = 3.44 mm

D_{60} = 3.44 mm

Effective size D_{10} = 2.86 mm.

The uniformity coefficient C_u, given as

$C_u = D_{60}/D_{10}$ is = 3.44/2.86

which = 1.203.

The sample can therefore be considered as highly uniform in gradation.

5.2. PERMEAMETER TEST

The permeameter test was carried out using the constant head permeameter (see Section 4.4 and Figure 4.3). The procedure for determining the hydraulic gradient and macroscopic velocity are described below.

5.2.1. Hydraulic Gradient:

Varying values of the hydraulic head Δ were established by adjusting the height of the constant

94A

FIG. 5.1

PARTICLE SIZE DISTRIBUTION ASTM D 422 – D 546

DATE OF TEST 22-11-85 SAMPLE No.

LOCATION DESCRIPTION CLASSIFICATION

DEPTH

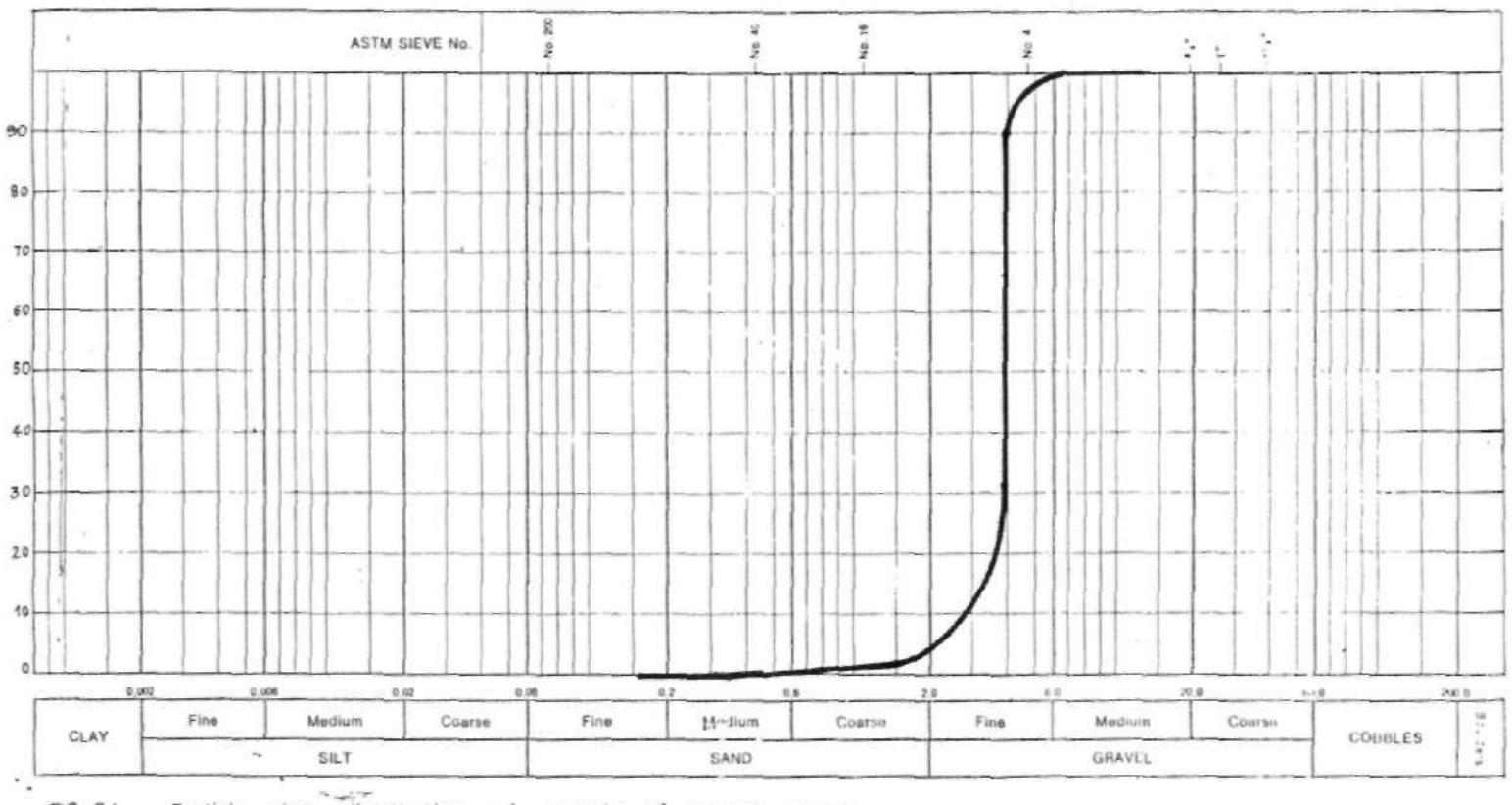


FIG. 5.1 *Particle size distribution of sample of porous matrix.*

Signed

head tank above the permeameter. For a given constant hydraulic head Δ, the hydraulic gradient I is given by

$$I = \Delta/h$$

where

Δ = average of the values Δ_1 and Δ_2;

h = distance between the two measurement points

= 10 cm.

thus $I = 0.1\Delta$, with Δ in cm.

5.2.2. Macroscopic Velocity:

With the given hydraulic head established between the two measurement points, the discharge was determined by measuring the time t in seconds it takes to fill a 250 ml measuring cylinder up to the 250 ml mark. The discharge is given by

$$Q_d = \frac{250}{t_{av}} \times 10^{-6} \text{ m}^3/\text{sec}$$

where

t_{av} = average of five readings taken for each value of constant head.

The internal diameter of the permeameter, as measured using Vernier sliding callipers = 7.57 cm.

$\therefore$ Cross sectional area of flow A is

$$A = \frac{\pi}{4}(7.57)^2 \text{ cm}^2$$

$$= 45.00 \text{ cm}^2$$

$$= 4.5 \times 10^{-3} \text{ m}^2.$$

Thus, the macroscopic velocity V is given by

$$V = Q_d/A$$

$$= \frac{250}{t_{av}} \times \frac{10^{-6}}{4.5 \times 10^{-3}}$$

therefore,

$$V = \frac{55.56}{t_{av}} \times 10^{-3} \text{ m/s} \quad \text{----------(5.1)}$$

TABLE 5.1: PARTICLE SIZE DISTRIBUTION OF SAMPLE

Total weight of sample = 300 g.

SIEVE SIZE (mm)	WEIGHT RETAINED (g)	CUMMU-LATIVE WEIGHT RETAINED (g)	CUMMU-LATIVE PERCENTAGE RETAINED (%)	TOTAL PERCENTAGE PASSING (%)
6.35	0.00	0.00	0.000	100.000
5.60	1.00	1.00	0.333	99.667
4.75	5.55	6.55	2.183	97.817
2.40	270.30	276.85	92.283	7.717
1.20	19.80	296.65	98.883	1.117
0.60	2.60	299.25	99.750	0.250
0.434	0.10	299.35	99.783	0.217
0.30	0.10	299.45	99.817	0.183
0.208	0.10	299.55	99.850	0.150
0.150	0.10	299.65	99.883	0.117
0.075	0.10	299.75	99.917	0.083
Passing 0.075	0.25	300.00	100.000	0.000

Table (5.2) gives the various values of I and V obtained from the permeameter experiment. Due to the limitations in the height position of the constant head tank, it was not possible to establish a hydraulic gradient

greater than 0.3. Similarly, there was difficulty in maintaining the water levels in the manometers within the glass tube region for low discharge conditions. For this reason, it was not possible to obtain steady reliable readings for hydraulic gradients less than 0.5.

5.3. ANALYSIS OF PERMEAMETER DATA

For the sake of comparison, three theoretical velocity-gradient relations are herein postulated to describe the variation of the hydraulic gradient I with respect to the macroscopic velocity V. These relations are:

(1) The linear relation or Darcy's law: i.e.

$$I = aV \quad \text{----------(5.3)}$$

in which a = 1/k, where k is hydraulic conductivity;

(2) The Forchheimer quadratic relation: i.e.

$$I = aV + bV^2 \quad \text{----------(5.4)}$$

in which a, b are resistivity coeffieients; and

(3) A logrithmic relation of the form

$$\log I = A + B \log V \quad \text{----------(5.5)}$$

This relationship is also equivalent to Izbash's equation

$$V = MI^n \quad \text{----------(5.6)}$$

Equations (5.5) and (5.6) are alternate forms of the same relation. It can easily be deduced that

$$A = \frac{1}{n} \log \frac{1}{M} \; ; \; B = \frac{1}{n}$$

and $n = \frac{1}{B}$; $M = \exp(-A/B)$.

Each of the relations, i.e. equations (5.3) to (5.5) was fitted to the experimental data by a method of least

squares regression, and the mean square error of the experimental data from the calculated curves was determined for each of the three cases.

5.3.1. Regression Along The Linear Relation:

It is required to regress the experimental data to fit the equation (5.3) such that the sum of squares of deviation of the experimental data from the calculated line is a minimum. If I_j and V_i are the various experimental values of I and V respectively, it can easily be shown that the value of "a" for which the above requirement is satisfied is given by $\hat{a}$ where

$$\hat{a} = \sum_{j=1}^{n} I_j / \sum_{j=1}^{n} V_j \quad \text{----------(5.6)}$$

TABLE 5.2: PERMEAMETER DATA FOR DETERMINATION OF FLOW COEFFICIENTS

Δ (cm)			Hydraulic Gradient	Average Time t (secs)	Macroscopic velocity v ($x10^{-3}$ m/s)
Δ_1	Δ_2	Average Δ	i		
3.00	3.00	3.00	0.300	4.70	11.82
2.80	2.80	2.80	0.280	4.80	11.60
2.50	2.50	2.50	0.250	5.30	10.50
2.30	2.30	2.30	0.230	5.80	9.58
2.00	2.00	2.00	0.200	6.80	8.17
1.80	2.00	1.90	0.190	6.80	8.17
1.60	1.90	1.75	0.175	7.20	7.72
1.50	1.70	1.60	0.160	7.57	7.33
1.50	1.50	1.50	0.150	8.50	6.54
1.20	1.20	1.20	0.120	10.60	5.24
1.00	1.00	1.00	0.100	12.50	4.44
0.70	0.70	0.70	0.070	17.00	3.27
0.50	0.50	0.50	0.050	23.40	2.38

Table 5.6 shows the summation of the 13 values each of I_j and V_j; from the table

$$\sum_{j=1}^{13} I_j = 2.275;$$

and $$\sum_{j=1}^{13} V_j = 96.78 \times 10^{-3};$$

Hence from equation (5.6),

$$\hat{a} = 2.275/(96.78 \times 10^{-3}) = 23.5069 \text{ s/m}.$$

Figure 5.2 shows a graphical plot of the experimental data and the calculated straight line.

If the deviation between an experimental value I_j and the calculated value, i.e. $I = \hat{a}v$, is ε_j, then the mean square error, MSE, an unbiased estimate of the variance of the experimental values along the calculated line is given as

$$MSE = \sum_{j=1}^{N} \varepsilon_j^2/(N-1)$$

where

$\sum_{j=1}^{N} \varepsilon_j^2$ = Residual sum of squares RSS

N = Number of sets of experimental data which for this case = 13.

Table 5.3 shows a summation of the squares of deviations for this case. From the table,

$$MSE = \frac{9.736 \times 10^{-4}}{12} = 81.1333 \times 10^{-6}$$

5.3.2. Regression Along The Quadratic Relation:

The least squares regression of experimental data to calculate a curve of the equation (5.4) requires the use of equations (2.7) and (2.8) described in Section 2.4.3.

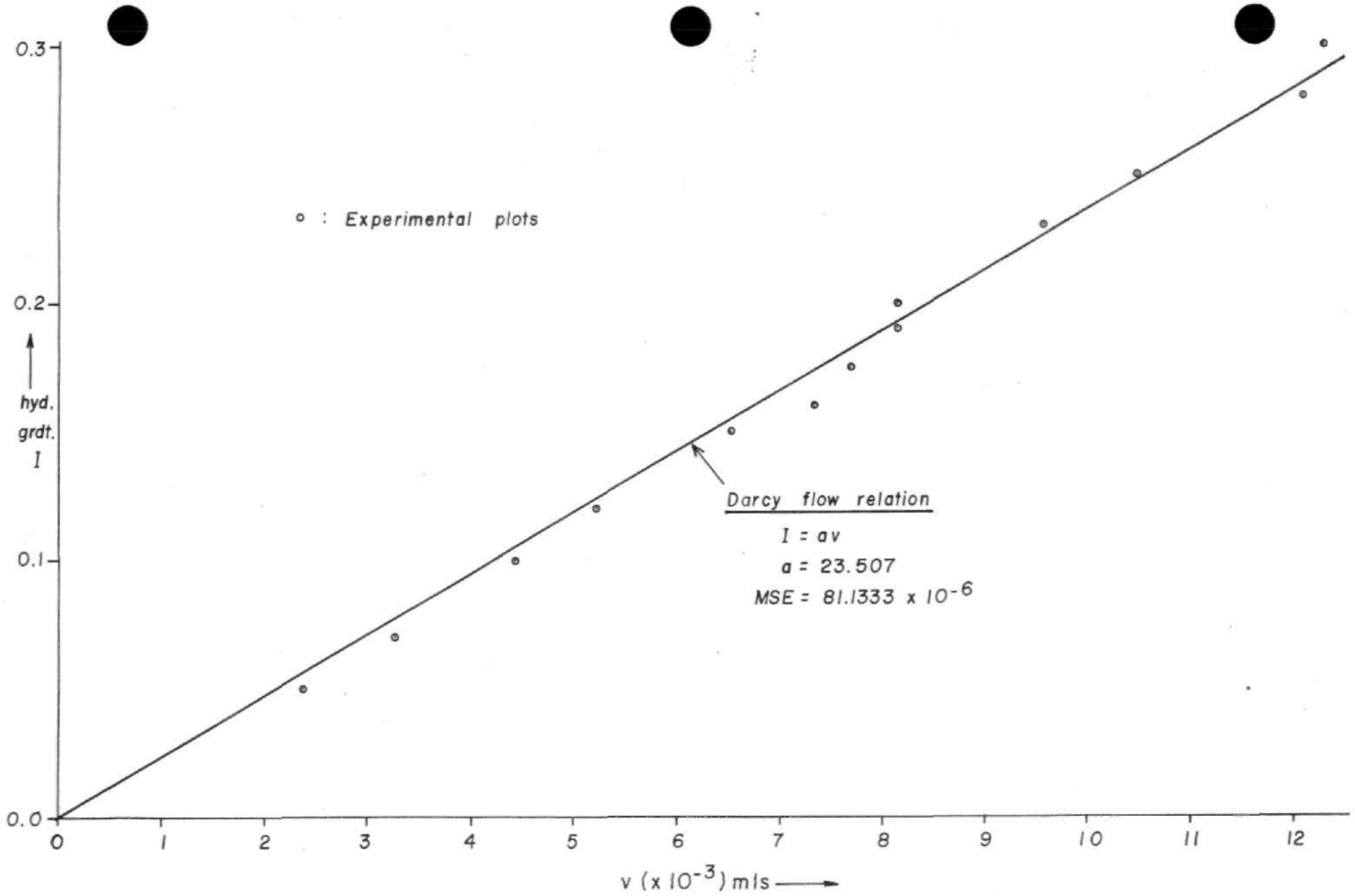


FIG. 5.2 : Regression of experimental plots to fit Darcy flow relation.

TABLE 5.3: CALCULATION OF THE MEAN SQUARE ERROR, MSE, FOR REGRESSION OF EXPERIMANTAL DATA UNTO I = av

Macroscopic Velocity v $x10^{-3}$ m/sec	Experimental I	Theoretical i from Darcian flow equation: I = av a = 23.5069 s/m		
		I Theoretical	Variation ε_j from Exptal.	Sq. of dev. x 10^{-4}
11.82	0.300	0.2779	0.0221	4.8841
11.60	0.280	0.2727	0.0073	0.5329
10.50	0.250	0.2468	0.0032	0.1024
9.58	0.230	0.2252	0.0048	0.2304
8.17	0.190	0.1921	0.0079	0.6241
8.17	0.190	0.1921	0.0021	0.0441
7.72	0.175	0.1815	0.0065	0.4225
7.35	0.160	0.1728	0.0128	1.6384
6.54	0.150	0.1537	0.0037	0.1369
5.24	0.120	0.1232	0.0032	0.1024
4.44	0.100	0.1044	0.0044	0.1936
3.27	0.070	0.0769	0.0069	0.4761
2.38	0.050	0.0559	0.0059	0.3481
Residual sum of squares =				9.736 x 10^{-4}
MSE (= $\frac{RSS}{12}$)				81.1333 x 10^{-6}

as done by Gill (1977). These equations are reproduced below:

$$\hat{a} = \frac{\sum_{1}^{N} V_j^4 \sum_{1}^{N} V_j I_j - \sum_{1}^{N} V_j^3 \sum_{1}^{N} V_j^2 I}{\sum_{1}^{N} V_j^4 \sum_{1}^{N} V_j^2 - (\sum_{1}^{N} V_j^3)^2} \quad \text{----------(5.7)}$$

$$\hat{b} = \frac{\sum_{1}^{N} V_j^2 \sum_{1}^{N} V_j^2 I_j - \sum_{1}^{N} V_j^3 \sum_{1}^{N} V_j I_j}{\sum_{1}^{N} V_j^4 \sum_{1}^{N} V_j^2 - (\sum_{1}^{N} V_j^3)^2} \quad \text{----------(5.8)}$$

Table 5.4 shows a summation of the various quantities involved in equations (5.7) and (5.8) above. From the table the following summations are obtained:

$$\sum_{1}^{13} V_j^4 = 7.6702 \times 10^{-8}$$

$$\sum_{1}^{13} V_j I_j = 19.7374 \times 10^{-3}$$

$$\sum_{1}^{13} V_j^3 = 7.7565 \times 10^{-6}$$

$$\sum_{1}^{13} V_j^2 I_j = 18.6083 \times 10^{-5}$$

$$\sum_{1}^{13} V_j^2 = 8.2971 \times 10^{-4}$$

Substituting these values into equations (5.7) and (5.8), ewe obtain

$$\hat{a} = \frac{7.05818 \times 10^{-11}}{3.47803 \times 10^{-12}}$$

$$= 20.29 \text{ s/m}$$

$$\hat{b} = \frac{1.300099 \times 10^{-9}}{3.478030 \times 10^{-12}}$$

$$= 373.80 \text{ (s/m)}^2$$

KASHIM IBRAHIM LIBRARY
RECEIVED
13 AUG 1987
ZARIA, NIGERIA

TABLE 5.4: SUMMATIONS FOR LEAST SQUARES REGRESSION OF EXPERIMENTAL DATA TO FIT INTO: $I = av + bv^2$

v $\times 10^{-3}$ m/sec	I	v^4 $\times 10^{-8}$	vI $\times 10^{-3}$	v^3 $\times 10^{-6}$	$v^2 I$ $\times 10^{-5}$	v^2 $\times 10^{-4}$
11.82	0.300	1.9520	3.5460	1.6514	4.1914	1.3971
11.60	0.280	1.8106	3.2480	1.5609	3.7677	1.3456
10.50	0.250	1.2155	2.6250	1.1576	2.7563	1.1025
9.58	0.230	0.8423	2.2034	0.8792	2.1109	0.9178
8.17	0.200	0.4455	1.6340	0.5453	1.3350	0.6675
8.17	0.190	0.4455	1.5523	0.5453	1.2682	0.6675
7.72	0.175	0.3552	1.3510	0.4601	1.0430	0.5960
7.35	0.160	0.2918	1.1760	0.3971	0.8644	0.5402
6.54	0.150	0.1829	0.9810	0.2797	0.6416	0.4277
5.24	0.120	0.0754	0.6288	0.1439	0.3295	0.2746
4.44	0.100	0.0389	0.4440	0.0875	0.1971	0.1971
3.27	0.070	0.0114	0.2289	0.0350	0.0749	0.1069
2.38	0.050	0.0032	0.1190	0.0135	0.0283	0.0566
	Σ	7.6702 $\times 10^{-8}$	19.7374 $\times 10^{-3}$	7.7565 $\times 10^{-6}$	18.6083 $\times 10^{-5}$	8.2971 $\times 10^{-4}$

Figure 5.3 shows a graphical plot of the experimental data and the calculated curve. Similarly, Table 5.5 shows a summation of the squares of deviations of experimental from calculated values of I. From the table, the mean square error is calculated as

$$MSE = \frac{3.2351}{12} \times 10^{-4} = 26.9592 \times 10^{-6}$$

Finally, the nonlinear parameter C, defined as b/a^2 is

$373.80/20.29^2 = 0.908$

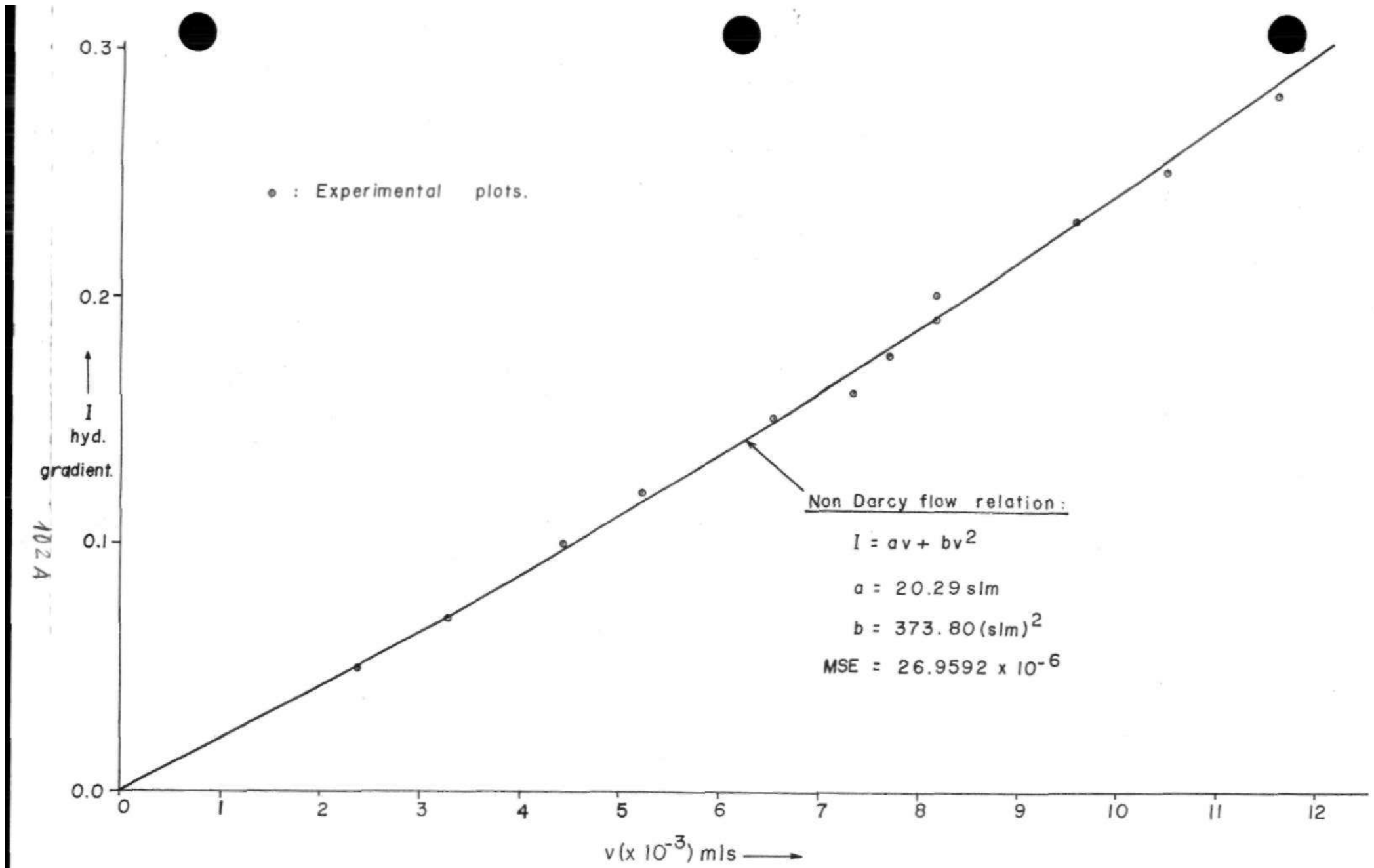


FIG 5.3: Regression of experimental plots to fit non Darcy flow relation.

TABLE 5.5: CALCULATION OF THE MEAN SQUARE ERROR (MSE) FOR REGRESSION OF EXPERIMENTAL DATA UNTO $I = av + bv^2$

Macroscopic Velocity v $\times 10^{-3}$ m/sec	Experimental I	Non-Darcian Flow Equation $I = av + bv^2$ $a = 20.29$ s/m; $b = 373.80(s/m)^2$		
		I Theoretical	Deviation ε_j from Exptal.	Sq. of Deviation $\times 10^{-4}$
11.82	0.300	0.2921	0.0079	0.6241
11.60	0.280	0.2857	0.0057	0.3249
10.50	0.250	0.2543	0.0043	0.1849
9.58	0.230	0.2287	0.0013	0.0169
8.17	0.200	0.1907	0.0093	0.8649
8.17	0.190	0.1907	0.0007	0.0049
7.72	0.175	0.1789	0.0039	0.1521
7.35	0.160	0.1693	0.0093	0.8649
6.54	0.150	0.1487	0.0013	0.0169
5.24	0.120	0.1166	0.0034	0.1156
4.44	0.100	0.0975	0.0025	0.0625
3.27	0.070	0.0703	0.0003	0.0009
2.38	0.050	0.0504	0.0004	0.0016
Residual sum of squares				3.2351×10^{-4}
MSE $(= \frac{RSS}{12})$				26.9592×10^{-6}

5.3.3. Regression Along The Logrithmic Relation:

In order to regress the experimental data so as to calculate a curve with an equation of the form written as equation (5.5), we regard logV as the regresso

and log I as the response variable in a linear regression between the two variables. Accordingly, it can be shown that the values of B and A which minimize the squares of deviations of the experimental from the calculated values of logV and log I are given as:

$$\hat{B} = \frac{\sum_{1}^{N}(\log V)_j(\log I)_j - \frac{1}{N}\sum_{1}^{N}(\log I)_j \sum_{1}^{N}(\log V)_j}{\sum_{1}^{N}(\log V)_j^2 - \frac{1}{N}(\sum_{1}^{N}(\log V)_j)^2} \quad \text{---(5.9)}$$

$$\hat{A} = (\overline{\log I}) - B(\overline{\log V}) \quad \text{----------(5.10)}$$

where

$$(\overline{\log I}) = \frac{1}{N}\sum_{1}^{N}(\log I)_j$$

$$(\overline{\log V}) = \frac{1}{N}\sum_{1}^{N}(\log V)_j$$

i.e. mean values of (log I) and (logV) respectively.

Table 5.6 shows a summation of the various quantities involved in equation (5.9) above. From the table, the following summations are obtained:

$$\sum_{1}^{13}(\log V)_j(\log I)_j = 123.8311$$

$$\sum_{1}^{13}(\log V)_j^2 = 327.4028$$

$$\sum_{1}^{13}(\log V)_j = -24.1537$$

$$\sum_{1}^{13}(\log I)_j = -64.9529$$

We also deduce that

$$(\overline{\log V}) = \frac{-64.9529}{13} = -4.9964$$

$$(\overline{\log I}) = \frac{-24.1537}{13} = -1.8580$$

TABLE 5.6: SUMMATIONS FOR LEAST SQUARES REGRESSION OF EXPERIMENTAL DATA TO FIT INTO log I = A+B log\

V x 10^{-3} (m/sec)	I	$\log_e V$	$\log_e I$	$(\log_e V)^2$	$(\log_e V)(\log_e I)$
11.82	0.300	-4.4380	-1.2040	19.6955	5.3422
11.60	0.280	-4.4568	-1.2730	19.8626	5.6733
10.50	0.250	-4.5564	-1.3863	20.7606	6.3165
9.58	0.230	-4.6481	-1.4697	21.6046	6.8312
8.17	0.200	-4.8073	-1.6094	23.1100	7.7370
8.17	0.190	-4.8073	-1.6607	23.1100	7.9836
7.72	0.175	-4.8639	-1.7430	23.6579	8.4777
7.35	0.160	-4.9131	-1.8326	24.1381	9.0036
6.54	0.150	-5.0298	-1.8971	25.2991	9.5422
5.24	0.120	-5.2514	-2.1203	27.5776	11.1344
4.44	0.100	-5.4171	-2.3026	29.3450	12.4733
3.27	0.070	-5.7230	-2.6593	32.7523	15.2189
2.38	0.050	-6.0407	-2.9957	36.4895	18.0962
96.78 x 10^{-3}	2.275	-64.9529	-24.1537	327.4028	123.8311

Substituting these values into equations (5.9) and (5.10), A and B are obtained as:

$$B = \frac{3.1501}{2.8736} = 1.0962$$

$$A = 3.6191$$

Figure 5.4 shows a graphical plot of the experimental data and the calculated curve. Similarly, Table 5.7 shows a summation of the squares of deviations of experimental from calculated values of I, using the

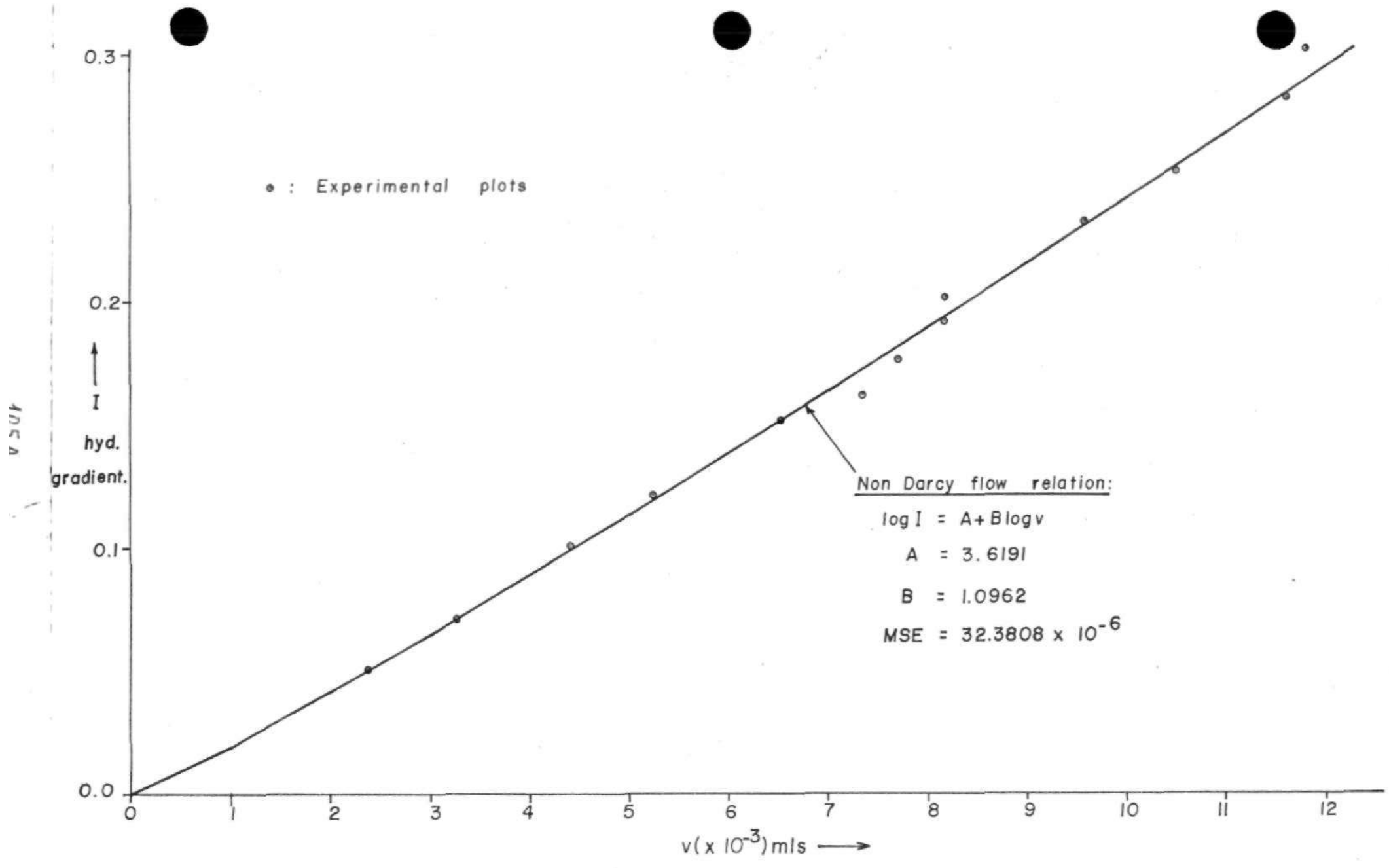


FIG 5.4: Regression of experimental plots to fit non Darcy flow relation.

TABLE 5.7: CALCULATION OF THE MEAN SQUARE ERROR (MSE) FOR REGRESSION OF EXPERIMENTAL DATA UNTO log I = A + B logV

Macroscopic Velocity v $x10^{-3}$ m/sec	Experimental I	None-Darcian Flow Equation log I = A + B logV A = 3.6191; B = 1.0962		
		I Theoretical	Deviation ε_j from Exptal.	Sq. of Deviation $x\ 10^{-4}$
11.82	0.300	0.2877	0.0123	1.5129
11.60	0.280	0.2818	0.0018	0.0324
10.50	0.250	0.2527	0.0027	0.0729
9.58	0.230	0.2295	0.0015	0.0225
8.17	0.200	0.1919	0.0081	0.6561
8.17	0.190	0.1919	0.0019	0.0361
7.72	0.175	0.1804	0.0054	0.2916
7.35	0.160	0.1709	0.0109	1.1881
6.54	0.150	0.1504	0.0004	0.0016
5.24	0.120	0.1179	0.0021	0.0441
4.44	0.100	0.0984	0.0016	0.0256
3.27	0.070	0.0703	0.0003	0.0009
2.38	0.050	0.0497	0.0003	0.0009
Residual sum of squares				$3.8857\ x\ 10^{-4}$
MSE $(= \frac{RSS}{12})$				$32.3808\ x\ 10^{-6}$

logrithmic equation. From the table the mean square error MSE is calculated as

$$MSE = \frac{3.8857}{12} \times 10^{-4} = 32.3808 \times 10^{-6}$$

5.4. CALCULATION OF PRECIPITATION RATES

In the calculation of the precipitation rates unto the bed of the porous matrix, the following assumptions are made:

1. The total precipitation unto the model is distributed uniformly over the surface area of the porous matrix bed.

2. At steady state, the total precipitation unto the model equals the discharge seeping out from the porous medium.

While it is recognized that the precipitation rates may not be exactly uniform from one point to another in the model, these assumptions, however, provide the simplest approach under the given conditions to the determination of the precipitation rate. They are also expected to give the best mean value to the actual variations in the experiment because they follow from the conditions of continuity, i.e. that inflow into the porous medium = outflow from the porous medium at steady state. Furthermore, such assumptions are also widely employed in the theoretical analyses of actual field drainage problems.

In the determination of the discharge out of the pipe P_1 in Figure 4.2, a container (drum) is used with the following dimensions:

Internal diameter = 0.56 m

Height = 0.86 m

$\therefore$ Volume = $\frac{\pi}{4} \times (0.56)^2 \times 0.86\ m^3 = 0.2118\ m^3$

Therefore if t = average time (in seconds) it takes to fill the container with water discharged from pipe P_1, then discharge Q_d is given by:

$$Q_d = \frac{0.2118}{t} \quad m^3/sec$$

Q_d is also the total precipitation over the surface area of the porous matrix bed. The total surface area A of the bed is

$$A = 4.87 \times 0.76 \ m^2$$

$$= 3.7012 \ m^2$$

and therefore, the precipitation rate R, assumed uniform over the surface area is:

$$R = \frac{Q_d}{A}$$

$$= \frac{0.2118}{3.7012 \ t} \quad m/sec.$$

In this way, the precipitation rates for the four experiments carried out are calculated as follows:

1. Experiment 1:

Average time t = 316.8 seconds.

$$R = \frac{0.2118}{3.7012 \times 316.8}$$

$$= 1.8063 \times 10^{-4} \ m/sec.$$

2. Experiment 2:

Average time t = 263.4 seconds

$$R = \frac{0.2118}{263.4 \times 3.7012}$$

$$= 2.1725 \times 10^{-4} \ m/sec.$$

3. Experiment 3:

Average time t = 259.8 seconds.

$$R = \frac{0.2118}{259.8 \times 3.7012}$$

$$= 2.2026 \times 10^{-4} \text{ m/sec.}$$

4. Experiment 4:

Average time t = 232.2 seconds.

$$R = \frac{0.2118}{232.2 \times 3.7012}$$

$$= 2.4645 \times 10^{-4} \text{ m/sec.}$$

5.5. DETERMINATION OF THEORETICAL WATER TABLE PROFILES FROM RAINFALL RATES

The precipitation rate values calculated above are now used in calculating the theoretical water tables as in the following sections.

5.5.1. Assumption Of Linear Flow:

Under the assumption of the applicability of Darcy's law as described by the equation

$$I = av ;$$

the ellipse equation, (equation 3.10c) is used for the determination of y for given values of x. Thus

$$y^2 = h^2 + Q_x (9.74 - x) \text{----------(5.11)}$$

The value of the drain spacing substituted for the S in equation (3.10c) equals twice the length of the model, which represents only half of the field of flow. Thus, S = 2 x 4.87 = 9.74 m.

Also in the equation (5.11) above

$$Q = a\,R$$

where a is the value calculated from the regression on Figure 5.2 and = 23.507 s/m; and R = the precipitation rate in m/sec.

5.5.2. Assumption of Nonlinear Flow:

Quadratic Relation:

Under the assumption of nonlinear flow described by the equation

$$I = av + bv^2$$

the equation derived in Section 3.4, i.e. equation (3.23b) is used. Thus

$$[y + \frac{P}{2Q}(4.87 - x)]^2 - [h + 8.87\frac{P}{2Q}]^2$$

$$= Qx\,(9.74 - x) \text{ ----------(5.12)}$$

where

$Q = a\,R$

$P = b\,R^2$

and the values of a and b as determined from the regression on Figure 5.3, i.e. a = 20.29; b = 373.80; and 9.74m= the drainage spacing.

5.5.3. Assumption of Nonlinear Flow:

Logrithmic Relation:

Under the assumption of nonlinear flow described by the logrithmic equation:

$$\log I = A + B \log V$$

We recognize that the logrithmic equation written above

is equivalent to the Izbash flow equation which is of the form:

$$V = MI^n \text{ ----------(5.13)}$$

from which we deduce that

$$\left.\begin{aligned} A &= \frac{1}{n} \log \frac{1}{M};\ B = \frac{1}{n};\ \text{and} \\ n &= \frac{1}{B};\ M = \exp(-A/B) \end{aligned}\right\} \text{ ----------(5.13a)}$$

Values of A and B have already been obtained from the regression of Figure 5.4 (see also Table 5.6 of Section 5.3.3) as

$$A = 3.6191;$$

$$B = 1.0962$$

We thus obtain from equations (5.13a) above

$$\left.\begin{aligned} n &= 1/1.0962 = 0.912242 \\ M &= \exp(-3.6191/1.0962) = 0.03628 \end{aligned}\right\} \text{ ----------(5.13b)}$$

Obtaining the water table profile equation for non-linear flow subject to equation (5.13) above requires the use of equation (2.40) discussed in Section 2.6.3 derived by Basak (1977). This equation is reproduced below

$$Y^{1+1/n} - Y_o^{1+1/n} = \left(\frac{R}{M}\right)^{1/n} \left(\frac{S/2}{H}\right)^{1+1/n} [1 - (1 - X)^{1+1/n}]$$

where

$$Y = y/H,\ Y_o = h/H$$

Multiplying through by $H^{1+1/n}$, we obtain

$$y^{1+1/n} + h^{1+1/n} = \left(\frac{R}{M}\right)^{1/n} (S/2)^{1+1/n} [1 - (1 - X)^{1+1/n}]$$

Substituting the values of n, M quoted in equation ((5.13b) gives

$$y^{2.0962} - h^{2.0962} = \left(\frac{R}{0.036828}\right)^{1.0962} (4.87)^{2.0962}$$

$$[1 - (1 - X)^{2.0962}] \quad \text{----------(5.14)}$$

where

$$X = \frac{x}{S/2} = \frac{x}{4.87}$$

Equation (5.14) is used in obtaining the theoretical water table profiles for this case.

Figures 5.5, 5.6, 5.7, 5.8, show the theoretical water table profiles in the porous medium for the various values of precipitation rates calculated for each of the three assumed flow conditions, viz:

(i) Darcy's flow $I = av$

$a = 23.507$

(ii) Non-Darcy flow: $I = av + bv^2$

$a = 20.29$; $b = 373.80$

(iii) Non-Darcy flow: $\log I = A + B \log V$

$A = 3.6191$

$B = 1.0962$

In the plots of Figures 5.5 - 5.8, the experimental water levels along the manometric glass tubes are also indicated for comparison. Tables 5.8, 5.9, 5.10, 5.11 show for each precipitation rate, a summary of the various water levels in each of the six manometric glass tubes, both experimental and theoretical.

The variation of the dimensionless drainage spacing i.e. S/H with the ratio h/H have also been calculated on

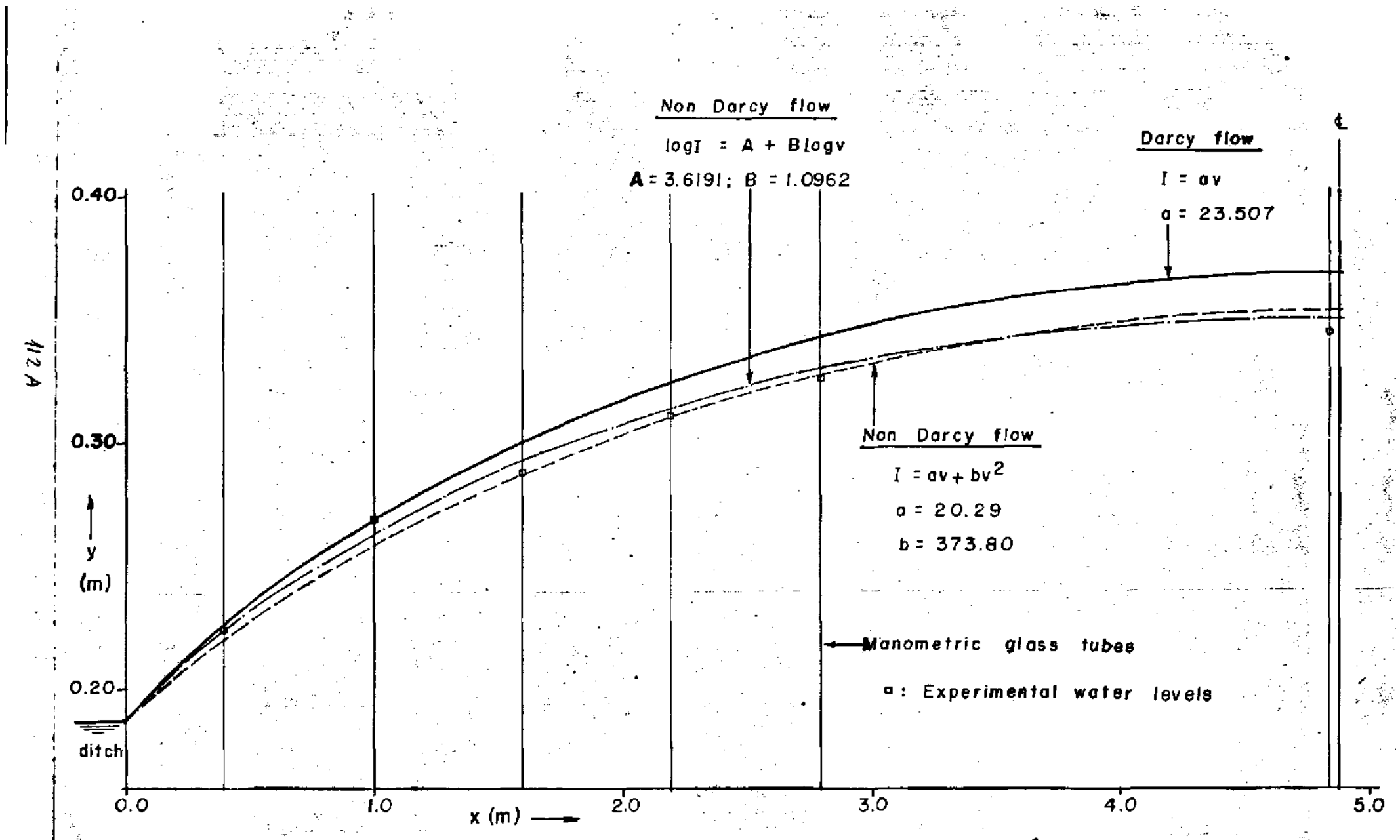


FIG.5.5: Experimental and theoretical water table profiles; R = 1.8063 x 10^{-4} mls.

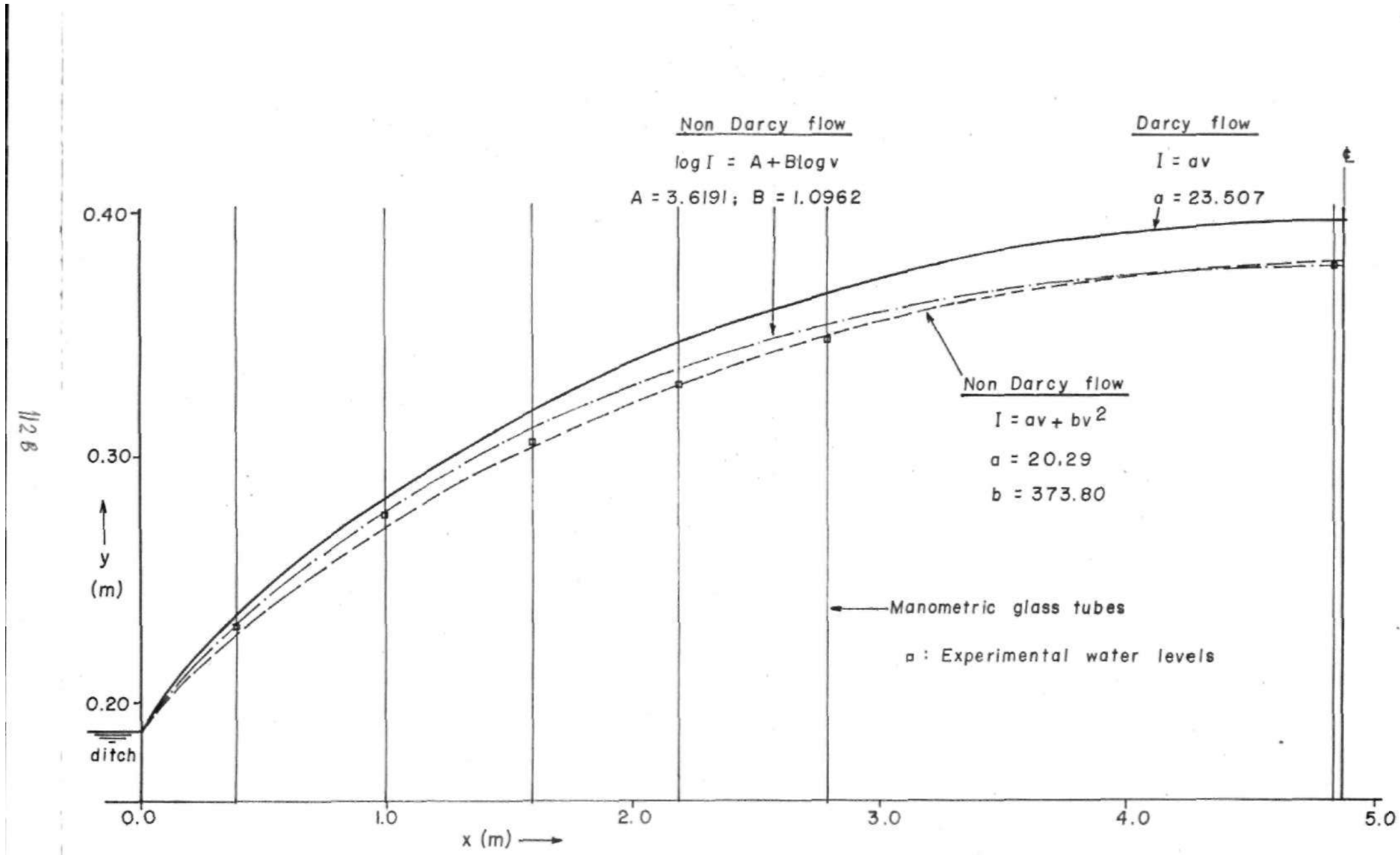


FIG 5.6: Experimental and theoretical water profiles; $R = 2.1725 \times 10^{-4}$ m/s

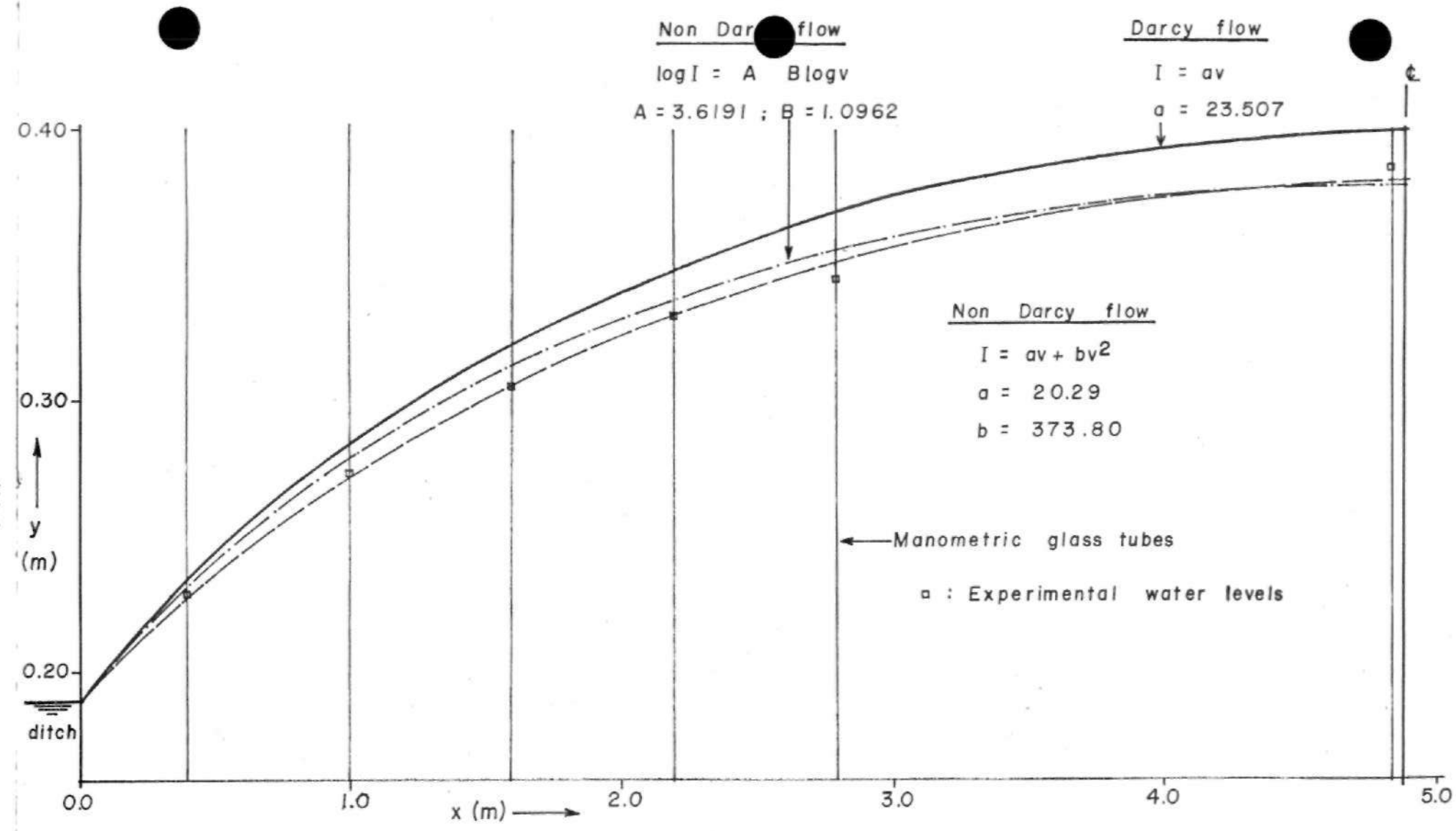


FIG 5.7: Experimental and theoretical water table profiles , $R = 2.2026 \times 10^{-4}$ m/s

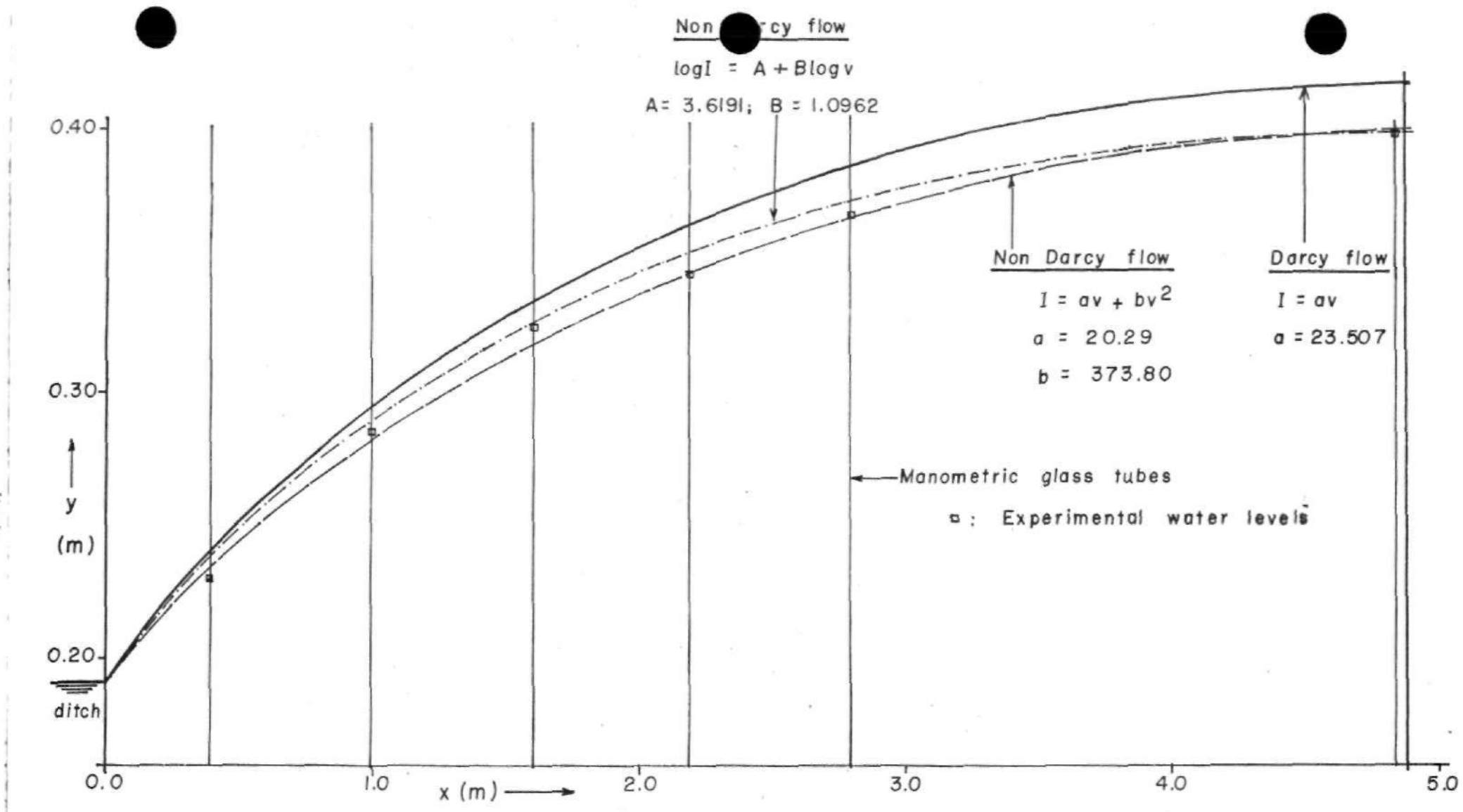


FIG 5.8: Experimental and theoretical water table profiles, $R = 2.4645 \times 10^{-4}$ m/s

the basis of each of the three assumed flow conditions enumerated above. The variations are shown in Figure 5.9 for the typical precipitation rate

$$R = 2.4645 \times 10^{-4} \text{ m/sec.}$$

TABLE 5.8: WATER TABLE PROFILES

$$R = 1.8063 \times 10^{-4} \text{ m/sec.}$$

Distance from ditch (m) X	Manometer No.	Water Table Elevations y (m)				
		Experimental	Theoretical			
			i=av a=20.29	i=av i=23.507	$i=av+bv^2$ a=20.29 b=373.80	log I = A+BlogV A=3.6191 B=1.0962
0.00		0.187	0.1870	0.1870	0.1870	0.1870
0.395	1	0.224	0.2202	0.2250	0.2197	0.228
0.995	2	0.268	0.2585	0.2682	0.2580	0.2627
1.595	3	0.287	0.2873	0.3002	0.2871	0.2918
2.190	4	0.310	0.3090	0.3243	0.3095	0.3132
2.790	5	0.325	0.3255	0.3425	0.3267	0.3291
4.835	6	0.344	0.3490	0.3683	0.3533	0.3504
4.870			0.3490	0.3683	0.3534	0.3504

TABLE 5.9: WATER TABLE PROFILES

$R = 2.1725 \times 10^{-4}$ m/sec.

Distance from ditch (m) X	Manometer No.	Water Table Elevations y (m)				
			Theoretical			
		Experimental	I=av a=20.29	I=av =23.507	$I=av+bv^2$ a=20.29 b=373.80	log I = A+BlogV A=3.6191 B=1.0962
0.000		0.188	0.1880	0.1880	0.1880	0.1880
0.395	1	0.230	0.2271	0.2328	0.2263	0.2308
0.995	2	0.276	0.2713	0.2825	0.2704	0.2773
1.595	3	0.305	0.3041	0.3189	0.3037	0.3107
2.190	4	0.3285	0.3288	0.3461	0.3291	0.3351
2.790	5	0.347	0.3474	0.3666	0.3486	0.3531
4.835	6	0.377	0.3738	0.3956	0.3787	0.3772
4.870			0.3738	0.3956	0.3788	0.3772

TABLE 5.10: WATER TABLE PROFILES

$R = 2.2026 \times 10^{-4}$ m/sec.

Distance from ditch (m) X	Manometer No.	Water Table Elevations y (m)				
			Theoretical			
		Experimental	I=av a=20.29	I=av a=23.507	$I=av+bv^2$ a=20.29 b=370.80	log I = A+BlogV A=3.6191 B=1.0962
0.000		0.189	0.1890	0.1890	0.1890	0.1890
0.395	1	0.229	0.2295	0.2342	0.2277	0.2322
0.995	2	0.273	0.2732	0.2842	0.2722	0.2790
1.595	3	0.306	0.3063	0.3209	0.3058	0.3127
2.190	4	0.331	0.3311	0.3483	0.3314	0.3374
2.790	5	0.345	0.3499	0.3690	0.3511	0.3555
4.835	6	0.386	0.3765	0.3981	0.3815	0.3797
4.870			0.3765	0.3982	0.3815	0.3797

TABLE 5.11: WATER TABLE PROFILES

$R = 2.4645 \times 10^{-4}$ m/sec.

Distance from ditch (m) X	Manometer No.	Water Table Elevations y (m)				
		Experimental	Theoretical			
			i=av a=20.29	i=av a=23.507	i=av+bv² a=20.29 b=373.80	log I = A+BlogV A=3.6191 B=1.0962
0.000		0.191	0.1910	0.1910	0.1910	0.1910
0.395	1	0.230	0.2344	0.2406	0.2333	0.2387
0.995	2	0.285	0.2828	0.2948	0.2816	0.2898
1.595	3	0.325	0.3815	0.3343	0.3178	0.3263
2.190	4	0.345	0.3452	0.3637	0.3453	0.3529
2.790	5	0.367	0.3653	0.3858	0.3665	0.3724
4.835	6	0.398	0.3938	0.4170	0.3992	0.3984
4.870			0.3938	0.4170	0.3993	0.3984

5.6. FLOW REGIMES

The coefficients a and b of flow resistivity are theoretically, slightly variable with the regime of flow, essentially the Reynold's number. They may, however, normally be assumed constant but only over a restricted range of Reynold's numbers (Volker, 1975). For this reason, it becomes important to ascertain whether the flow regime in the sand tank model does fall in the range of Reynold's numbers that was investigated in the permeameter experiment for the determination of the flow coefficients a and b of the sample porous matrix.

Furthermore, this study is concerned with the range of laminar flow regimes for which Darcy's law does not apply, i.e. transitional or steady inertial flow regimes. This regime of flow falls within a specified range of Reynold's numbers: ranging from a lower limit of 1 to 10 to an upper limit from 60 to 150, according to Schneebelli (1955), Wright (1968) and others. It is therefore desirable for the study to determine, in addition, whether the range of flow regimes in the sand tank model falls in the range of the transitional flow regime.

The Reynold's number Re is defined as

$$Re = \frac{VD}{(\mu/\rho)}$$

where

(μ/ρ) = kinematic viscosity of water at the relevant temperature

V = macroscopic velocity of flow

D = average grain size.

The kinematic viscosity of water at 20°C is $= 1.00 \times 10^{-6}$ m²/sec and at 40°C is $= 0.685 \times 10^{-6}$ m²/sec. (Bolz & Tuve, 1973). The temperature of water in the experiment, measured at its outflow from the porous medium, is = 23°C.

Interpolating these values the kinematic viscosity of water at 23°C, which is the water temperature in the experimental conditions is $= 0.953 \times 10^{-6}$ m²/sec $= (\mu/\rho)$.

Similarly, the average grain diameter, determined

from the grain size analysis of the sample is = 3.44 mm.

i.e. $D = 3.44 \times 10^{-3}$ m

Consequently, the Reynold's number range in the permeameter and sand box model experiments can now be determined.

5.6.1. Range For Permeameter Test:

The range of macroscopic velocities applied in the permeameter test was as follows:

$$V_{max} = 11.82 \times 10^{-3} \text{ m/sec}$$

$$V_{min} = 2.38 \times 10^{-3} \text{ m/sec.}$$

The corresponding range of Reynold's numbers, i.e. $Re = VD/(\mu/\rho)$ is:

$$(Re)_{max} = \frac{V_{max} D}{(\mu/\rho)}$$

$$= \frac{11.82 \times 3.44 \times 10^{-6}}{0.953 \times 10^{-6}}$$

$$= 42.666$$

$$(Re)_{min} = \frac{V_{min} D}{(\mu/\rho)}$$

$$= \frac{2.38 \times 3.44 \times 10^{-6}}{0.953 \times 10^{-6}}$$

$$= 8.591$$

Thus, the maximum Reynold's number clearly falls in the range of transitional non-Darcy flow regimes. The minimum Reynold's number on the other hand falls within the range of the lower limit for transitional non-Darcy flow. The nonlinearity of flow is however rather weak.

(b) For $R = 2.1725 \times 10^{-4}$ m/sec

Total discharge Q_d into ditch is

$R \times 4.87 \times 0.76$

i.e. $Q_d = 2.1725 \times 10^{-4} \times 4.87 \times 0.76$

$= 8.0409 \times 10^{-4}$ m³/sec

Cross-sectional area of flow at exit face is

$A = 0.76 \times 0.188$

$\therefore$ macroscopic velocity is

$V = Q_d/A$

$= 5.628 \times 10^{-3}$ m/sec

$\therefore$ $Re = \frac{VD}{(\mu/\rho)}$

$= \frac{5.628 \times 3.44 \times 10^{-6}}{0.953 \times 10^{-6}}$

$= 20.3151$

(c) For $R = 2.2026 \times 10^{-4}$ m/sec

Total discharge Q_d into ditch is

$Q_d = 2.2026 \times 10^{-4} \times (4.87 \times 0.76)$

$= 8.1523 \times 10^{-4}$ m³/sec

Cross-sectional area of flow at exit face is

$A = 0.189 \times 0.76$

$\therefore$ macroscopic velocity is

$V = \frac{Q_d}{A}$

$= 5.675 \times 10^{-3}$ m/sec

$$\therefore \quad Re = \frac{VD}{(\mu/\rho)}$$

$$= \frac{5.675 \times 3.44 \times 10^{-6}}{0.953 \times 10^{-6}}$$

$$= 20.4848$$

(d) For R = 2.4645×10^{-4} m/sec

Total discharge Q_d into ditch is

$$Q_d = 2.4645 \times 10^{-4} \times (4.87 \times 0.76)$$

$$= 9.1216 \times 10^{-4} \ m^3/sec$$

Cross-sectional area of flow at exit face is

$$A = 0.191 \times 0.76$$

$\therefore$ macroscopic velocity is

$$V = Q_d/A$$

$$= 6.284 \times 10^{-3} \ m/sec$$

$$\therefore \quad Re = \frac{VD}{(\mu/\rho)}$$

$$= \frac{6.284 \times 3.44 \times 10^{-6}}{0.953 \times 10^{-6}}$$

$$= 22.683.$$

Two conclusions are drawn from the analyses presented above:

1. The flow regimes in the sand tank model experiments (Re = 16.980, 20.315, 20.485, and 22.683) fall in the range that was investigated in the permeameter experiments (Re = 8.591 to 44.66) for the determination of the resistivity coefficients of the material. The

application of the values of the flow parameters (coefficients a, and b) obtained from the permeameter experiment, to the sand tank model experiments can therefore be considered valid.

2. The flow regimes in both the permeameter and the sand tank model experiments fall into the range of transitional non-Darcy flow regimes.

5.7. DISCUSSION OF RESULTS

5.7.1. On Permeameter Test Results:

The determination of the conductivity characteristics of a soil is the first requirement for the design of subsurface drainage for an agricultural land. In the determination of these properties for a coarse sand using a constant head permeameter, the results and analyses obtained herein have shown that different interpretations can be given to the data obtained from the permeameter test to postulate a flow equation relating the hydraulic gradient with the macroscopic velocity. The first of these, which assumes a linear relationship between the hydraulic gradient and the velocity (Darcy's law) is the most widely used. The two others are both based on nonlinear velocity-gradient relationships. Experimental results have shown that although Darcy's law gives a good fit to the experimental data (mean square error MSE = 81.1333×10^{-6}), the nonlinear relationships give better fits (MSE = 26.9592×10^{-6} and 32.3808×10^{-6}) as seen from Figures 5.2 to 5.4. In other words a 66.8% and a 60.1% reduction

water table profiles based on non-Darcy flows could be attributable to a number of factors with the experimental set up. These include:

1. The uneven surface of the container base of the rainfall simulator which resulted in unequal water levels along the length of the rainfall simulator. This caused slight variations in precipitation rates along the length of the container, contrary to assumptions of uniform precipitations.

2. Non-uniformity in the geometry and roughness of the surfaces of the discharge holes of the rainfall simulator. This meant that the discharges from the holes, which were of equal diameters were nonetheless unequal, due to variations in discharge coefficients of the holes from one area of the container to another.

3. Slight leakages in locations along intersections of wall and flow surfaces and at points of entry of the manometric glass tubes. However, additional measures were taken in sealing these leakage points and effectively reducing them to negligible quantities.

5.7.3. On Drain Spacing Equations:

Figure 5.9 presents three curves showing the variation between the nondimensional spacing S/H and the ratio h/H for each of three assumed flow conditions represented by the equations (5.3), (5.4), and (5.5) respectively, for a typical precipitation rate R = 2.4645×10^{-4} m/sec. falling on the porous medium used in the model experiment.

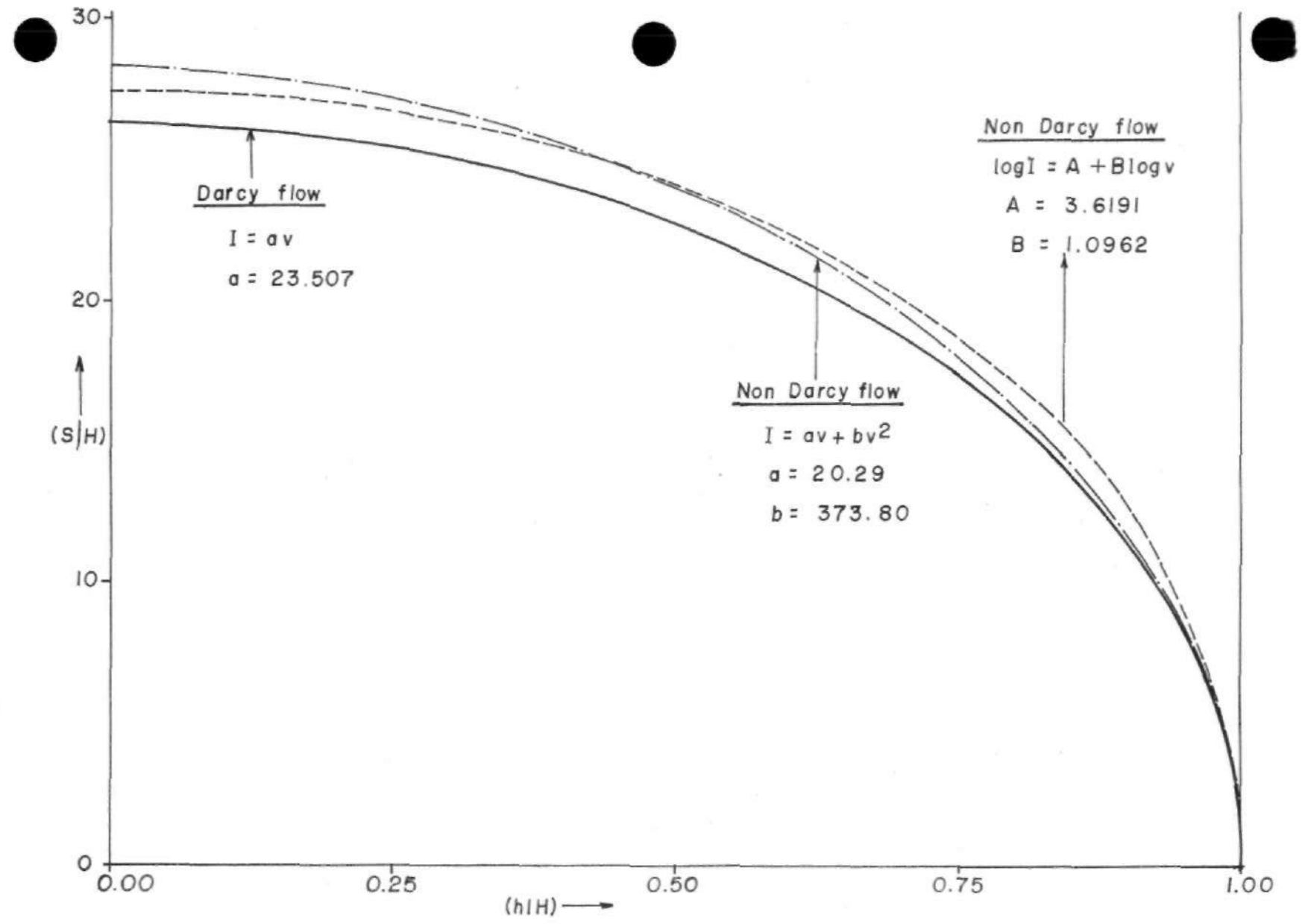


FIG. 5.9: Variation of dimensionless spacing (S/H) with the ratio (h/H) for three assumed flow conditions ; $R = 2.4645 \times 10^{-4}$ m/s

The curves are represented by the equations (3.11), (3.24) and (5.41), respectively. It could not be possible to determine the experimental plot of the spacing (S/H) against the water level (h/H) because the model length, representing L could not be altered with the given set up. From the figure 5.9, the non Darcy flow drain spacing equation (equation 2.41) based on Izbash's nonlinear flow equation (equation 5.13) gives higher drainage spacing than that given by equation(3.24) based on the quadratic flow relation (equation 5.4) for h/H ratio ≥ 0.44. For h/H < 0.44 the reverse obtains. Both equations, however, give consistently higher drainage spacings than predicted by the ellipse equation (equation 3.11) based on the Darcy flow equation (equation 5.3) for all values of h/H.

For instance, for a typical ratio of h/H = 0.25, the spacing S/H is increased from 25.4 to 27.1 by using the spacing formula of equation (3.24) instead of equation (3.11) based on Darcian linearity; i.e. a 6.7% increase in spacing. Conversely, it is deduced that for a given drain spacing, the formula based on non-Darcy flow gives greater lowering of the water table height, H for a given water level in the drainage ditch, h, or depth of drain tube.

CHAPTER SIX

CONCLUSIONS AND RECOMMENDATIONS

From the analytical solution proposed in this study and the various experimental results and their analyses, the following conclusions can be drawn.

6.1 CONCLUSIONS

(1) An approximate analytical solution has been developed which shows close agreement with experimental data, for non-Darcy flow toward parallel ditch drains through a porous medium consisting of coarse sand of effective size 2.86 mm. Same agreement is expected to be obtained for other sizes of soil. For fine grain soils in which Darcy flow is known to occur, the proposed solution reduces to the more conventional ellipse equation for drain spacing, which applies for cases of Darcy flow.

(2) Water table profiles given by the proposed analytical solution agree closely with those given by analytical solutions obtained earlier by other researchers, based on nonlinear flow equations for the given porous medium and flow regimes obtained in the sand tank model experiments.

(3) The water table profiles obtained in the sand tank experimental model are identical to those theoretically expected in one symmetrical half of a flow domain between two parallel ditch drains. This therefore confirms

the assumption that the centreline between two ditch drains could be represented in a model study by an impermeable vertical boundary.

(4) The close agreements of the theoretical water table profiles with the experimental water levels obtained in the manometric glass tubes of the sand tank model verify the assumptions made in the calculation of the precipitation rate, R, i.e. that the steady discharge supplied to the model is uniformly precipitated over the surface area of the porous matrix bed, and that at steady state it equals the discharge out of the porous medium.

(5) The shape of the water table profile between two parallel ditch drains under the non-Darcy flow conditions obtained in the sand tank model experiments is not elliptic, and, for a given water level in the drain would lie below the water table that would be expected if the flow were assumed to be linear and subject to Darcy's law.

(6) For the porous medium used in the experiment (coarse sand, effective size 2.86 mm), the interpretation of data from permeameter experiments in terms of a non-linear flow equation rather than a linear one, gives a better description of the conductivity characteristics of the material. The same is expected to apply for other sizes of coarse grained soils under similar flow conditions.

(7) It is also found that if the conductivity characteristics of a coarse grained porous medium are evaluated in terms of its nonlinear flow parameters and a drain spacing formula is used which considers the nonlinearity of flow, the resulting spacing so obtained would be greater than that predicted on the basis of linear flow assumption. The difference becomes greater with increasing nonlinearity of flow. In a typical instance, the calculated spacing for a weakly nonlinear flow at a certain given precipitation rate and a h/H ratio = 0.25, was found to be 6.7% greater if calculated from the proposed solution obtained herein than if on the basis of a linear flow assumption.

(8) The above fact reveals that the identification of the existence of non-Darcy flow in the soil and calculation of the drain spacing accordingly would enhance great savings of costs in any large agricultural land drainage or reclamation project.

6.2. RECOMMENDATIONS

The results obtained in this study can be considered to constitute an initial step towards providing a practical drainage design approach based on non-Darcy flow for the steady state condition. In order to evolve more comprehensive design procedures based on non-linear flow however, a number of factors would still need to be put into consideration in separate studies in order to take account of varying conditions such as:

(a) the effect of an increasing depth h of the impervious layer from the ditch water level on the seepage flow pattern as well as the flow regimes (the calculated Re). Very high values of h are known to affect the validity of the D-F assumptions employed in the analysis of the seepage flow contained in this study;

(b) transient response of the ground water table to a pattern of precipitation events;

(c) the effect of capillary storage and flow above water table (partially saturated soil);

(d) rate of fall of water table at the instant precipitation ceases.

The sand tank experimental model can be adopted to study unsteady state flow conditions such as the rates of fall or rise of the ground water table or under conditions of non-uniform (spatially varied) precipitation rates. It can also be used to study the performance of different drain tube materials by monitoring the behaviour of the water table fluctuations between drains buried in the porous medium of the model using the manometric glass tubes.

The results of this study could find wide application in river basin areas containing aquifers of medium to coarse grained material under relatively high discharge conditions. In this country, such areas exist, notably in the lower sedimentary basins such as the lower catchment areas of the Sokoto-Rima Basin; eg. the Gwandu

aquifer in the lower Rima valley, and soils in the Goronyo area of the middle Rima valley in Sokoto State. Such soils contain thick sandy deposits with significant ground water storage.

REFERENCES

1. AHMED, N. & SUNADA, D.K. (1969): Non-Linear Flow in Porous Media. J. Hyd. Div., ASCE: Vol, 95, No. HY6, pp. 1847 - 1857.

2. ALLISON, L.E. (1962): Salinity status of irrigation schemes of Northern Nigeria. Consultants report No. 4, Min. of Agric., N. Nigeria.

3. ALLISON, L.E. (1964): Salinity in relation to irrigation; in Advances in Agronomy (Norman, A.G. ed.) Vol. 16, Academic Press, N.York.

4. ANANDAKRISHNAN, M. and VARADARAJULU, G.H. (1963): Laminar and Turbulent flow of water through sand. J. Soil Mech. and Foundation Div., ASCE, 89(SM5): pp. 1 - 15.

5. ARBHABHIRAMA, A. and DINOY, A.A.(1973): Friction Factor and Reynold's number in Porous Media Flow. J. Hydraulics Div. ASCE, Vol.99, No. HY6, pp. 901 - 911.

6. ARONOVICI, V.S. and DONNAN, W.W.(1946): Soil permeability as a criterion for drainage design. Trans. Amer. Geophys. Union 27: pp. 95 - 101.

7. BASAK, P.(1976): Steady non-Darcian seepage through embankments. J. Irrig. and Drainage Div. ASCE, Vol. 102, No. 1R4, pp. 435 - 443.

8. BASAK, P.(1977): Non-Darcy flow and its implication to seepage problems. J. Irrig. and Drainage Div. ASCE, Vol. 103, No. 1R4, pp. 459 - 473.

9. BEAR, J.(1972): Dynamics of Fluids in Porous Media. American Elsevier, N. York.

10. BEAR, J., ZASLAVSKY, D. and IRMAY, S.(1968): Physical principles of water percolation and seepage. UNESCO, Paris, 1968.

11. BERNSTEIN, L.(1974): Crop growth and salinity. In Drainage for Agric. (Van Schilfgaarde, J. ed.). Am. Soc. Agrm. Inc. Monograph No. 17, pp. 39-54, Madison, Wisconsin.

12. BOER, S.A.D. and VAN DER MOLEN, W.H.(1972) Electrical Models: Conductive Sheet Analogues. In Int. Inst. for land Reclamation and Improvement; Wageningen, the Netherlands. Publ. 16 Vol. 1; Drainage Principles & Applications, pp. 201 - 221.

13. CHILDS, E.C.(1969): An introduction to the Physical Basis of soil Water Phenomenon. John Wiley & Sons, N. York. 493 pp.

14. BOLZ, R.E. and TUVE, G.L.(1973): Handbook of Tables for applied Engineering Science. C.R.C. Press, Inc.

15. BOUWER, H.(1974): Developing Drainage Design Criteria. In Van Schilfgaarde (ed.). Drainage for Agriculture. Am. Soc. Agron. Inc. Monograph No. 17, Madison, Wisconsin, pp. 67 - 81.

16. DAGAN, G.(1964); Spacing of Drain by an approximate method. Journal of Irrigation and Drainage Division, ASCE, Vol. 90, No. 1R1, pp. 41 - 66

17. DONNAN, W.W.(1959): Drainage of agricultural lands using interceptor lines. J. Irrig. and Drainage Div. ASCE Vol. 85, No. 1R1, pp. 13 - 23.

18. DONNAN, W.W. and SCHWAB, G.D.(1974): Current Drainage Methods in the U.S.A. In Van Schilfgaarde (ed): Drainage for Agriculture. American Society of Agronomy Monograph No. 17, Madison, Wisconsin, pp. 93 - 114.

19. ENGELUND, F.(1957): The Water Table in Equilibrium with Rainfall or Irrigation Water. In Luthin, J.N. (ed), Drainage of Agricultural Lands. Am. Soc. Agron. Monograph No. 7, Madison, Wisconsin.

20. FIREMAN, M.(1957): Salinity and Alkalinity Problem in Relation to High Ground Water Tables in Soils. In Luthin, J.N. (ed), Drainage of Agricultural Lands. Am. Soc. Agron. Monograph No. 7, Madison, Wisconsin.

21. FOX, J.A.(1974): An Introduction to Engineering Fluid Mechanics. Macmillan Press, London, 446 pp.

22. FRAMJI, K.K.(1974): A Review of Waterlogging and Drainage Problem and their Solutions in India. Int. Comm. Irrigation & Drainage Bulletin, Jan., 1974.

23. GILL, M.A.(1976): Analysis of one-dimensional vertical Non-Darcy Infiltration. J. Hydrology 31: 1 - 11.

24. GILL, M.A.(1977): Analysis of Permeameter Data to obtain Parameters of Non-Darcy Flow. Journal of Hydrology 32: 165 - 173.

25. GLOVER, R.E.(1978): Transient Ground Water Hydraulics. 2nd printing, Water Resources Publications Fort Collins, pp. 413.

26. GRABLE, A.R.(1966): Soil Aeration and Plant growth in Norman, A.G.(ed): Advances in Agronomy Vol. 18, Academic Press, New York.

27. GUITJENS, J.C.(1974): Hydraulic Models. Chp. 22 in Van Schilfgaarde, J. (ed); Drainage for Agriculture. Am. Soc. Agron. Inc. Agronomy Monograph No. 17, Madison, Wisconsin.

23. HARDING, S.W. and WOOD, J.K.(1941): Model tests of flow into drains. Soil Science Society of American Proc. V6, pp. 6 - 9.

29. HARRIS, C.I., ERICSON, H.T., ELLIS, M.K., LARSON, J.E.(1962): Water level control in agricultural soils as related to subsidence rate, crop yield, and response to Nitrogen. Soil Science 94, 158 - 161.

30. HAYWARD, H.E. and WADLEIGH, C.H.(1949): Plant growth in saline and alkali soils. Advances in Agronomy 1: 1 - 38. Academic Press, New York.

31. IRMAY, S.(1958): On the theoretical derivation of Darcy and Forchheimer Formulas. Trans. Amer. Geophysics Union No. 4; 39: pp. 702 - 707.

32. KIRKHAM, D.(1939): Artificial Drainage of Land: Streamline Experiments. Trans. American Geophysical Union 20, p. 677.

33. KIRKHAM, D.(1940): Artificial drainage of land: streamline experiments. The Artisian Basin II American Geophys. Union 21: 587 - 593.

34. KIRKHAM, D.(1945): Artificial drainage of land: streamline experiments. The Artesian Basin III. Amer. Geophys. Union 26: No. 3, pp. 393 - 406.

35. KIRKHAM, D.(1957): The ponded water case. In "Theory of land Drainage" in Luthin, J.N. (ed): Drainage of agricultural lands. Amer. Soc. Agron. Monograph No. 7, Madison, Wisconsin.

36. KIRKHAM, D.(1958): Seepage of steady Rainfall through soil into Drains. Trans. Amer. Geophys. Union 39: pp. 892 - 908.

37. KIRKHAM, D.(1961): An upper limit for the heights of the water table in drainage design formulas. Proc. 7th Int. Congress of Soil Science Soc., Madison, Wisconsin Comm. VI: August, 1960, I, 486 - 492.

38. KIRKHAM, D.(1967): Explanation of Paradoxes in Dupuit-Forchheimer Seepage Theory. Water Resources Research Vol. 3, No. 2, pp. 609 - 622.

39. KIRKHAM, D., TOKSOZ, S., VAN DER PLOCG, R.R.(1974): Steady flow to drains and wells. In Van Schilfgaarde, J. (ed). Drainage for agriculture. Am. Soc. Agron. Inc. Monograph No. 17, Madison, Wisconsin.

40. LAMB, H.(1932): Hydrodynamics. 6th Edition Reprint. Dover, New York.

41. LELIAVSKY, S.(1965): Design of Dams for Percolation and Erosion. Vol. 3: of Design Textbooks in Civil Engineering. Chapman & Hall Ltd., London.

42. Luthin, J.N.(1957): Drainage of Irrigated Lands. In Luthin, J.N. (ed) Drainage of Agricultural Lands. Am. Soc. Agron. Inc. Monograph No. 7, Madison, Wisconsin.

43. LUTHIN, J.N. and HAIG, A.(1971): Some factors affecting flow into drain pipes. Hilgardia 41(10): 235 - 245.

44. LUTHIN, J.N.(1973): Drainage Engineering. Second Reprint. Robert Krieger, New York. pp. 250.

45. LUTHIN, J.N.(1974): Drainage analogues. In Van Schilfgaarde, J. (ed). Drainage for agriculture. Am. Soc. Agron. Monograph No. 17. Madison, Wisconsin.

46. MAAS, E.V. and HOFFMAN, G.J.(1977): Crop Salt Tolerances; Current Assessment. J. Irrig. and Drainage Div., ASCE, Vol. 103, No. 1R2, pp. 115 - 134.

47. MAASLAND, M.(1959): Water Table Fluctuations induced by intermittent Recharge. J. Geophys. Research. Vol. 64, No. 5, pp. 549 - 559.

48. MAASLAND, M.(1964): Water Table Fluctuations induced by Irrigation. Transactions, ASCE Vol. 128, Part III, pp. 142 - 161.

49. MAURYA, P.R. and SINGH (1979): Salinity Status and Waterlogging in Irrigated Agriculture of Northern Nigeria. Trans. 6th National Irrigation Seminar, A.B.U., Zaria, pp. 146 - 163.

50. MAURYA, P.R.(1982): Problems of Weed, Salinity, Erosion, and Drainage in Irrigation Projects. Proc. 4th Afro-Asian Congress, Int. Commission on Irrigation and Drainage, Lagos, 1982.

51. MAC-DONALD & PARTNERS (1973): Feasibility Report of South Chad Irrigation Project. Consultants Report. Chad Basin Dev. Authority.

52. McNEAL, B.L.(1974: Soil salts and their Effects on Water Movement. Chp. 15 in Van Schilfgaarde (ed). Drainage for Agriculture. Am. Soc. Agron. Monograph 17, Madison, Wisconsin.

53. McWHORTER, D.B. and DUKE (1976): Transient Drainage with nonlinearity and capillarity. J. Irrigation & Drainage Div. ASCE Vol. 102, No. 1R2, pp. 193 - 204.

54. McWHORTER, D.B.(1977): Drain spacing Based on Dynamic Equilibrium. J. Irrigation & Drainage Div. ASCE. Vol. 103, No. 1R2, pp. 259 - 271.

55. MEHTA, M.L.(1957): The Behaviour of subsoil water table under the Punjab Canals. Trans. Int. Comm. Irrig. and Drainage, 3rd Congress, Vol. 5, pp. 10.71 - 10.88.

56. MOODY, W.T.(1966) Non-linear Differential equation for Drain Spacing. J. Irrig. & Drainage Division, ASCE 92(1R2), pp. 1 - 9.

57. MUSKAT, M.(1937): The Flow of Homogeneous Fluids Through Porous Media. McGraw-Hill, New York, 2nd Reprint: Edwards, Ann Arbour, Michigan, (1946).

58. NICOLA, F. and AMER, M.H.(1969): Effect of Sub-surface Drainage in increasing production of crops in the Delta area of U.A.R.

59. NWA, E.U.(1979): Drainage of Irrigation areas using the Bamboo (Arundinaria Amabilis) as field drainage material. Proc. 6th National Irrigation Seminar, A.B.U., Zaria, pp.164-170.

60. NWA, E.U.(1982): Ground water problems of the Kano River Irrigation Project of Nigeria. Proc. 4th Afro-Asian Conference Int. Comm. Irrig. Drainage, Lagos, 1982.

61. POLUBARINOVA-KOCHINA, P.Ya (1962): Theory of Ground Water Movement (1952) Translated by R.G.M De. Weist, Princeton University Press, Princeton N.J., p. 500.

62. PONNAMPERUMA, F.N.(1972): The Chemistry of Submerged Soils in Brady, N.C.(ed). Advances in Agronomy Vol. 24, Academic Press, New York.

63. RAATS, P.A.C.(1970): Steady Infiltration from line sources and furrows. Soil Science Soc. Amrica, 34, 709 - 714.

64. REEVE, R.C. and FAUSEY, W.R.(1974): Drainage and Timeliness of Farming Operations in Van Schilf gaarde, J. (ed). Drainage for Agriculture.

Agronomy Monograph No. 17, Am. Soc. Agron. Inc., Madison, Wisconsin, Chp.4. pp. 55 - 66.

65. RHOADES, J.C.(1974): Drainage for Salinity Control In Van Schilfgaarde (ed). Drainage for Agriculture. Am. Soc. Agronomy Inc. Monograph No. 17, Madison, Wisconsin, pp. 433 - 462.

66. RUSSEL, E.U.(1973): Soil conditions and plant growth. 10th ed. Longman, London, 849 pp.

67. SCHEIDEGGAR, A.E.(1960): The Physics of Flow through Porous Media. Second ed., University of Toronto Press, Toronto.

68. SCHNEEBELLI, G.(1955): Experiments on the Range of Validity of Darcy's law and the appearance of turbulence in a filtering flow. La Huile Blanche No. 2 Grenoble, France, 10. pp.141-149.

69. SCHWAB, G.O., FREVERT, R.K., EDMINSTER, T.W. and BARNES, K.K.(1966): Soil and Water Conservation Engineering. 2nd ed. John Wiley & Sons, New York.

70. SHALHEVET, J. and ZWERMAN, P.J.(1962): Nitrogen Responses of Corn Under Variable Conditions of Drainage: A Lysimeter Study. Soil Science 93: 172 - 182.

71. TERZAGHI, K. and PECK, R.B.(1967): Soil Mechanics in Engineering Practice. Second ed. John Wiley & Sons, N. York.

72. TODD, D.K.(1959): Ground Water Hydrology. John Wiley, New York.

73. TOKSOZ, S. and KIRKHAM, D.(1961): Graphical solution and interpretation of a new Drain Spacing Formula. J. Geophysical Research Vol. 66, pp. 509 - 511.

74. U.P. IRRIGATION RESEARCH INSTITUTE, ROORKEE, INDIA (1964): Steady State Saturation Line of Seepage from an unlined canal - its variation with water-table depth and depth of Impervious Stratum, and assessment of the water-logging condition thereof: I.C.I.D. Bulletin, p. 42.

75. U.S. SALINITY LABORATORY (1954): Diagnosis and Improvement of Saline and Alkali Soils. U.S.D.A. Handbook 60.

76. VAN DE GOOR (1972): Plant Growth in Relation to Drainage in International Institute for Land Reclamation and Improvement, the Netherlands, Publ. 16, Vol. 1, Drainage Principles and Applications I.

77. VAN SCHILFGAARDE, J.(1957): Approximate Solutions to Drainage Flow Problems. In Drainage of Agricultural Lands (Luthin, J.N. ed.). Am. Soc. Agron. Inc. Monograph No. 7, Madison, Wisconsin.

78. VAN SCHILFGAARDE, J.(1965): Transient Design of Drainage Systems. J. Irrig. and Drainage Div. ASCE Vol. 91, No. 1R3, pp. 9 - 22.

79. VAN SCHILFGAARDE, J.(1970): Theory of Flow to drains In Advances in Hydro-Science (V.T. Chow, ed) Vol. 6, pp. 43 - 106.

80. VAN SCHILFGAARDE, J.(1974): Non steady flow to drain. In Drainage for Agriculture (Van Schilfgaarde, J., ed.). Am. Soc. Agron. Inc. Monograph No. 17, Madison, Wisconsin, Chpt. 11.

81. VANT WOUDT, B.D. and HAGAN, R.M.(1957): Crop Responses at excessively High Moisture Levels In Drainage of Agricultural Lands (Luthin, J.N. ed). Am. Soc. Agron. Inc. Monograph No. 7. Madison, Wisconsin.

82. VOLKER, R.E.(1975): Solutions for Unconfined Non-Darcian Seepage. J. Irrigation & Drainage Div. ASCE Vol. 101, No. 1R1, pp. 53 - 65.

83. WESSELING, J. and VAN WIJK, W.R.(1957): Soil Physical Conditions in relation to drain depth. In Drainage of Agric. Lands (Luthin, J.N. ed) Am. Soc. Agron. Inc. Monograph No. 7, Madison, Wisconsin.

84. WESSELING, J.(1964): Comparison of the Steady State Drain Spacing Formulas of HOoghoudt and Kirkham in connection with Design Practice. J. Hydrology 2(1), pp. 25 - 32.

85. WESSELING, J.(1974): Crop growth and wet soils. Chp. 1 in Drainage for Agric. (Van Schilfgaarde, J. ed). Am. Soc. Agron. Inc. Monograph No. 17, Madison, Wisconsin.

86. WRIGHT, D.E.(1968): Non Linear Flow Through granular Media. J. Hydraulics Div. ASCE, Vol. 94, No. HY4, pp. 851 - 872.